Phenotypic modulation of smooth muscle cells in atherosclerosis is associated with downregulation of *LMOD1, SYNPO2, PDLIM7, PLN* and *SYNM*

Perisic L[1], Rykaczewska U[1], Razuvaev A[1], Sabater-Lleal M[2], Lengquist M[1], Miller CL[3], Ericsson I[1], Röhl S[1], Kronqvist M[1], Aldi S[1], Magné J[2], Vesterlund M[4], Li Y[2], Yin H[2], Gonzalez Diez M[2], Roy J[1], Baldassarre D[5,6], Veglia F[6], Humphries SE[7], de Faire U[8,9], Tremoli E[5,6], on behalf of the IMPROVE study group, Odeberg J[10], Vukojević V[11], Lehtiö J[4], Maegdefessel L[2], Ehrenborg E[2], Paulsson-Berne G[2], Hansson GK[2], Lindeman JHN[12], Eriksson P[2], Quertermous T[3], Hamsten A[2], Hedin U[1]

[1]Department of Molecular Medicine and Surgery, Karolinska Institutet, Sweden, [2]Department of Medicine, Karolinska Institutet, Sweden, [3]Division of Vascular Surgery, Stanford University, USA, [4]Science for Life Laboratory, Sweden, [5]Dipartimento di Scienze Farmacologiche e Biomolecolari, Università di Milano, Milan, Italy, [6]Centro Cardiologico Monzino, IRCCS, Milan, Italy, [7]British Heart Foundation Laboratories, University College of London, Department of Medicine, Rayne Building, London, United Kingdom, [8]Division of Cardiovascular Epidemiology, Institute of Environmental Medicine, Karolinska Institutet, [9]Department of Cardiology, Karolinska University Hospital Solna, Karolinska Institutet, Stockholm, Sweden, [10]Science for Life Laboratory, Department of Proteomics, Sweden, [11]Department of Clinical Neuroscience, Center for Molecular Medicine, Karolinska Institutet, Sweden, [12]Department of Vascular Surgery, Leiden University Medical Center, Netherlands

Running title: Markers of smooth muscle cells

Words 7989; Figures 8; Supplementary Figures 10; Supplementary Tables 10

Key Words: atherosclerosis, smooth muscle cells, phenotypic modulation

Subject codes: smooth muscle proliferation and differentiation, vascular biology, atherosclerosis, biomarkers

TOC category: basic; TOC subcategory: atherosclerosis

Correspondence to:

Ljubica Perisic Matic

Department of Molecular Medicine and Surgery, Solna

Karolinska Institute, L8:03

SE-171 76 STOCKHOLM

Tel: +46-76-0237008, E-mail: Ljubica.Perisic@ki.se

Abstract

Key augmented processes in atherosclerosis have been identified, whereas less is known about downregulated pathways. Here we applied a systems biology approach to examine suppressed molecular signatures, with hypothesis that they may provide insight into mechanisms contributing to plaque stability.

'Muscle contraction', 'muscle development' and 'actin cytoskeleton' were the most downregulated pathways (FDR=6.99e-21, 1.66e-6, 2.54e-10 respectively) in microarrays from human carotid plaques (n=177) vs. healthy arteries (n=15). In addition to typical SMC markers, these pathways also encompassed cytoskeleton-related genes previously not associated with atherosclerosis. *SYNPO2, SYNM, LMOD1, PDLIM7*, and *PLN* expression positively correlated to typical SMC markers in plaques (Pearson r>0.6, p<0.0001) and in rat intimal hyperplasia (r>0.8, p<0.0001). By immunohistochemistry, the proteins were expressed in SMCs in normal vessels, but largely absent in human plaques and intimal hyperplasia. Subcellularly, most proteins localised to the cytoskeleton in cultured SMCs and were regulated by active enhancer histone modification H3K27ac by ChIP-seq. Functionally, the genes were downregulated by PDGFB and IFNg, exposure to laminar shear stress and oxLDL loading. Genetic variants in *PDLIM7, PLN* and *SYNPO2* loci associated with progression of carotid intima-media thickness in high-risk subjects without symptoms of cardiovascular disease (n=3378). By eQTL, rs11746443 also associated with *PDLIM7* expression in plaques. Mechanistically, silencing of *PDLIM7 in vitro* lead to downregulation of SMC markers and disruption of the actin cytoskeleton, decreased cell spreading and increased proliferation.

We identified a panel of genes that reflect the altered phenotype of SMCs in vascular disease and could be early sensitive markers of SMC dedifferentiation.

Abbreviations

AF- amaurosis fugax
AHA- American Heart Association
AS-asymptomatic
BiKE- Biobank of Karolinska Endarterectomies
CEA- carotid endarterectomy
CP- carotid plaque
CHip- chromatin immunoprecipitation
CNN- calponin
cIMT- carotid intima-media thickness
ECM- extracellular matrix
LMOD1-leiomodin 1
GEO- Gene Expression Omnibus
IHC- immunohistochemistry
IFL- immunofluorescence
MS- minor stroke
MYOCD- myocardin
MYH11- myosin heavy chain 11
NA- normal artery
NCA- normal carotid artery
PCNA- proliferating cell nuclear antigen
PDGF- platelet derived growth factor
PLN- phospholamban
PDLIM7- PDZ and LIM domain containing 7
RNAseq- RNA sequencing
qPCR- quantitative polymerase chain reaction
FDR- false discovery rate
S- symptomatic
SMC- smooth muscle cell
SMA- smooth muscle actin
SYNM- synemin
SYNPO2- synaptopodin 2
TIA- transitory ischemic attack
TAGLN- transgelin

Introduction

Unstable atherosclerosis in the carotid bifurcation is a common cause of stroke, and guidelines recommend treatment with stroke-preventive carotid endarterectomy (CEA) in patients with signs of cerebral embolism[1]. Stable, asymptomatic (AS) carotid lesions are generally rich in extracellular matrix (ECM) and smooth muscle cells (SMCs), whereas unstable (symptomatic, S) plaques contain abundant inflammatory cells and a thin fibrous cap prone to rupture[2]. Inflammation, cytokines, mitogens, ECM degradation and altered cell-matrix interactions have been associated with intraplaque processes in atherogenesis which promote activation of contractile SMCs in the media into a secretory and replicating phenotype that engage in intimal remodeling and formation of the fibrous cap.

Contractile SMCs are distinguished from other cell types by expression of a unique repertoire of markers including Smooth Muscle Actin (SMA, ACTA2), Calponin (CNN1), Transgelin (TAGLN), Myocardin (MYOCD) and Myosin Heavy Chain 11 (MYH11), mostly associated with the acto-myosin cytoskeleton. These genes are downregulated in activated SMCs and may be undetectable using traditional immunohistochemical staining methods[3, 4]. However, it is unclear whether altered expression of these genes takes place concomitantly or successively during phenotypic modulation. This problem is notable in atherosclerotic lesions where SMA positive (SMA+) cells define several distinct regions and can be found in the necrotic core and the fibrous cap (Figure 1A). Recently, SMC transdifferentiation into CD68+ macrophage-like cells has been demonstrated in atherosclerosis[5, 6] which further emphasizes the complexity in characterizing SMC phenotypes in vascular disease. Apart from atherogenesis, activation of SMCs also dominates in healing reactions aimed to repair the vessel after injury, healing of ruptured atheromas[7], restenosis after arterial interventions[8] and in the failure of vein grafts and dialysis fistulas[9].

Understanding the molecular and cellular processes that convert asymptomatic plaques into symptomatic ones may facilitate the development of preventive pharmacotherapy with unprecedented impact on cardiovascular mortality and morbidity. For this purpose, intensive efforts have been dedicated to the identification of suitable targets through analysis of augmented pathways and molecules in vulnerable lesions[10, 11]. In contrast, less is known about pathways that are inhibited in atherogenesis and in the process of plaque instability. Since identification of such inherent functional changes within the vessel wall may give clues to therapies that can sustain arterial resistance to atherogenic stimuli or improve stability of established complex lesions, studies of downregulated genes and suppressed pathways may be equally important[12]. Identifications of ultimately translatable target molecules are bound to be more successful when generated directly from human disease, followed by clinical and experimental exploration.

Recently we performed a comprehensive transcriptomic analysis of late-stage human carotid atherosclerosis based on defined clinical patient phenotypes[13]. Our findings confirmed a central role for lipid accumulation, inflammation and proteases in plaque instability, and highlighted haemoglobin metabolism and bone resorption as important enriched pathways in plaques. Here, we instead analysed downregulated molecular signatures in carotid plaques by applying an integrative framework based on collaboration of three large human biobanks: initial discoveries were made using material from the Biobank of Karolinska Endarterectomies (BiKE, n=177 plaques from end-stage atherosclerosis patients and n=15 macroscopically healthy, normal arteries); data was further validated using atheroprogression samples from the SOKRATES biobank (n=28 patients tissues); and genetic analyses were performed in the IMPROVE cohort (n=3378 high-risk patients without symptoms or signs of cardiovascular disease). We found that SMC-related functional categories were the most significantly affected in plaques and identified a set of downregulated SMC-related genes previously poorly studied in vascular disease. Temporal changes in the expression of these genes were followed in the rat carotid injury model and in primary SMCs *in vitro* in comparison with typical SMC markers. Genetic association with progression of carotid

intima-media thickness (cIMT) as a surrogate marker of atherosclerosis, was investigated in the large cohort of high-risk subjects and mechanistic studies were performed for one of these genes *in vitro*. We report a panel of novel SMC markers that are suppressed in vascular disease in humans and reflect the altered phenotype of SMCs during vascular remodelling.

Material and Methods

Material and Metods are available in the online-only Data Supplement.

Results

Genes and pathways associated with SMCs are repressed in atherosclerosis

Pathways associated with 'muscle contraction', 'muscle development' and 'actin cytoskeleton' were the most significantly downregulated in microarrays comparing late-stage human carotid plaques (CP) vs. normal arteries (NA) as well as in plaques extracted from symptomatic vs. asymptomatic patients (e.g. in CP vs. NA comparison FDR=6.99e-21, 1.66e-6 and 2.54e-10 respectively, Supplementary Table I). Genes clustered in these categories were the typical markers of SMCs and acto-myosin cytoskeleton (Supplementary Fig IA). Among the most significantly downregulated genes appeared several whose function in SMCs was previously unexplored in the context of atherosclerosis: *LMOD1* (Leiomodin 1), *SYNPO2* (Synaptopodin 2), *PLN* (Phospholamban), *PDLIM7* (PDZ and LIM domain containing 7) and *SYNM* (Synemin). By constructing functional networks from their extended protein-protein interactions and expression profiles across tissues [14-16], we noted that these genes were co-expressed with actin and microtubule markers (Figure 1B) and some of them also co-interacted with the cytoskeleton based on available public data (i.e. PDLIM7, SYNM, LMOD1 and SYNPO2; Supplementary Figure IB). Strong downregulation of these transcripts was found in two non-overlapping microarray datasets comparing carotid plaques to normal arteries (n=127 CP vs. n=10 NA and n=50 CP vs. n=5 NA, p<0.0001 for most transcripts) and downregulation was also noted in plaques from symptomatic vs. asymptomatic patients (n=87 S vs 40 AS, p<0.01) (Figure 1C, full list in Supplementary Table II). In support of these findings, their protein levels were also lower in plaques from S vs. AS patients, as determined by mass spectrometry (n=10 S vs 10 AS, Supplementary Figure II). Additionaly, a trend towards downregulation of these genes was observed in publicly available microarray datasets comparing n=12 human carotid plaques vs. n=9 normal arteries [10] and n=32 carotid plaques vs. matched adjacent tissue (GSE43292). Strong positive correlations were seen between mRNA expression of *LMOD1, SYNPO2, PLN, PDLIM7* and *SYNM* in carotid plaques and typical SMC markers such as *ACTA2, MYH11, CNN1, MYOCD* (Pearson r>0.6, p<0.0001, representative examples in Figure 1D, full data in Supplementary Table III). Similarly, strong correlations between corresponding protein levels, as determined by mass spectrometry, were also demonstrated (Pearson r>0.8, p<0.0001, Supplementary Table III). To further investigate the association of the selected genes with SMCs, we analyzed a publicly available microarray dataset (GSE23303) comparing microdissected SMC-rich subintimal regions of carotid plaques with macrophage-rich regions from the necrotic core. We found that mRNA levels of these genes were strongly downregulated in macrophage-rich compared with SMC-rich regions, while no significant difference was seen in this comparison for ACTA2 (Supplementary Table II).

To experimentally corroborate our findings from human plaques, we analyzed the expression of the selected genes in an inducible plaque rupture model on ApoE background, where mice present atherothrombotic events and morphological signs of plaque instability [17]. Expression of all 5 genes of interest was strongly downregulated in ligated vs. non-ligated arteries (i.e. mRNA fold change= -114, p<0.0001 for *Synpo2*; fold change= -45, p<0.0001 for *Lmod1*), and marginally also in comparison between ruptured vs. stable plaques, thus replicating results from the human datasets (Supplementary Table IV).

Collectively, these results demonstrated that we have identified a set of previously poorly characterised genes through transcriptomic profiling of late-stage human atherosclerosis, likely associated with loss of contractile SMC features in the disease.

LMOD1, SYNPO2, PDLIM7, SYNM and PLN are expressed by SMCs

The localisation of selected genes and proteins in normal human vessels and carotid plaques was performed by *in situ* RNA hybridization and immunohistochemistry and compared with typical SMC markers such as MYH11, CNN1 and SMA, including proliferating cell nuclear antigen (PCNA) as a marker of cell proliferation. By immunohistochemistry, MYH11, considered to be an early marker of phenotypic changes in SMCs[3], was only detected in PCNA- SMCs in normal carotid artery media but was absent in late-stage plaques, while CNN1 was detectable in the normal artery as well as in subintimal SMA+/PCNA- cells and in SMA+ cells in the fibrous cap of carotid plaques (Figure 2A). By co-immunostaining, SMA, LMOD1, SYNPO2, PDLIM7, SYNM and PLN were all abundantly expressed in SMCs in normal arteries (carotid artery stainings shown in Figure 2B). The stainings appeared mostly cytosolic, except in the case of PLN, which exhibited nuclear staining. In late-stage plaques, PDLIM7 was present in subintimal SMCs and weak expression was also detected in stellate-shaped SMA+ cells in the fibrous cap. SYNM showed a similar staining pattern in subintimal SMCs but was absent from the fibrous cap. SYNPO2, LMOD1 and PLN were not detectable in these plaques by immunohistochemistry. RNA transcripts of *MYH11, CNN1, ACTA2* and selected genes were all detectable in the normal artery media and to a lesser extent also in cells with elongated nuclei in the fibrous cap (except *PLN*, Supplementary Figure III).

We further investigated the expression of these genes during atheroprogression, using human aortic lesions from different stages of disease graded according to the modified American Heart Association criteria[18], ranging from adaptive intimal thickening and xantomas (stages I and II), via pathological intimal thickening (stage III) to early and thin-cap fibroatheromas (stages IV and V). In these lesions, SMA and CNN1 were detectable in SMCs from early stages to advanced lesions, while MYH11 as expected, was absent from PCNA+ SMCs already at stage I (Supplementary Figure IV). LMOD1 and SYNPO2 were mostly absent already from stage I, PLN was not detectable from stage III, whereas SYNM and PDLIM7 were present in subintimal SMCs but sparsely in cells that build the fibrous cap from stage III. Interestingly, in human intimal hyperplasia, we observed the reappearance of both typical SMC markers and the selected genes in SMA+/PCNA- areas (Figure 2). Abundant signal was observed for CNN1 as well as for PDLIM7 and SYNM, while LMOD1, SYNPO2 and PLN were sparsely present. Our results confirm that these genes localise to quiescent SMCs in normal artery media and undergo various degrees of downregulation at both transcript and protein levels in activated SMA+ cells of lesions, with reappearance in mature intimal hyperplasia. Of note, these proteins were also detected in SMA+ cells in several other smooth muscle-rich tissues (Supplementary Figure V).

***Lmod1, Synpo2, Pdlim7, Synm* and *Pln* are downregulated early in reponse to experimental vascular injury but reappear in mature neointima**

Time-dependent alterations in expression of SMC markers were examined by transcriptomic analysis from rat carotid arteries after balloon injury (Figure 3). Typical SMC genes along with *Lmod1, Synpo2, Pdlim7, Synm* and *Pln* showed similar gene expression profiles with gradual downregulation in the early phases after injury, but upregulation after 2-12 weeks in the mature neointima. Expression correlations of *Lmod1, Synpo2, Pln, Pdlim7* and *Synm* with typical SMC markers in this model were strongly positive (mostly Pearson $r>0.8$, $p<0.0001$, Figure 3C, Supplementary Table III) and negative with cytokines such as *Pdgfb*, *Igf1* and *Tgfb1* (Figure 3C). By IHC, we observed loss of CNN1 from PCNA+ SMC layers closer to the lumen, while the staining was still present in deeper medial layers at day 5 and again abundant in the mature intima with reduced PCNA staining 12 weeks after injury (Figure 4A). Staining for LMOD1, SYNPO2, PDLIM7, SYNM and PLN was absent at day 5 with gradual reappearance in medial SMCs in tissues with pronounced intimal hyperplasia 12 weeks after injury (Figure 4B). No similar changes in gene expression patterns were found in contralateral uninjured arteries (Supplementary Figure VI). These analyses indicated that downregulation of *Lmod1, Synpo2, Pln, Pdlim7* and *Synm* might functionally relate to SMC activation in response to injury.

LMOD1, SYNPO2, SYNM, PDLIM7 and PLN localise mostly to actin-cytoskeleton in SMCs and relate to phenotypic changes in vitro

To address the expression of the selected genes during the process of SMC phenotypic modulation, rat aortic SMCs were isolated by collagenase digestion, seeded on fibronectin and cultured in serum-free medium or medium supplemented with PDGFBB for 7 days[19]. Directly upon isolation (day 0), almost 90% of the cells were SMA+ by flow cytometry, although lower SMA levels in a subgroup of cells were detectable (Figure 5A). After 7 days, 95% of the population cultured in serum-free medium uniformly expressed higher levels of SMA, while cells stimulated with PDGFBB showed presence of two subpopulations of which one expressed lower signal for SMA (totally 77% SMA+ cells, Figure 5A, detailed analysis shown in Supplementary Figure VII). By qPCR, mRNA levels of *Acta2, Myocd* and *Myh11* as well as *Lmod1, Synpo2, Pdlim7, Synm* and *Pln* strongly decreased from day 1 to day 3 in culture, but on day 5 and 7 the expression of most of these genes (except *Synm*) gradually increased. At each reference time-point, cells cultured in the presence of PDGFBB showed downregulation of the target genes compared to cells in serum-free medium (Figure 5B). By RNA-sequencing, downregulation of *LMOD1, SYNPO2, PDLIM7, SYNM* and *PLN* was also observed in low-passage human SMCs cultured in serum-supplemented (de-differentiation condition) vs. serum-free medium (Supplementary Table V).

By ChIP-sequencing, we observed that all these genes were under the regulation of active enhancer histone modification H3K27ac (Supplementary Table VI). Prediction of putative binding motifs in genomic sequences using MSigDB software searching a span of ±2000 basepairs around the transcription start site, we found 3 CArG motifs present upstream of human *PDLIM7* (at positions +650, +654, +667) and one SRF binding site in the *PLN* gene, but no such motifs were found in either *SYNPO2, LMOD1* or *SYNM* in this analysis. Another prediction program MotifMap, searching a wider region within 8000 basepairs around the transcription start, suggested regulation by several other transcription factors previously associated with SMCs or control of cell proliferation. Here, TEF1 and MAFA were predicted to regulate *LMOD1*; AP1 and SRF to regulate *PDLIM7*; TEF1 and SRF to regulate *PLN*; and CTCF and NEUROD to control *SYNPO2* (full list in Supplementary Table VII).

Subcellular localization of SMC markers was also assessed in low-passage human SMCs (Figure 5C, additional images shown in Supplementary Figure VIII). CNN1, PDLIM7 and SYNPO2 were localized to the actin cytoskeleton by overlap with phalloidin staining; SYNM localized to cellular filopodia and to the cortical cytoskeleton; PLN exhibited nuclear staining while MYH11 and LMOD1 could not be detected in these cells. Taken together, our data confirm that SMCs maintain phenotypic plasticity *in vitro* and show that the expression changes and cytoskeletal localization of the selected genes strongly correlate with those of typical SMC markers *in vitro*, as initially observed *in situ*.

Downregulation of *LMOD1, SYNPO2, SYNM, PDLIM7* and *PLN* in response to inflammatory-, hemodynamic- and lipid stimuli

Next, we explored processes relevant in the environment of an atherosclerotic lesion that may influence expression of the genes identified in our study. The expression of standard SMC markers as well as *LMOD1, SYNPO2, SYNM, PDLIM7* and *PLN* was rapidly downregulated in human SMCs in vitro by stimulation with IFNg (Figure 6A). Downregulation of all genes was observed within 24h of IFNg treatment, whereas expression of *PLN*, *PDLIM7, SYNM and SYNPO2* was suppressed already after 2h. These genes were also downregulated in human SMCs after 48-72hrs stimulation with oxLDL (in particular *SYNPO2, LMOD1* and *PLN*, Figure 6B), which was validated by analyzing a public microarray dataset comparing cholesterol-loaded primary mouse aortic SMCs with baseline controls (GSE47744, Supplementary Figure IX)[20]. In this model, the typical SMC markers *ACTA2* and *CNN1* were also downregulated, whereas the macrophage marker *CD68* was upregulated. Finally, we analyzed expression of these genes in an in vitro model of SMC exposure to laminar shear stress, mimicking the exposure of the injured vessel surface to the hemodynamic forces of

the flowing blood[21]. In microarrays comparing shear stress vs. static conditions, we have previously observed apoptosis as an enriched pathway through activation of *CASP3* (dataset accession nr GSE19909) and all genes (as well as other typical SMC markers) were also found to be downregulated in this model (Figure 6C).

Collectively, our results demonstrate that downregulation of *LMOD1, SYNPO2, SYNM, PDLIM7* and *PLN* along with standard SMC markers, functionally relates to clinical symptoms of plaque instability, vascular injury, as well as to key molecular processes in atherosclerosis such as apoptosis, shear stress, inflammatory stimuli and lipid-uptake.

Polymorphisms in *PDLIM7, SYNPO2* and *PLN* associate with surrogate markers of atherosclerosis

In order to investigate the involvement of *LMOD1, SYNPO2, PDLIM7, SYNM* and *PLN* in early processes shown to be predictive of carotid and coronary artery disease in humans, we examined the association of genetic variants in these loci with severity and rate of cIMT progression. Several variants in the *PDLIM7, SYNPO2* and *PLN* genomic regions were found to be associated with cIMT phenotypes in a large cohort of high-risk subjects (n=3378, IMPROVE)[22] after adjustment for age, gender and population stratification (Supplementary Table VIII). Variants rs11746443 and rs35716097 (*PDLIM7*) associated with the maximum thickness of the common carotid artery (p=0.002) and the fastest cIMT progression (p=0.0009, p=0.002, respectively), and variants rs67456868 (*PLN*) and rs4833611 (*SYNPO2*) were associated with the maximum common carotid artery thickness (p=0.00004, p=0.0007, respectively). Full functional information obtained from Haploreg for these variants is presented in Supplementary Tables IX and X. The *SYNPO2* variant rs4833611 was located in the intronic region of the *USP53* gene and by eQTL analyses marginally linked to *SYNPO2* (p=0.09) and *USP53* (p=0.02) gene expression in plaques. Of particular interest, *PDLIM7* variant rs35716097 was predicted to constitute a putative binding site for HNF4A transcription factor. The other *PDLIM7* variant rs11746443 was localised in the genomic region of *RGS14* and predicted to constitute the binding site for the HEY1 transcription factor, while its proxy (rs4075958, Rsquared=0.927, Dprime=0.963) was mapped within the putative binding site for the ETS1 transcription factor. By eQTL analysis in plaques, rs4075958 was found to be significantly associated with the expression of both *PDLIM7* and *RGS14* (p=0.007 and p=0.0002 respectively, Figures 7A and 7B) and the expression levels of both genes were strongly correlated (Pearson r=0.61, p<0.0001) (Figure 7C). PDLIM7 and RGS14 also appeared to be linked in a protein interaction network via actin cytoskeleton and markers of differentiated SMCs, SMTN and CNN2 (Figure 7D). Altogether, our results underline the possiblity that genetic variants associated with *PDLIM7* may be causal to altered intima-media phenotypes and predisposition to atherosclerosis.

Silencing of *PDLIM7* leads to downregulation of other SMC markers and increased SMC proliferation

Of the five genes that were identified, *PDLIM7* emerged as one of the key drivers of pathological processes in atherosclerosis[13]. Since *PDLIM7* was causally implicated in atherogenesis at the genetic level, localised to SMC actin cytoskeleton and in addition, interconnected with other cytoskeletal proteins, we decided to mechanistically investigate its role in SMCs. Silencing *PDLIM7* expression in human carotid SMCs in vitro, resulted in downregulation of other SMC markers (*ACTA2* by approximately 30%, *MYH11* by 50%, *LMOD1* by 30%, and particularly *SYNPO2* by 70% and *PLN* by 50% on the mRNA level). Cell adhesion and spreading on fibronectin were defective compared with controls, and proliferation was significantly increased in these cells as evaluated by BrdU incorporation (Figure 8, Supplementary Figure X). These findings add mechanistic support that PDLIM7 is a critical structural molecule in the regulation of SMC phenotype.

Discussion

A large biobank of carotid endarterectomies obtained from patients undergoing surgery for symptomatic or asymptomatic carotid stenosis was used to identify suppressed processes in atherosclerosis. We found molecular pathways related to SMC function and phenotype but also a panel of genes *(SYNPO2, SYNM, LMOD1, PDLIM7, PLN)* previously not associated with vascular disease, not only to be the most repressed in end-stage atherosclerosis but also in relation to clinical symptoms of plaque instability, both on the transcriptomic and proteomic level. We hypothesized that some of these genes may show early expression variations and demarcate the initiation of SMCs phenotypic switching. Most of these genes were linked to the SMC cytoskeleton, downregulated during neointima formation after rat carotid balloon injury, and polymorphisms in *PDLIM7, PLN* and *SYNPO2* genomic regions were associated with cIMT phenotypes in high-risk subjects. In addition, expression of these genes was sensitive to predominant processes in the atherosclerotic lesion such as apoptosis, inflammation, hemodynamic stress, and lipid exposure. We propose that these SMC genes may improve definition of the phenotypic state of these cells in vascular disease and may be further explored related to the capacity of SMCs to contribute to plaque stabilization.

Previously, transition of SMCs from a contractile and quiescent phenotype into synthetic, matrix-producing and replicating cells has been widely accepted as a central feature in early atherogenesis and an essential part of lesion stability and repair. This process, where the typical contractile features of SMCs are lost, represents an example of disturbed vessel wall homeostasis in disease progression. However, it has become evident that these conclusions oversimplify the complexity of SMC function in vascular disease and that these phenotypes probably represent the extremes of a spectrum of intermediate phenotypes that may to various extents coexist in the vessel wall, as dictated by exposure to environmental cues affecting gene expression patterns[23]. Recent studies have presented strong evidence that SMCs and macrophages can activate the same genes by demonstrating that 50% of foam cells within advanced human coronary artery lesions express the SMC marker SMA besides the macrophage marker CD68, while lineage tracing in mice confirmed that up to 80% of the lesion cells (including mesenchymal stem cells and macrophage-like cells) are SMC-derived[5, 6]. Here, we demonstrated that a number of SMC markers remain repressed on the protein level in stellate-shaped SMA+ cells of the fibrous cap, whereas expression was still detectable on the transcript level in situ, as previously reported by others[24]. Together, these observations highlight the problem of correct SMC identification with respect to our understanding of human disease. Other studies seeking to establish the earliest determinants of SMC phenotypic switch have shown that e.g. mitochondrial fragmentation represents an early mark of SMC activation[25]. Currently, changes in histone modifications, novel SMC-enriched transcription factors such as TCF21 and TET2[26-29] and epigenetic regulation of SMC phenotype by noncoding RNAs[30] are also being intensively investigated. Nevertheless, our study highlights that we have not yet fully explored the transcriptomic landscape in relation to the plethora of SMC phenotypes and adds to elucidation of molecular signatures that characterize their plasticity.

Here, we confirmed that muscle-contraction, muscle-development and acto-myosin cytoskeleton were some of the most repressed categories in atherosclerotic tissue, including typical markers of SMCs as well as a number of genes previously poorly characterised in the context of SMC function. Synemin (SYNM) is an intermediate filament protein whose knockdown in saphenous vein SMCs in vitro leads to increased collagen production, downregulation of typical SMC markers and disassembly of actin fibers[31]. Phospholamban (PLN), a regulator of Ca2+ homeostasis, was previously immunolocalized to the nuclear envelope and sarcoplasmic reticulum of cardiac SMCs[32]. In a recent study, PLN mutations were linked to dilated cardiomyopathy, ventricular arrhythmias and interstitial fibrosis[33]. Nanda V et al.[34] described Leiomodin 1 (LMOD1) as a new SMC-restricted, myofilament-related, SRF/MYOCD target gene enriched in SMCs in embryonic and adult mouse tissues.

Earlier, LMOD1 was predicted to belong to a 'gene battery' involved in SMC differentiation by a bioinformatics screen for regulators of conserved functional gene modules in mammals[35]. Interestingly, Synaptopodin (SYNPO) and PDLIM proteins have been discovered as neuronal components and also investigated as adaptor molecules orchestrating actin-cytoskeletal organization in foot processes of podocytes[36-39], but sparsely linked to SMCs[40-43]. Apart from these few publications, limited information exists about these genes in the literature up to date, and to the best of our knowledge, this study is the first to systematically examine their implication in human atherosclerosis and vascular remodelling.

SMCs are currently considered to be the main cell type responsible for intimal repair after balloon injury in the rat carotid artery, although cells of mesenchymal origin may also contribute [44]. In this model, intimal hyperplasia develops in three major stages[45, 46] with initial SMC activation, replication and beginning of migration to the luminal surface during the first two days after injury. Between days two and five, SMCs colonise the intimal surface following activity related to chemoattractants and ECM degradation. In the next few weeks, the number of SMCs in the neointima continues to increase, but from one month after injury, SMC proliferation ceases, the cells become quiescent and regain ultrastructural features typical for the contractile state[46]. Our results show that expression profiles for both typical SMC markers and for *Synm, Pln, Lmod1, Synpo2* and *Pdlim7* reflect these stages by gradual downregulation until five days after injury, followed by subsequent upregulation later as SMCs become quiescent and regain contractile features. In a similar fashion, immunohistochemical staining for typical SMC markers as well as for SYNM, PLN, LMOD1, SYNPO2, and PDLIM7 was detected in human intimal hyperplasia, especially in large PCNA-areas. Based on these results we hypothesize that SYNM, PLN, LMOD1, SYNPO2, and PDLIM7 functionally relate to the phenotypic state of SMCs.

Freshly isolated rat aortic SMCs seeded on fibronectin and cultured under serum-free conditions have previously been used to study the subcellular properties related to SMC phenotypic modulation *in vitro*. Under these conditions, interactions between fibronectin, integrin $\alpha_5\beta_1$ and FAK-dependent intracellular signalling promote cell cycle entry and dedifferentiation into a synthetic state, accompanied by structural reorganisation and loss of myofilaments[19, 47, 48]. Here, we observed that *Synm, Pln, Lmod1, Synpo2* and *Pdlim7* (as well as *Acta2, Myocd, Myh11*) were indeed downregulated in primary rat SMCs during the first days of culture on fibronectin, but reexpressed from about 5 days of culture, suggesting that SMCs retain their inherent plasticity *in vitro*. Several of the examined genes were localised to the actin cytoskeleton in human SMCs implying that they may be involved in reorganisation of cytoskeletal structures. Interestingly, while plasticity of SMCs and re-expression of target genes and proteins was apparent in human and rat intimal hyperplasia, expression of the proteins remained repressed in stellate-shaped SMA+ cells of the fibrous cap in carotid plaques. As discussed, this may either be due to a heterogeneous population of cells expressing SMA[5, 6] or repression of these genes in SMCs by disease specific factors such as inflammatory-, apoptotic-, or lipid mediators.

Therefore, in order to explore whether dominant processes in the atherosclerotic environment may influence the genes of interest in our study, we investigated the expression of *SYNM, PLN, PDLIM7, LMOD1* and *SYNPO2* as well as other typical SMC markers in SMCs exposed to disease-associated stimuli *in vitro*. To summarize, while we have not yet fully dissected which specific, or combination of, stimuli may repress expression of *SYNM, PLN, PDLIM7, LMOD1* and *SYNPO2* in atherosclerosis, we showed that they were downregulated in response to shear stress (and apoptosis), inflammatory stimuli and cholesterol-uptake. In support of these observations, exposure to lipids has previously been associated with dramatic effects on SMC phenotype and transdifferation into CD68+ macrophage-like foam cells, as also demonstrated in our study [20].

Intima–media thickness of extracranial carotid arteries, measured by ultrasound is a commonly accepted non-invasive marker of subclinical atherosclerosis. Several studies have established that cIMT changes over time are associated with vascular risk factors[22] and

prediction of vascular events both in subjects with plaques at baseline and in those without. Here, genetic variants in *PDLIM7, SYNPO2* and *PLN* showed association with cIMT measurements, suggesting that these genes could have a causal role in carotid disease. Of note, *SYNPO2* variants were located in the intron of *USP53* gene and marginally linked to expression in BiKE atherosclerotic plaques. USP53 (Ubiquitin Specific Peptidase 53) is a poorly studied protein, highly expressed in the heart muscle and found to be genetically associated with the Cantu syndrome, a rare condition characterized clinically by hypertrichosis, cardiomegaly and bone abnormalities[49]. Of particular interest, *PDLIM7* SNPs linked to fastest-IMTmax-progression were shown to influence expression of *PDLIM7* in plaques and predicted to constitute binding sites for transcription factors previously implicated in cardiovascular development, SMC migration, and SMC proliferation in response to cytokine stimulation[50, 51]. One of these SNPs was positioned in the intronic region of the *RGS14* gene, and interestingly, the expression of *RGS14* also strongly correlated with the expression of *PDLIM7* in plaques. *RGS14* has been shown to act as a positive modulator of microtubule polymerisation and spindle organization during cell division by integrating G protein and MAPK signaling pathways[52, 53]. It inhibits PDGF-stimulated ERK1/ERK2 phosphorylation and may indirectly interact with PDLIM7 via the actin-cytoskeleton.

The importance of *PDLIM7* for SMC phenotype was confirmed by silencing experiments that resulted in perturbed cytoskeletal structure, adhesion and spreading as well as SMC proliferation. Previous studies in other cell types have shown similar effects of *PDLIM7* knock-down on proliferation (i.e. periodontal ligaments[54]) and studies of other PDLIM family members have shown that they can directly interact with actin-cytoskeleton proteins such as α-actinin-4 to stabilise actin fibres[39]. Similarly, missense mutations of *ACTA2* in humans are associated with diminished gene expression, defective actin-filaments and actin-based spreading in SMCs, and formation of occlusive lesions due to increased SMC proliferation and intimal hyperplasia[55, 56]. Overall, our findings suggest a critical structural and mechanistic role for PDLIM7 in SMCs, with possible genetic influence on disease development.

Because the BiKE cohort comprises only late-stage lesions and cannot provide information about gene expression variations during atheroprogression, expression data was complemented with immunohistochemistry on aortic lesions collected from different stages of atherosclerotic disease. Of note, PCNA that was used as a proliferation marker in the immunohistochemical analysis, has been reported to overestimate the number of replicating cells. Consensus is lacking regarding the selection of appropriate control tissues, and in the BiKE study, control vessels contained outer media that is not included in the endarterectomy samples. Furthermore, the discovery approach in our study was based on microarrays and the complexity of microarray data was reduced by pathway analyses and construction of functional networks where genes were clustered based on biological functions or protein interactions. While this method is limited to semantic mining of existing knowledge from published literature and databases, it still permits for discovery of poorly explored genes in a certain context.

In conclusion, using a systems biology approach by integrating transcriptomic, in situ, in vivo, in vitro and genetic studies we were able to overcome these limitations and discover several novel candidates that demarcate early phenotypic modulation of SMCs in vascular disease. In perspective, the full knowledge of key expression signatures is likely to help us derive a better definition of various SMC phenotypes that coexist in the vessel wall, and provide targets for prevention and therapy in vascular disease.

Acknowledgments

None.

Funding sources

The BiKE study was conducted with support from the Swedish Heart and Lung Foundation, the Swedish Research Council, Uppdrag Besegra Stroke, the Strategic Cardiovascular Programs of Karolinska Institutet and Stockholm County Council, the Stockholm County Council, the Foundation for Strategic Research and the European Commission (CarTarDis, AtheroRemo, VIA and AtheroFlux projects). The SOKRATES study has been supported by the Foundation “De Drie Lichten” in The Netherlands. The IMPROVE study was supported by the European Commission (Contract number: QLG1- CT- 2002- 00896), Ministero della Salute Ricerca Corrente, Italy, the Swedish Heart-Lung Foundation, the Swedish Research Council (projects 8691 and 0593), the Foundation for Strategic Research, the Stockholm County Council (project 562183), the Foundation for Strategic Research, the Academy of Finland (Grant #110413) and the British Heart Foundation (RG2008/014). The funders had no role in study design, data collection and analysis, decision to publish, or preparation of the manuscript.

Disclosures

Authors have no competing interests to declare.

References#

#

1. Abbott AL, Paraskevas KI, Kakkos SK, Golledge J, Eckstein HH, Diaz-Sandoval LJ, Cao L, Fu Q, Wijeratne T, Leung TW, Montero-Baker M, Lee BC, Pircher S, Bosch M, Dennekamp M, Ringleb P. Systematic review of guidelines for the management of asymptomatic and symptomatic carotid stenosis. *Stroke; a journal of cerebral circulation*. 2015;46:3288-3301
2. Finn AV, Nakano M, Narula J, Kolodgie FD, Virmani R. Concept of vulnerable/unstable plaque. *Arteriosclerosis, thrombosis, and vascular biology*. 2010;30:1282-1292
3. Gomez D, Owens GK. Smooth muscle cell phenotypic switching in atherosclerosis. *Cardiovascular research*. 2012;95:156-164
4. Alexander MR, Owens GK. Epigenetic control of smooth muscle cell differentiation and phenotypic switching in vascular development and disease. *Annual review of physiology*. 2012;74:13-40
5. Allahverdian S, Chehroudi AC, McManus BM, Abraham T, Francis GA. Contribution of intimal smooth muscle cells to cholesterol accumulation and macrophage-like cells in human atherosclerosis. *Circulation*. 2014;129:1551-1559
6. Shankman LS, Gomez D, Cherepanova OA, Salmon M, Alencar GF, Haskins RM, Swiatlowska P, Newman AA, Greene ES, Straub AC, Isakson B, Randolph GJ, Owens GK. Klf4-dependent phenotypic modulation of smooth muscle cells has a key role in atherosclerotic plaque pathogenesis. *Nature medicine*. 2015;21:628-637
7. Schwartz SM, Virmani R, Rosenfeld ME. The good smooth muscle cells in atherosclerosis. *Current atherosclerosis reports*. 2000;2:422-429
8. Weintraub WS. The pathophysiology and burden of restenosis. *The American journal of cardiology*. 2007;100:3K-9K
9. Hedin U, Roy J, Tran PK. Control of smooth muscle cell proliferation in vascular disease. *Current opinion in lipidology*. 2004;15:559-565
10. Saksi J, Ijas P, Nuotio K, Sonninen R, Soinne L, Salonen O, Saimanen E, Tuimala J, Lehtonen-Smeds EM, Kaste M, Kovanen PT, Lindsberg PJ. Gene expression differences between stroke-associated and asymptomatic carotid plaques. *Journal of molecular medicine*. 2011;89:1015-1026
11. Sluimer JC, Kisters N, Cleutjens KB, Volger OL, Horrevoets AJ, van den Akker LH, Bijnens AP, Daemen MJ. Dead or alive: Gene expression profiles of advanced atherosclerotic plaques from autopsy and surgery. *Physiological genomics*. 2007;30:335-341
12. Clarke MC, Figg N, Maguire JJ, Davenport AP, Goddard M, Littlewood TD, Bennett MR. Apoptosis of vascular smooth muscle cells induces features of plaque vulnerability in atherosclerosis. *Nature medicine*. 2006;12:1075-1080
13. Perisic L, Aldi S, Sun Y, Folkersen L, Razuvaev A, Roy J, Lengquist M, Akesson S, Wheelock CE, Maegdefessel L, Gabrielsen A, Odeberg J, Hansson GK, Paulsson-Berne G, Hedin U. Gene expression signatures, pathways and networks in carotid atherosclerosis. *Journal of internal medicine*. 2015;3:293-308
14. Schmitt T, Ogris C, Sonnhammer EL. Funcoup 3.0: Database of genome-wide functional coupling networks. *Nucleic acids research*. 2014;42:D380-388
15. Alexeyenko A, Sonnhammer EL. Global networks of functional coupling in eukaryotes from comprehensive data integration. *Genome research*. 2009;19:1107-1116
16. Warde-Farley D, Donaldson SL, Comes O et al. The genemania prediction server: Biological network integration for gene prioritization and predicting gene function. *Nucleic acids research*. 2010;38:W214-220
17. Sasaki T, Nakamura K, Kuzuya M. Plaque rupture model in mice. *Methods in molecular medicine*. 2007;139:67-75
18. van Dijk RA, Virmani R, von der Thusen JH, Schaapherder AF, Lindeman JH. The natural history of aortic atherosclerosis: A systematic histopathological evaluation of the peri-renal region. *Atherosclerosis*. 2010;210:100-106

19. Hedin U, Bottger BA, Forsberg E, Johansson S, Thyberg J. Diverse effects of fibronectin and laminin on phenotypic properties of cultured arterial smooth muscle cells. *The Journal of cell biology*. 1988;107:307-319
20. Vengrenyuk Y, Nishi H, Long X, Ouimet M, Savji N, Martinez FO, Cassella CP, Moore KJ, Ramsey SA, Miano JM, Fisher EA. Cholesterol loading reprograms the microrna-143/145-myocardin axis to convert aortic smooth muscle cells to a dysfunctional macrophage-like phenotype. *Arteriosclerosis, thrombosis, and vascular biology*. 2015;35:535-546
21. Ekstrand J, Razuvaev A, Folkersen L, Roy J, Hedin U. Tissue factor pathway inhibitor-2 is induced by fluid shear stress in vascular smooth muscle cells and affects cell proliferation and survival. *Journal of vascular surgery*. 2010;52:167-175
22. Baldassarre D, Veglia F, Hamsten A, Humphries SE, Rauramaa R, de Faire U, Smit AJ, Giral P, Kurl S, Mannarino E, Grossi E, Paoletti R, Tremoli E, Group IS. Progression of carotid intima-media thickness as predictor of vascular events: Results from the improve study. *Arteriosclerosis, thrombosis, and vascular biology*. 2013;33:2273-2279
23. Shanahan CM, Weissberg PL. Smooth muscle cell heterogeneity: Patterns of gene expression in vascular smooth muscle cells in vitro and in vivo. *Arteriosclerosis, thrombosis, and vascular biology*. 1998;18:333-338
24. Gomez D, Shankman LS, Nguyen AT, Owens GK. Detection of histone modifications at specific gene loci in single cells in histological sections. *Nature methods*. 2013;10:171-177
25. Wang L, Yu T, Lee H, O'Brien DK, Sesaki H, Yoon Y. Decreasing mitochondrial fission diminishes vascular smooth muscle cell migration and ameliorates intimal hyperplasia. *Cardiovascular research*. 2015;106:272-283
26. Liu R, Jin Y, Tang WH, Qin L, Zhang X, Tellides G, Hwa J, Yu J, Martin KA. Ten-eleven translocation-2 (tet2) is a master regulator of smooth muscle cell plasticity. *Circulation*. 2013;128:2047-2057
27. Miller CL, Haas U, Diaz R, Leeper NJ, Kundu RK, Patlolla B, Assimes TL, Kaiser FJ, Perisic L, Hedin U, Maegdefessel L, Schunkert H, Erdmann J, Quertermous T, Sczakiel G. Coronary heart disease-associated variation in tcf21 disrupts a mir-224 binding site and mirna-mediated regulation. *PLoS genetics*. 2014;10:e1004263
28. Nurnberg ST, Cheng K, Raiesdana A et al. Coronary artery disease associated transcription factor tcf21 regulates smooth muscle precursor cells that contribute to the fibrous cap. *PLoS genetics*. 2015;11:e1005155
29. Sazonova O, Zhao Y, Nurnberg S, Miller C, Pjanic M, Castano VG, Kim JB, Salfati EL, Kundaje AB, Bejerano G, Assimes T, Yang X, Quertermous T. Characterization of tcf21 downstream target regions identifies a transcriptional network linking multiple independent coronary artery disease loci. *PLoS genetics*. 2015;11:e1005202
30. Miano JM, Long X. The short and long of noncoding sequences in the control of vascular cell phenotypes. *Cellular and molecular life sciences.* 2015;18:3457-88
31. Xiao Y, Huang Z, Yin H, Zhang H, Wang S. Desmuslin gene knockdown causes altered expression of phenotype markers and differentiation of saphenous vein smooth muscle cells. *Journal of vascular surgery*. 2010;52:684-690
32. Ferguson DG, Young EF, Raeymaekers L, Kranias EG. Localization of phospholamban in smooth muscle using immunogold electron microscopy. *The Journal of cell biology*. 1988;107:555-562
33. van der Zwaag PA, van Rijsingen IA, Asimaki A et al. Phospholamban r14del mutation in patients diagnosed with dilated cardiomyopathy or arrhythmogenic right ventricular cardiomyopathy: Evidence supporting the concept of arrhythmogenic cardiomyopathy. *European journal of heart failure*. 2012;14:1199-1207
34. Nanda V, Miano JM. Leiomodin 1, a new serum response factor-dependent target gene expressed preferentially in differentiated smooth muscle cells. *The Journal of biological chemistry*. 2012;287:2459-2467
35. Nelander S, Larsson E, Kristiansson E, Mansson R, Nerman O, Sigvardsson M, Mostad P, Lindahl P. Predictive screening for regulators of conserved functional gene modules (gene batteries) in mammals. *BMC genomics*. 2005;6:68

36. Mundel P, Heid HW, Mundel TM, Kruger M, Reiser J, Kriz W. Synaptopodin: An actin-associated protein in telencephalic dendrites and renal podocytes. *The Journal of cell biology*. 1997;139:193-204
37. Asanuma K, Yanagida-Asanuma E, Faul C, Tomino Y, Kim K, Mundel P. Synaptopodin orchestrates actin organization and cell motility via regulation of rhoa signalling. *Nature cell biology*. 2006;8:485-491
38. Sistani L, Rodriguez PQ, Hultenby K, Uhlen M, Betsholtz C, Jalanko H, Tryggvason K, Wernerson A, Patrakka J. Neuronal proteins are novel components of podocyte major processes and their expression in glomerular crescents supports their role in crescent formation. *Kidney international*. 2013;83:63-71
39. Sistani L, Duner F, Udumala S, Hultenby K, Uhlen M, Betsholtz C, Tryggvason K, Wernerson A, Patrakka J. Pdlim2 is a novel actin-regulating protein of podocyte foot processes. *Kidney international*. 2011;80:1045-1054
40. Watanabe T, Akishita M, Nakaoka T, He H, Miyahara Y, Yamashita N, Wada Y, Aburatani H, Yoshizumi M, Kozaki K, Ouchi Y. Caveolin-1, id3a and two lim protein genes are upregulated by estrogen in vascular smooth muscle cells. *Life sciences*. 2004;75:1219-1229
41. Krcmery J, Gupta R, Sadleir RW, Ahrens MJ, Misener S, Kamide C, Fitchev P, Losordo DW, Crawford SE, Simon HG. Loss of the cytoskeletal protein pdlim7 predisposes mice to heart defects and hemostatic dysfunction. *PloS one*. 2013;8:e80809
42. Weins A, Schwarz K, Faul C, Barisoni L, Linke WA, Mundel P. Differentiation- and stress-dependent nuclear cytoplasmic redistribution of myopodin, a novel actin-bundling protein. *The Journal of cell biology*. 2001;155:393-404
43. Turczynska KM, Sward K, Hien TT, Wohlfahrt J, Mattisson IY, Ekman M, Nilsson J, Sjogren J, Murugesan V, Hultgardh-Nilsson A, Cidad P, Hellstrand P, Perez-Garcia MT, Albinsson S. Regulation of smooth muscle dystrophin and synaptopodin 2 expression by actin polymerization and vascular injury. *Arteriosclerosis, thrombosis, and vascular biology*. 2015;35:1489-1497
44. Zhao W, Wang C, Liu R et al. Effect of tgf-beta1 on the migration and recruitment of mesenchymal stem cells after vascular balloon injury: Involvement of matrix metalloproteinase-14. *Scientific reports*. 2016;6:21176
45. Majesky MW, Schwartz SM, Clowes MM, Clowes AW. Heparin regulates smooth muscle s phase entry in the injured rat carotid artery. *Circulation research*. 1987;61:296-300
46. Thyberg J, Blomgren K, Hedin U, Dryjski M. Phenotypic modulation of smooth muscle cells during the formation of neointimal thickenings in the rat carotid artery after balloon injury: An electron-microscopic and stereological study. *Cell and tissue research*. 1995;281:421-433
47. Roy J, Tran PK, Religa P, Kazi M, Henderson B, Lundmark K, Hedin U. Fibronectin promotes cell cycle entry in smooth muscle cells in primary culture. *Experimental cell research*. 2002;273:169-177
48. Roy J, Kazi M, Hedin U, Thyberg J. Phenotypic modulation of arterial smooth muscle cells is associated with prolonged activation of erk1/2. *Differentiation; research in biological diversity*. 2001;67:50-58
49. Kurban M, Kim CA, Kiuru M, Fantauzzo K, Cabral R, Abbas O, Levy B, Christiano AM. Copy number variations on chromosome 4q26-27 are associated with cantu syndrome. *Dermatology*. 2011;223:316-320
50. Fischer A, Schumacher N, Maier M, Sendtner M, Gessler M. The notch target genes hey1 and hey2 are required for embryonic vascular development. *Genes & development*. 2004;18:901-911
51. Jiang H, Huang S, Li X, Li X, Zhang Y, Chen ZY. Tyrosine kinase receptor b protects against coronary artery disease and promotes adult vasculature integrity by regulating ets1-mediated ve-cadherin expression. *Arteriosclerosis, thrombosis, and vascular biology*. 2015;35:580-588
52. Wieland T, Lutz S, Chidiac P. Regulators of g protein signalling: A spotlight on emerging functions in the cardiovascular system. *Current opinion in pharmacology*. 2007;7:201-207

53. Vellano CP, Brown NE, Blumer JB, Hepler JR. Assembly and function of the regulator of g protein signaling 14 (rgs14).H-ras signaling complex in live cells are regulated by galphai1 and galphai-linked g protein-coupled receptors. *The Journal of biological chemistry*. 2013;288:3620-3631
54. Lin Z, Navarro VP, Kempeinen KM, Franco LM, Jin Q, Sugai JV, Giannobile WV. Lmp1 regulates periodontal ligament progenitor cell proliferation and differentiation. *Bone*. 2010;47:55-64
55. Guo DC, Pannu H, Tran-Fadulu V et al. Mutations in smooth muscle alpha-actin (acta2) lead to thoracic aortic aneurysms and dissections. *Nature genetics*. 2007;39:1488-1493
56. Papke CL, Cao J, Kwartler CS et al. Smooth muscle hyperplasia due to loss of smooth muscle alpha-actin is driven by activation of focal adhesion kinase, altered p53 localization and increased levels of platelet-derived growth factor receptor-beta. *Human molecular genetics*. 2013;22:3123-3137

#

Significance

A large biobank of carotid endarterectomies obtained from patients undergoing surgery for symptomatic or asymptomatic carotid stenosis was utilized to uncover genes and mechanisms repressed in atherosclerosis. Results demonstrated enrichment of molecular pathways related to smooth muscle cell (SMC) function and identified a panel of downregulated SMC genes previously not associated with vascular disease. These genes *(SYNPO2, SYNM, LMOD1, PDLIM7 and PLN)* were related to the SMC cytoskeleton, they were transiently downregulated during neointima formation after rat carotid balloon injury, and polymorphisms in *PDLIM7, PLN* and *SYNPO2* were associated with surrogate markers of atherosclerosis in high-risk subjects without symptoms of cardiovascular disease. Our work emphasizes the significance of SMC phenotypic modulation in atherosclerosis. In addition, these newly described SMC genes may improve definition of the phenotypic state of these cells in vascular disease and may be related to the capacity of SMCs to contribute to stabilizing processes in atherosclerotic lesions.

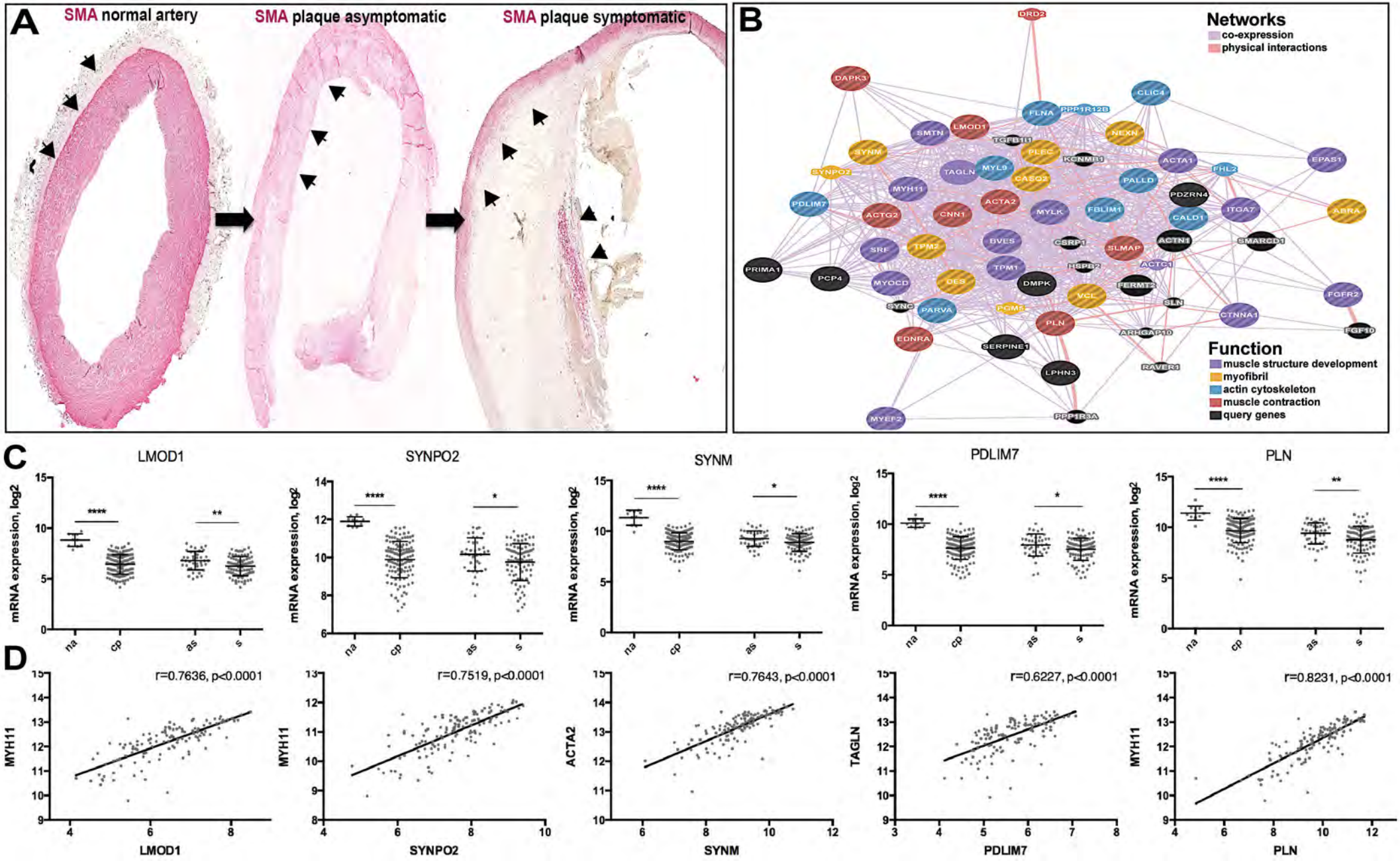

Figure 1. LMOD1, SYNPO2, SYNM, PDLIM7 and PLN were downregulated in carotid plaques. Microarray profiles comparing n=127 carotid plaques vs. n=10 normal arteries were used in discovery phase for analysis of downregulated genes and pathways. Arroweads showing SMA+ smooth muscle cells (SMCs) in the media of normal artery, remaining media at the plaque periphery and fibrous cap. Images were taken with 4x objective (A). Co-expression and co-interaction network of genes clusterred in pathways 'muscle contraction', 'muscle development', 'actin cytoskeleton' and 'myofibril cytoskeleton' shows the presence of typical markers of SMCs in these categories (i.e. CNN1, SMTN, TAGLN, ACTA2, MYH11) as well as other potentially interesting genes of which some were selected for further investigations. Network weighted for closeness in biological function based on publically available data (B). PDLIM7, LMOD1, SYNPO 2, SYNM and PLN were among the most downregulated genes in microarrays from plaques (CP) vs. normal arteries (NA) and symptomatic (S) vs. asymptomatic (AS) patients (C) and strongly correlated to standard markers of SMCs (D). Plots showing log mean±standard deviation in C and Pearson correlations in D.

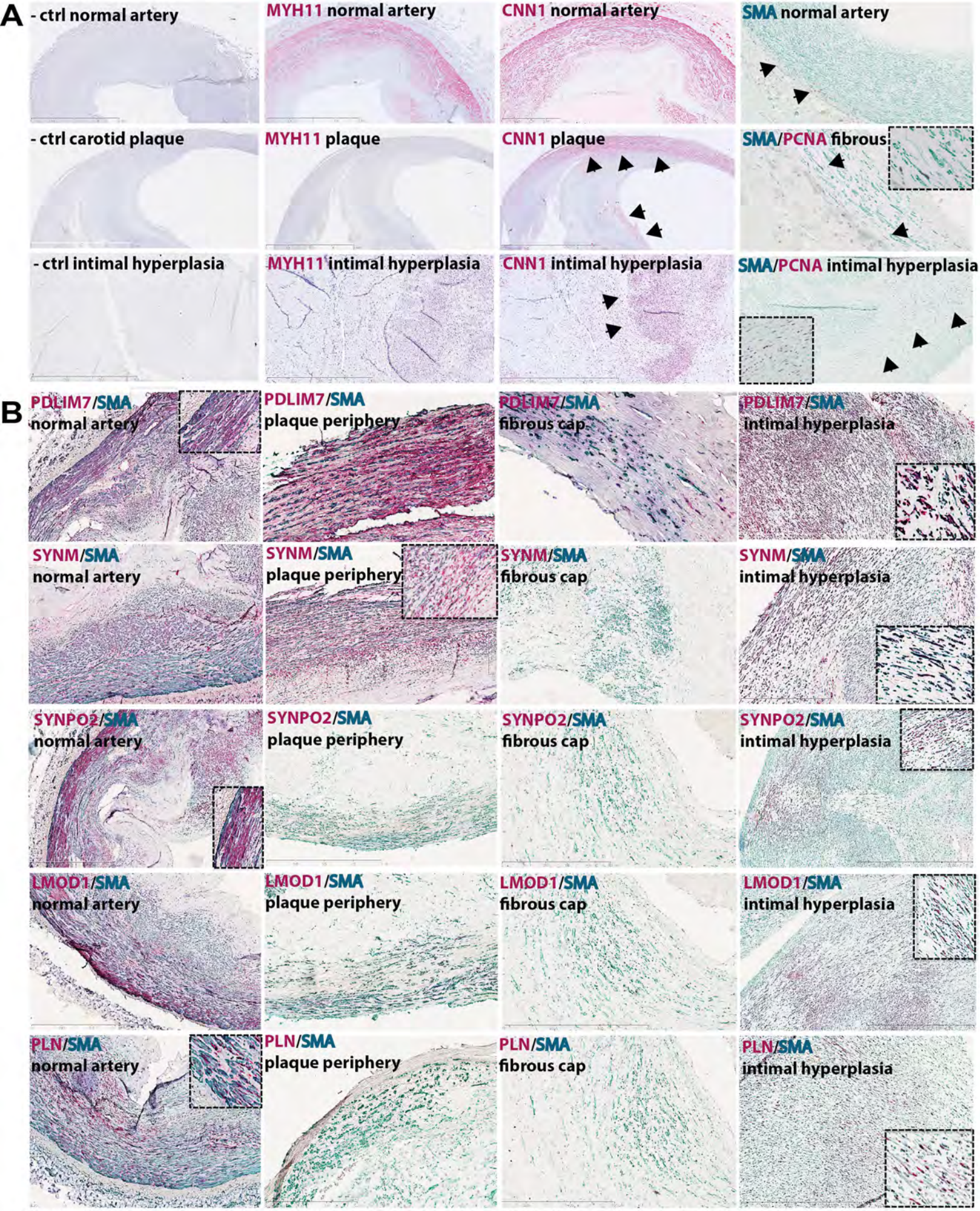

Figure 2. Selected candidates were localised to differentiated smooth muscle cells and reduced in late-stage plaques. By immunohistochemistry, Myh11 (red) was present only in normal carotid arteries while Calponin (red) and SMA (green) were detectable in normal arteries, in plaques as well as in human intimal hyperplasia tissue with large PCNA- areas (arrowheads, A). The identified SMCs markers (red) were all localised to SMCs in the normal carotid artery (left column panels, insets show higher magnification). Pdlim7 and Synm were also present in subintimal SMA+ cells at the plaque periphery and Pdlim7 was the only one still detectable in SMA+ cells in the fibrous cap. Signal for Lmod1, Synpo2 and Pln was lost in plaques. Abundant staning for Pdlim7 and Synm was seen in restenosis tissues, and Synpo2, Lmod1 and Pln were also observed in PCNA- areas (B). Images were taken with 10x objective, insets show 40x magnification.

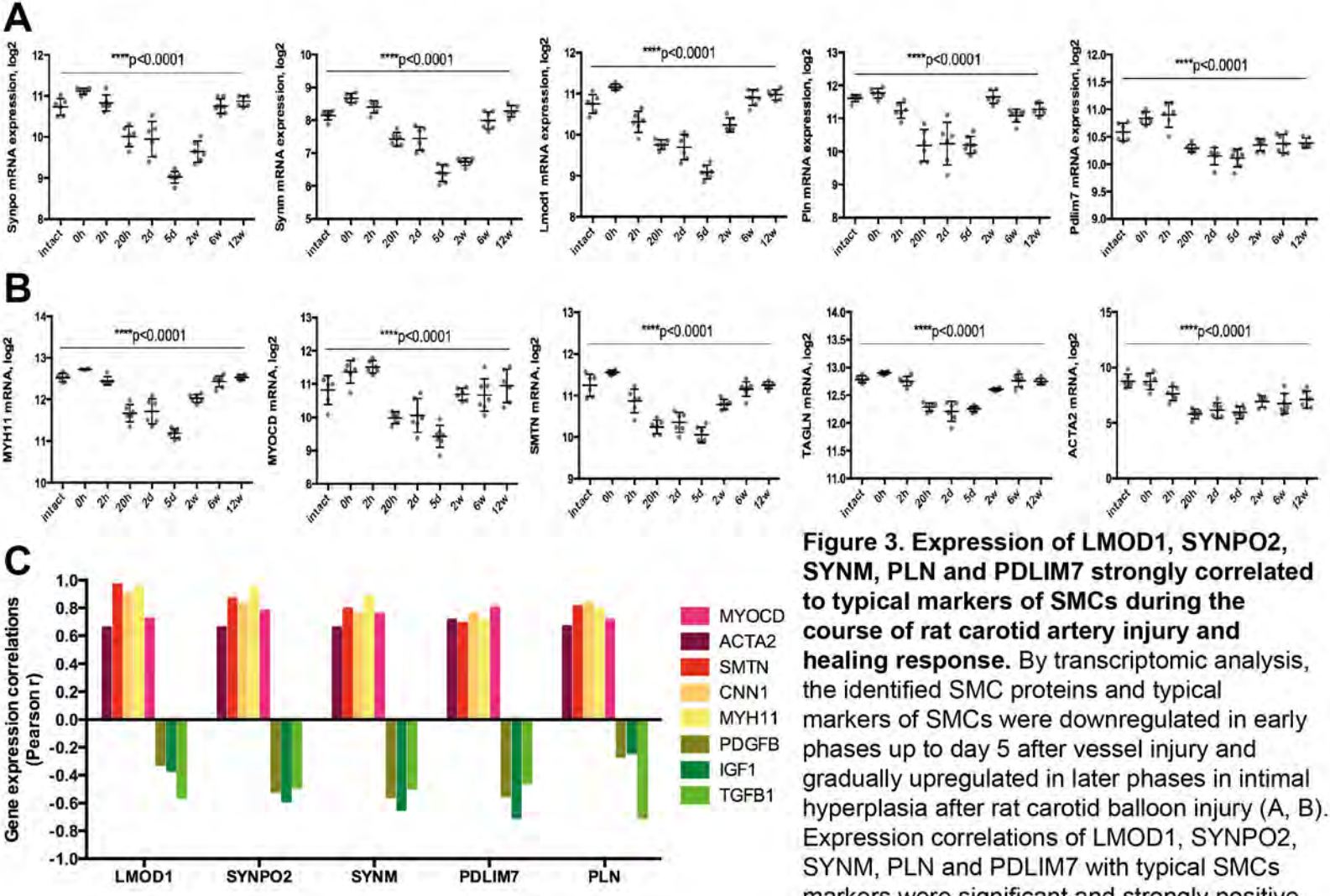

Figure 3. Expression of LMOD1, SYNPO2, SYNM, PLN and PDLIM7 strongly correlated to typical markers of SMCs during the course of rat carotid artery injury and healing response. By transcriptomic analysis, the identified SMC proteins and typical markers of SMCs were downregulated in early phases up to day 5 after vessel injury and gradually upregulated in later phases in intimal hyperplasia after rat carotid balloon injury (A, B). Expression correlations of LMOD1, SYNPO2, SYNM, PLN and PDLIM7 with typical SMCs markers were significant and strongly positive in this model (mostly Pearson r>0.8), and negative with PDGFB, IGF1 and TGFB1 (C).

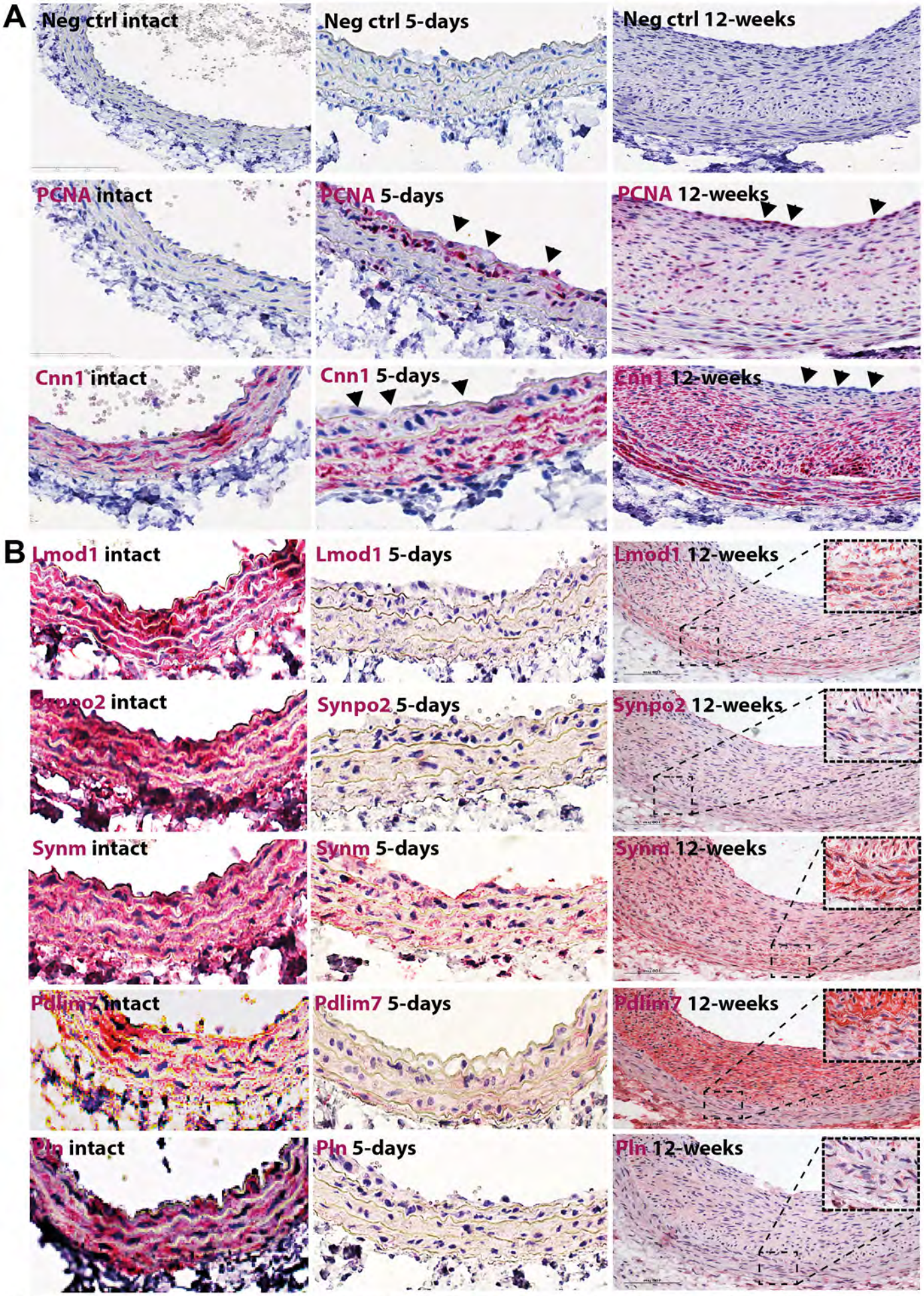

Figure 4. Lmod1, Synpo2, Synm, Pln and Pdlim7 were localised to SMCs in intact rat carotid artery and reduced in response to injury. By IHC the loss of Calponin (red) from highly proliferative PCNA+ SMCs layers in the injured rat artery closer to the lumen was observed (arrowheads), while staining was still present in deeper medial layers at day 5. At 12 weeks after injury Calponin was again abundant in the mature intima with less proliferative cells in the deeper layers but absent from luminal PCNA+ layers (arrowheads, A). The signal for identified SMCs markers (red) was completely absent at day 5 with gradual reappearance from the medial SMCs in tissues with pronounced intimal hyperplasia at 12 weeks after injury (B). Images were taken with 20x objective, insets show higher magnification (100x) of the media.

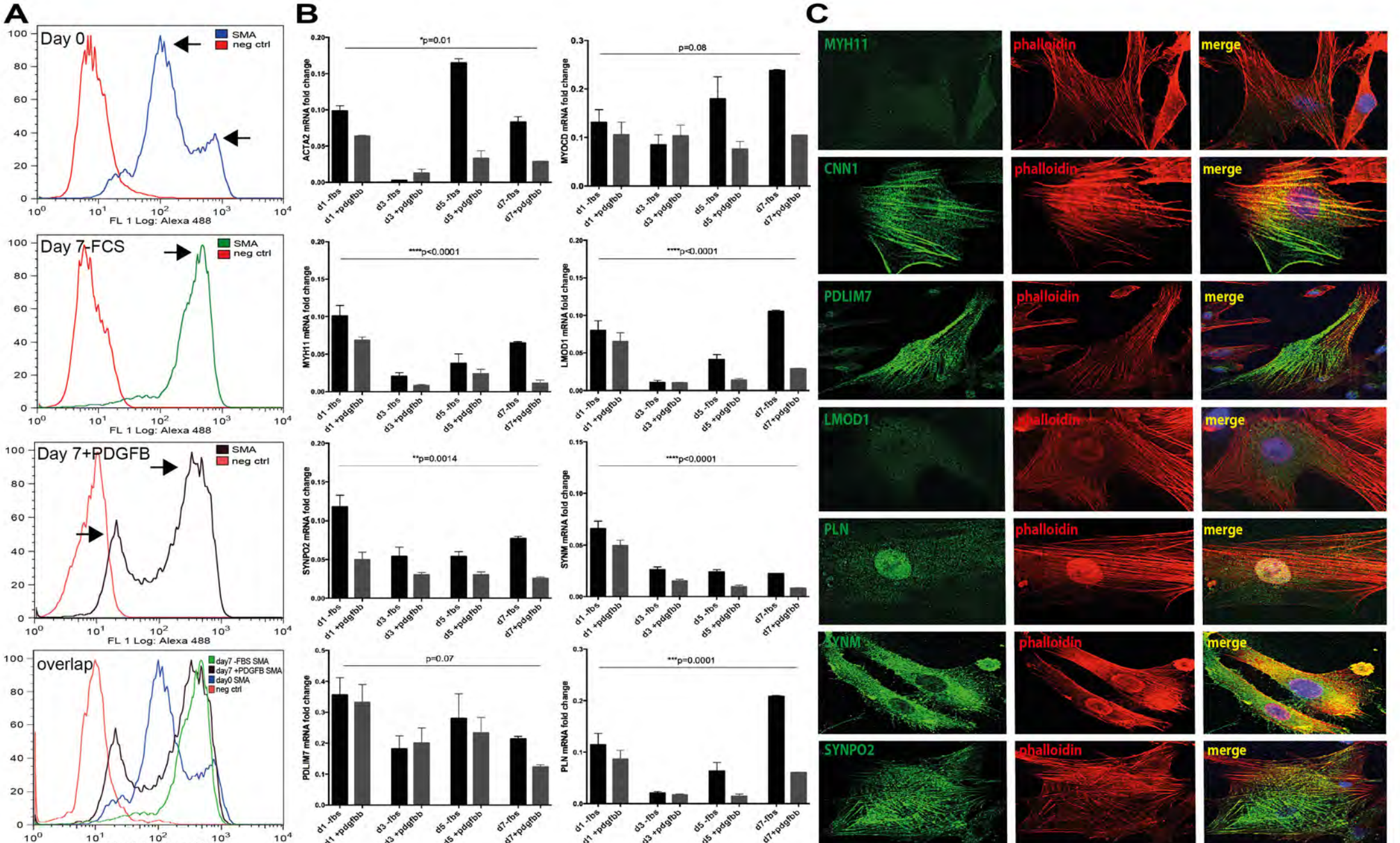

Figure 5. LMOD1, SYNPO2, SYNM, PLN and PDLIM7 were expressed by differentiated SMCs in vitro and localised to actin cytoskeleton. By flow cytometry 90% of the primary rat aortic cells were SMA+ on day 0 (after overnight collagenase treatment, top panel, A) as well as 7 days upon isolation when cultured in serum-free medium (second panel from the top, A). A subpopulation of cells with lower SMA+ signal was identified in culture at day 0, as well as 7 days upon isolation when stimulated with PDGFB (arrows, top and third panel, A). Bottom panel in A shows overlap of the upper 3 panels, indicating the change in SMA signal during 7 days of culture. By qPCR analysis rSMCs showed downregulation of conventional and identified SMCs markers at day 3 upon isolation and a trend towards upregulation after 5 days in culture. Graphs showing mean fold change ± SEM, ANOVA p-values, results representative of 3 independent primary cell isolations (B). In low-passage primary human carotid SMCs Pdlim7, Synm and Synpo2 colocalised with the actin cytoskeleton (as shown by phalloidin staining in red), Pln showed nuclear localisation and the signal for Lmod1 was beyond detection. For comparison, Calponin was localised to actin cytoskeleton (C). Images were taken with 100x objective.

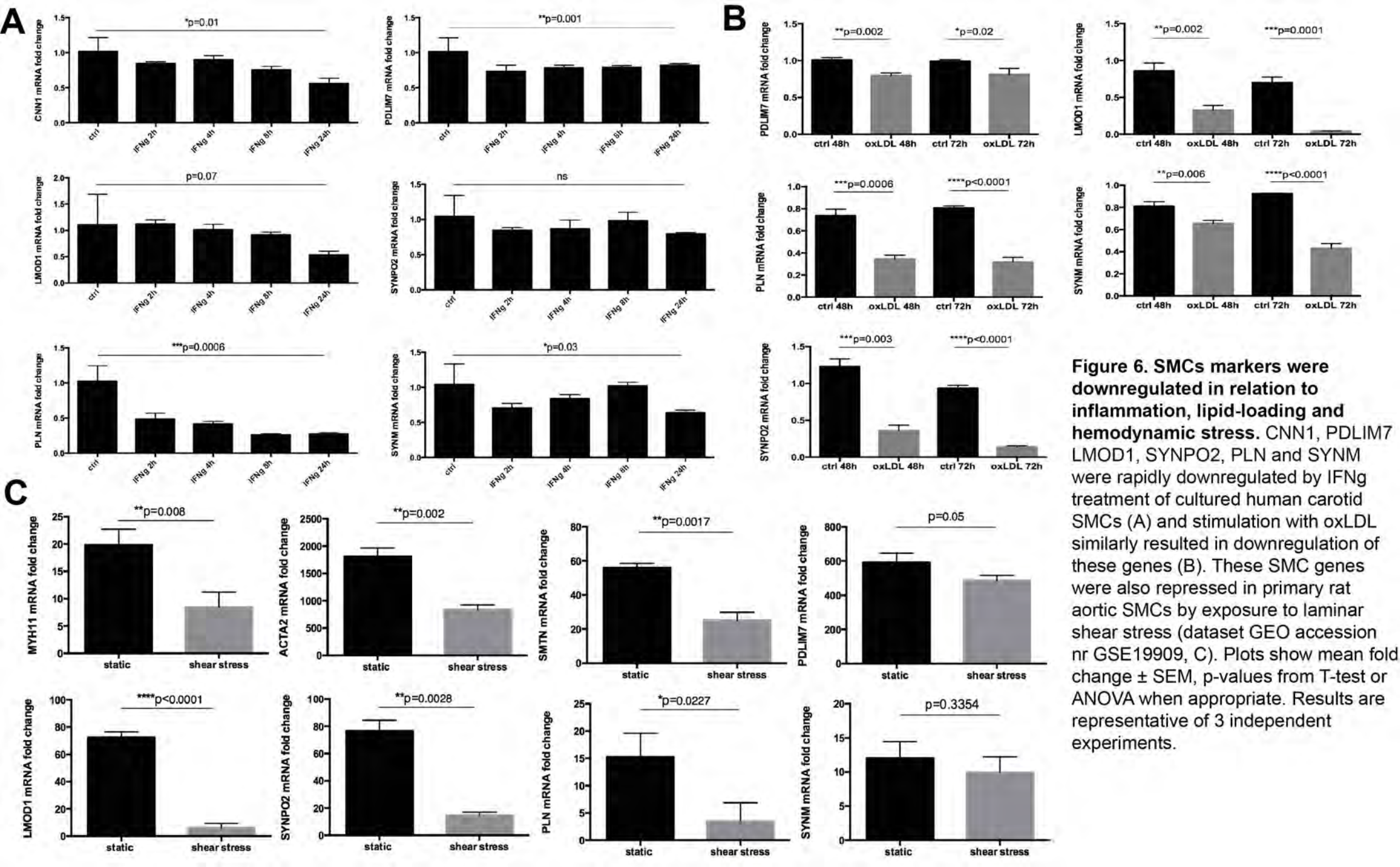

Figure 6. SMCs markers were downregulated in relation to inflammation, lipid-loading and hemodynamic stress. CNN1, PDLIM7 LMOD1, SYNPO2, PLN and SYNM were rapidly downregulated by IFNg treatment of cultured human carotid SMCs (A) and stimulation with oxLDL similarly resulted in downregulation of these genes (B). These SMC genes were also repressed in primary rat aortic SMCs by exposure to laminar shear stress (dataset GEO accession nr GSE19909, C). Plots show mean fold change ± SEM, p-values from T-test or ANOVA when appropriate. Results are representative of 3 independent experiments.

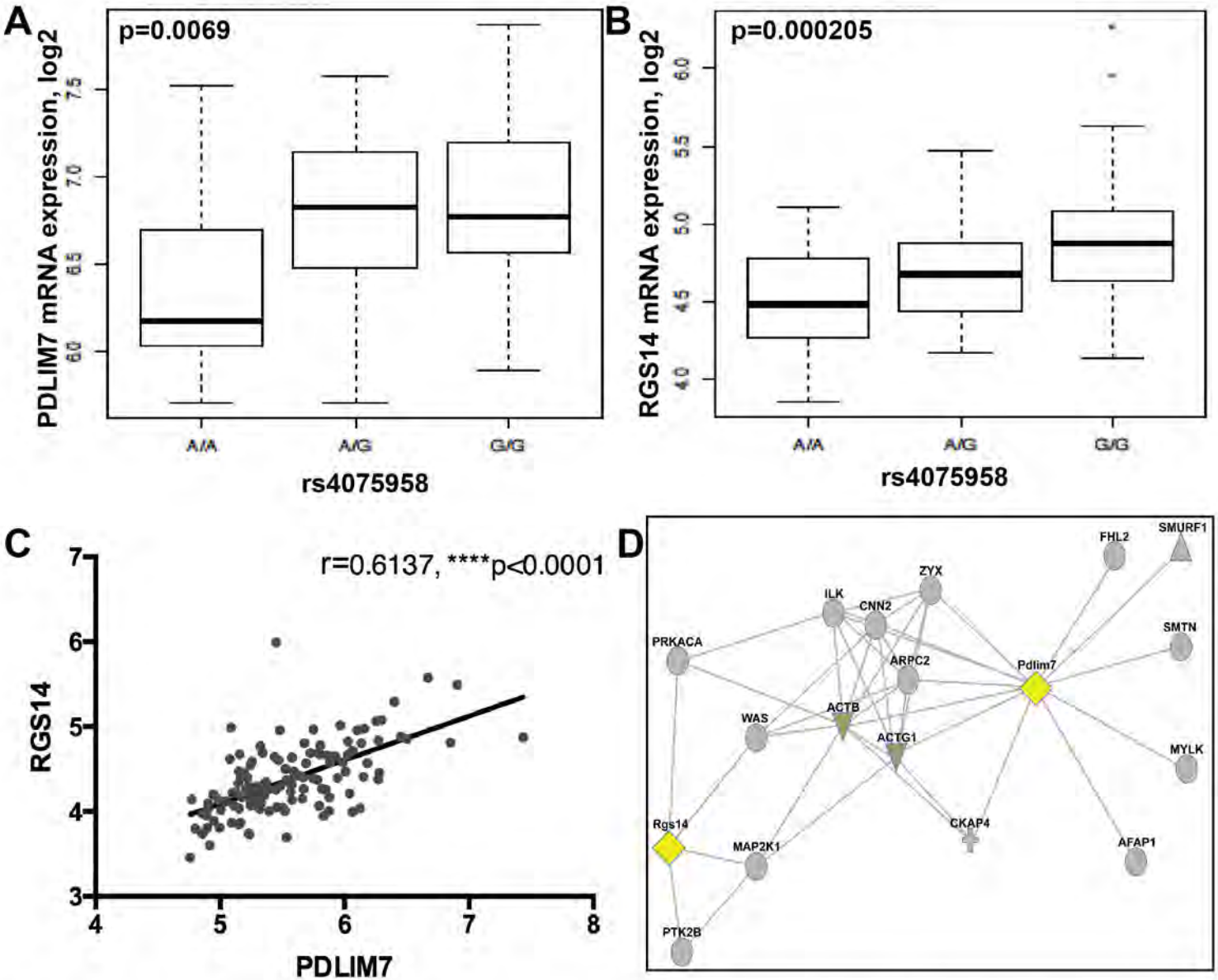

Figure 7. Polymorphism in the PDLIM7 genomic region associated with carotid intima-media thickness affects its expression in plaque tissue. By eQTL analysis variant rs4075958 was associated with the mRNA expression of both PDLIM7 and RGS14 in plaque tissue (A, B) and the expression levels of these two genes were strongly correlated (C). Functional network coupling based on protein-protein interactions links Pdlim7 and Rgs14 via actin cytoskeleton proteins (D). Plots in A and B show median with minimum and maximum.

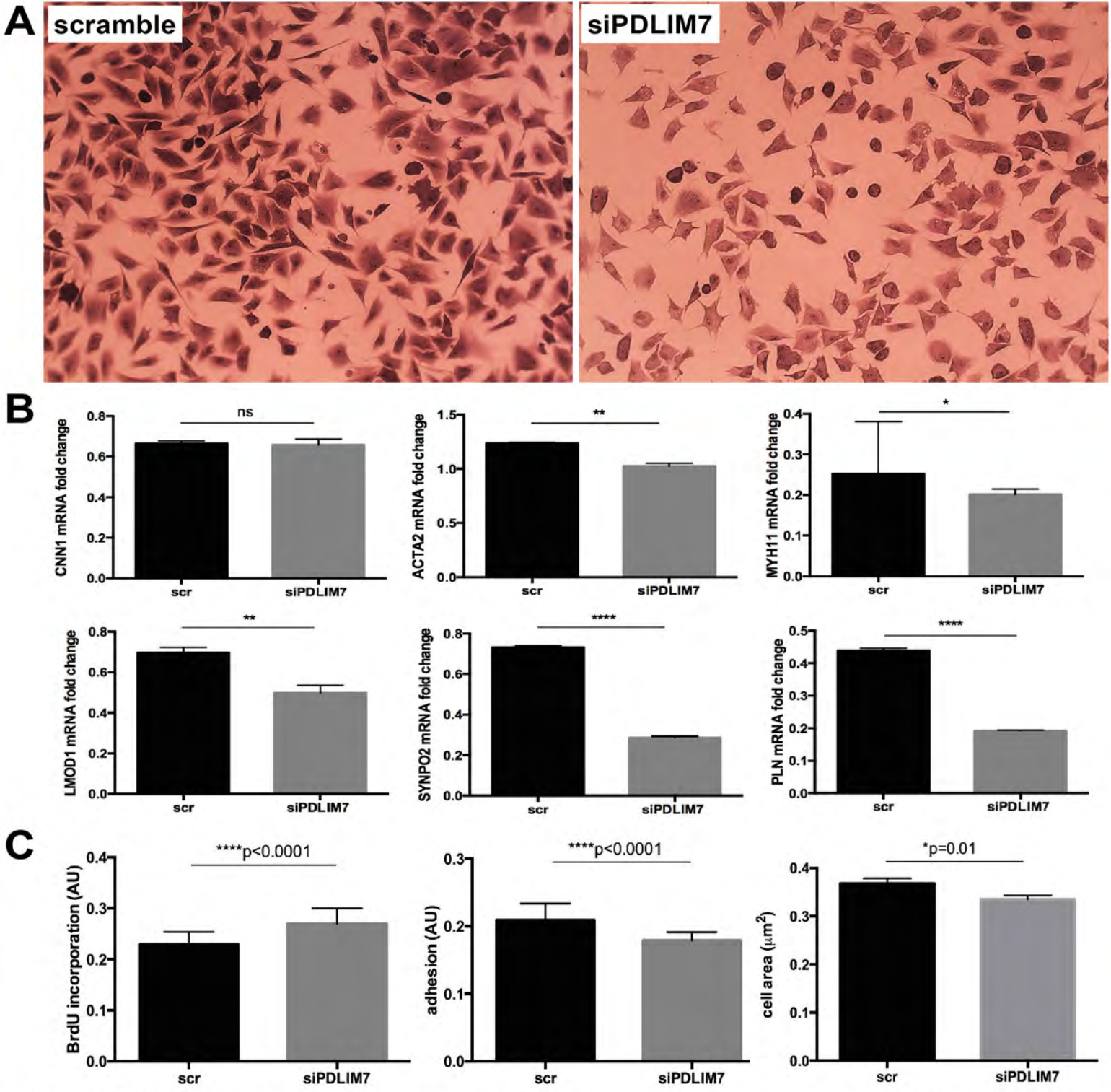

Figure 8. Silencing of PDLIM7 leads to downregulation of other SMC markers and increased SMC proliferation. PDLIM7 expression was silenced in human SMCs *in vitro* using siRNA (Crystal Violet staining, A), which resulted in downregulation of several other SMC markers (B), increased cell proliferation (as evaluated by BrdU incorporation) and impaired cell spreading/adhesion ability (C). Plots show mean ± SEM.

SUPPLEMENTAL MATERIAL

Phenotypic modulation of smooth muscle cells in atherosclerosis is associated with downregulation of *LMOD1, SYNPO2, PDLIM7, PLN* and *SYNM*

- Markers of smooth muscle cells -

Perisic L, Rykaczewska U, Razuvaev A, Sabater-Lleal M, Lengquist M, Miller CL, Ericsson I, Röhl S, Kronqvist M, Aldi S, Magné J, Vesterlund M, Li Y, Yin H, Gonzalez Diez M, Roy J, Baldassarre D, Veglia F, Humphries SE, de Faire U, Tremoli E, on behalf of the IMPROVE study group, Odeberg J, Vukojević V, Lehtiö J, Maegdefessel L, Ehrenborg E, Paulsson-Berne G, Hansson GK, Lindeman JHN, Eriksson P, Quertermous T, Hamsten A, Hedin U

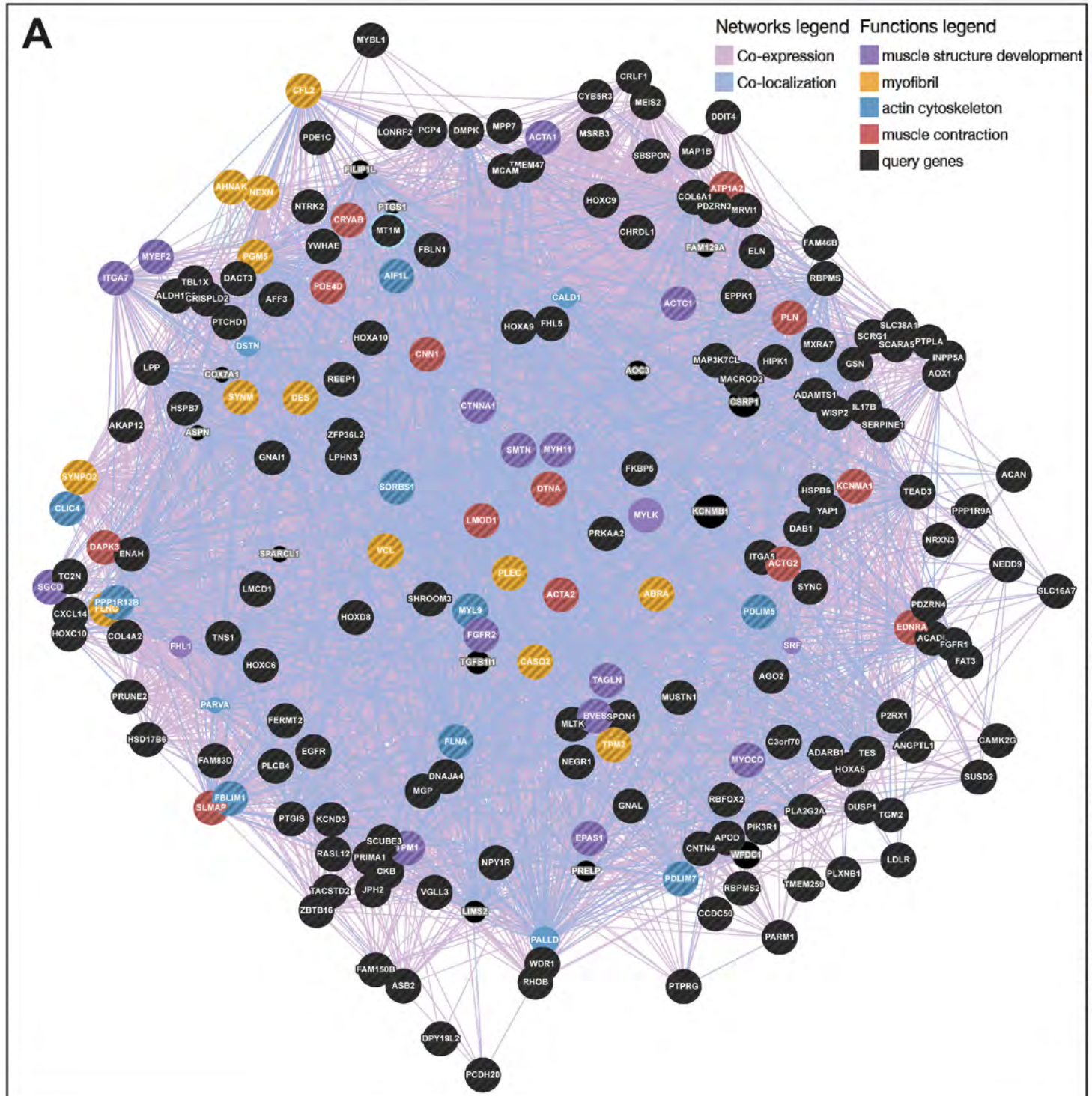

Supplementary Fig I. Network analyses of downregulated genes from microarrays comparing plaques vs. normal arteries. Network showing the 200 most downregulated genes, links connect those that were co-expressed and co-localised in tissues based on publicly available expression databases. Genes in functional category 'muscle contraction' are highlighted red, those in category 'myofibril cytoskeleton' are yellow, 'actin cytoskeleton' is blue and 'muscle development' is purple. Other queried genes, not assigned to the previous categories, are in black (A). Functional coupling network based on protein-protein interactions constructed from selected candidate SMCs markers, shows that Pdlim7 and Synm link to actomyosin cytoskeleton via other typical SMCs markers, such as Myh11, Smtn, Acta2 and Cnn1 (B).

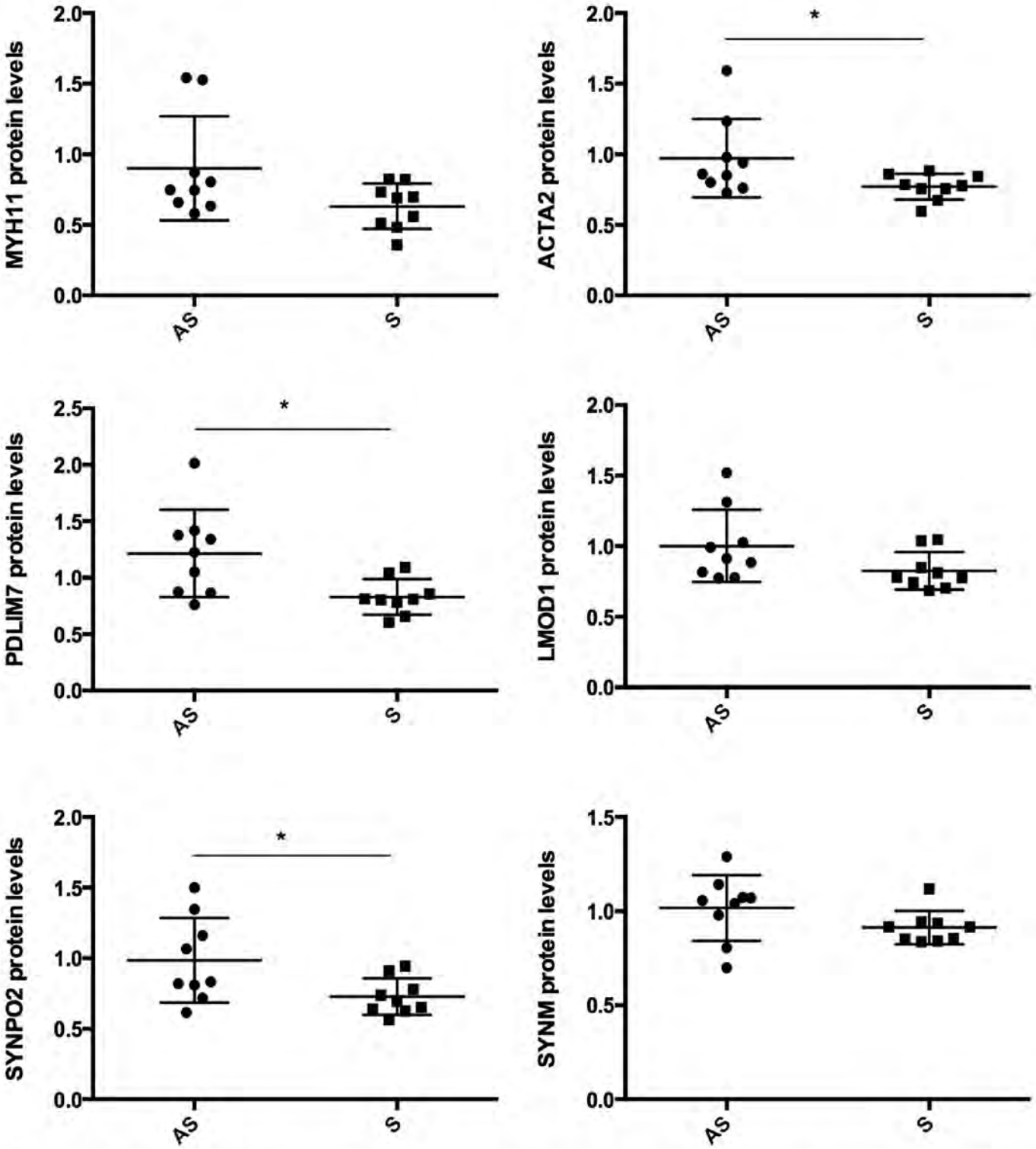

Supplementary Fig II. Proteomic analysis of human carotid plaques confirmed downregulation of typical and novel SMCs markers. Mass spectrometry analysis of plaques validated the findings from transcriptomic arrays and showed that MYH11, ACTA2, PDLIM7, SYNPO2, LMOD1 and SYNM proteins are less abundant in plaques from symptomatic vs. asymptomatic patients. N=10 patients analysed in each group.

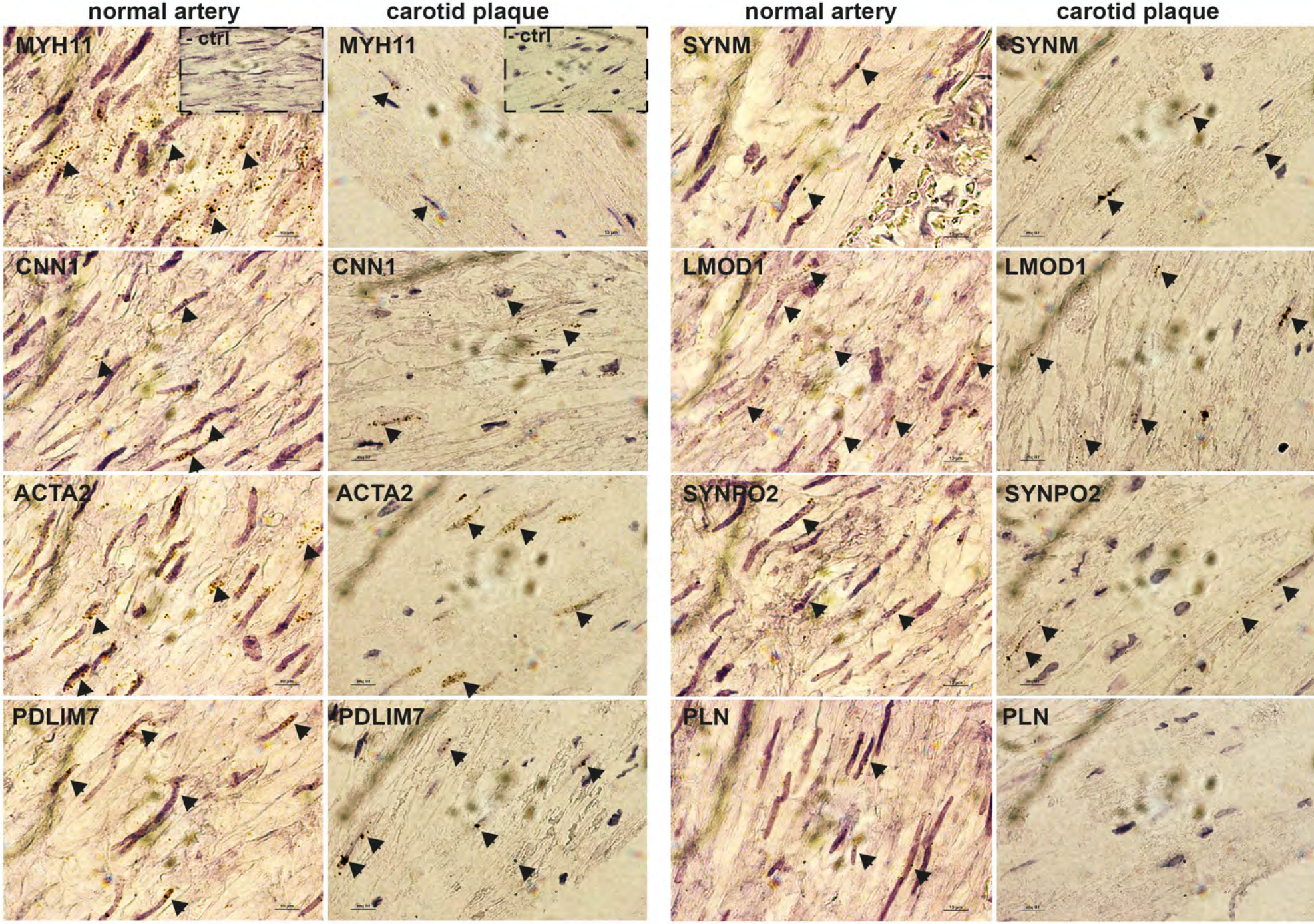

Supplementary Fig III. LMOD1, SYNPO2, PDLIM7 and SYNM transcript RNA was detectable in plaques fibrous cap. By in situ hybridization transcripts for typical (MYH11, ACTA2, CNN1) and identified candidate SMCs markers were found in normal artery media and were still detectable (except PLN) in stellate-shaped cells with elongated nuclei in the plaque fibrous cap. Arrowheads point to the RNA probe hybridization signal. Images were taken with 40x objective.

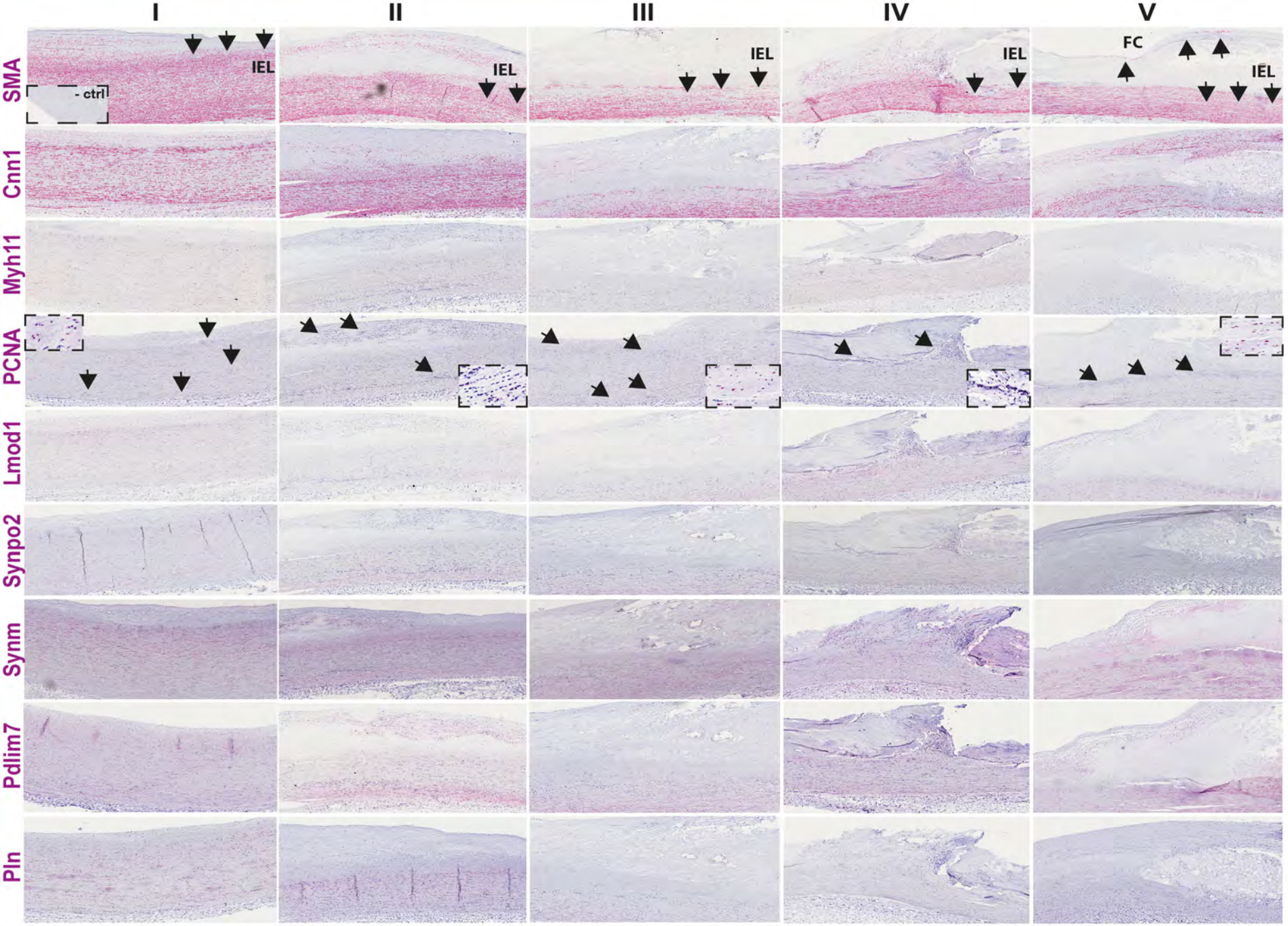

Supplementary Fig IV. Expression of SMCs markers during atheroprogression. By immunohistochemistry, SMA and Calponin (red) were continuosly expressed in lesions from all stages of atherosclerotic disease (modified American Heart Association grading I-V), while Myh11 was not detectable. Cells immunopositive for PCNA were found both in media and intima in all tissues (red signal, arrows, enlarged insets). Signal for Lmod1 and Synpo2 was rapidly lost and undetectable even in early lesions, while Pln (red) was present until stage III. Pdlim7 and Synm (red signal) were present in subintimal SMA+ cells and scarcely in the fibrous cap (FC). Arrows in SMA panels point to internal elastic lamina (IEL). Images were taken with the 5x objective.

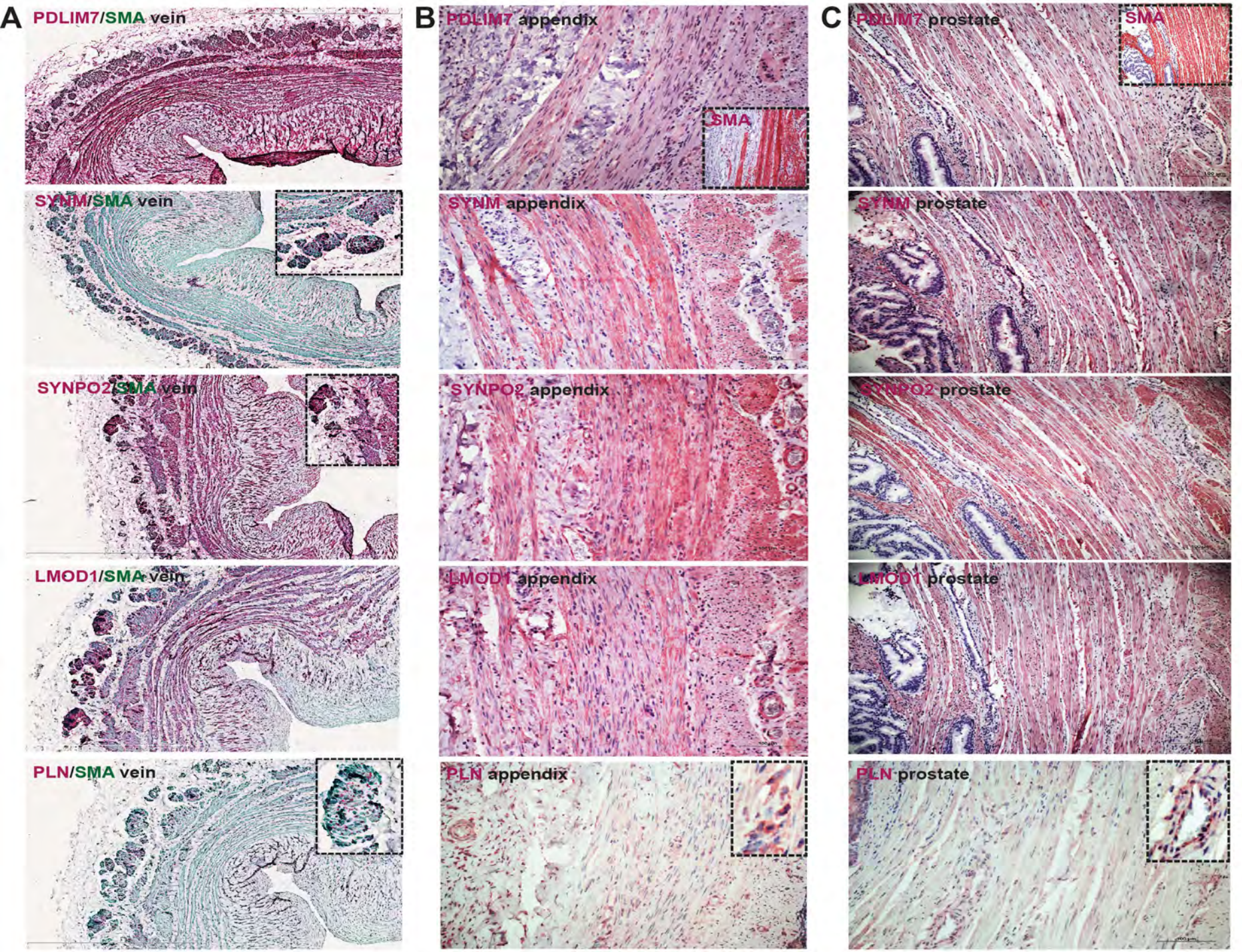

Supplementary Fig V. Localisation of candidate SMCs markers in SMC-enriched tissues. Immunohistochemistry shows localisation of Lmod1, Synpo2, Synm, Pln and Pdlim7 (red) in SMA+ cells in normal vein media (A), appendix (B) and prostate (C). Images were taken with 20x objective. By higher magnification (40x inset) it is possible to observe the nuclear localisation for Pln.

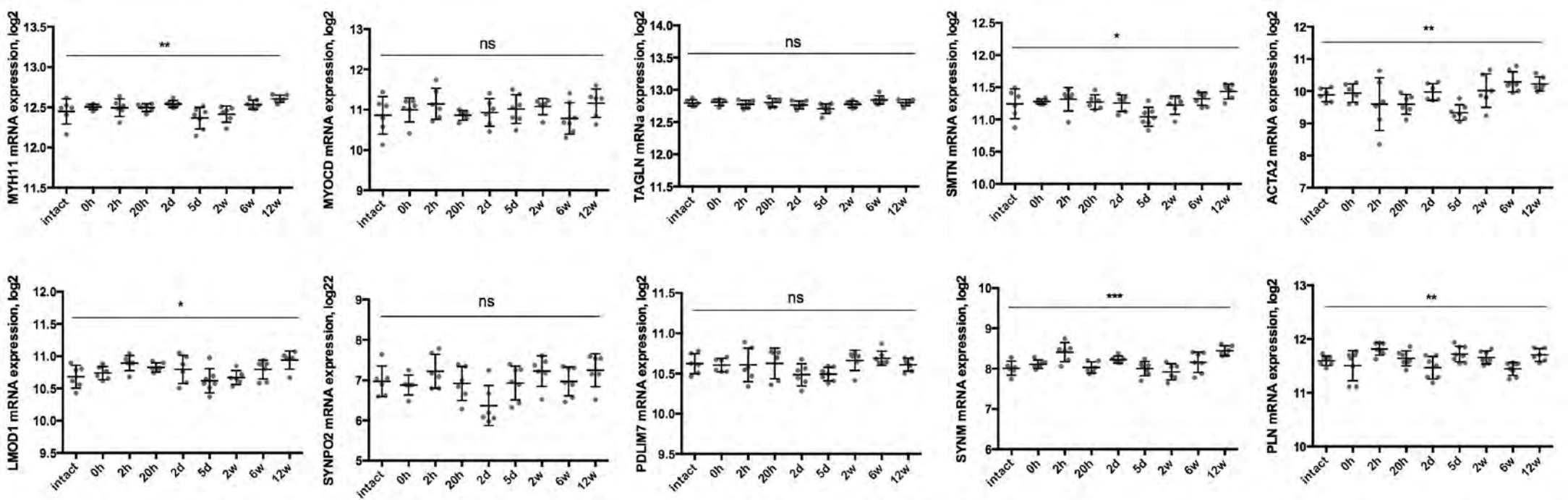

Supplementary Fig VI. Expression of SMCs markers in uninjured rat carotid arteries. The identified SMC genes as well as typical markers of SMCs show minor gene expression variations in uninjured contralateral arteries after rat carotid balloon injury.

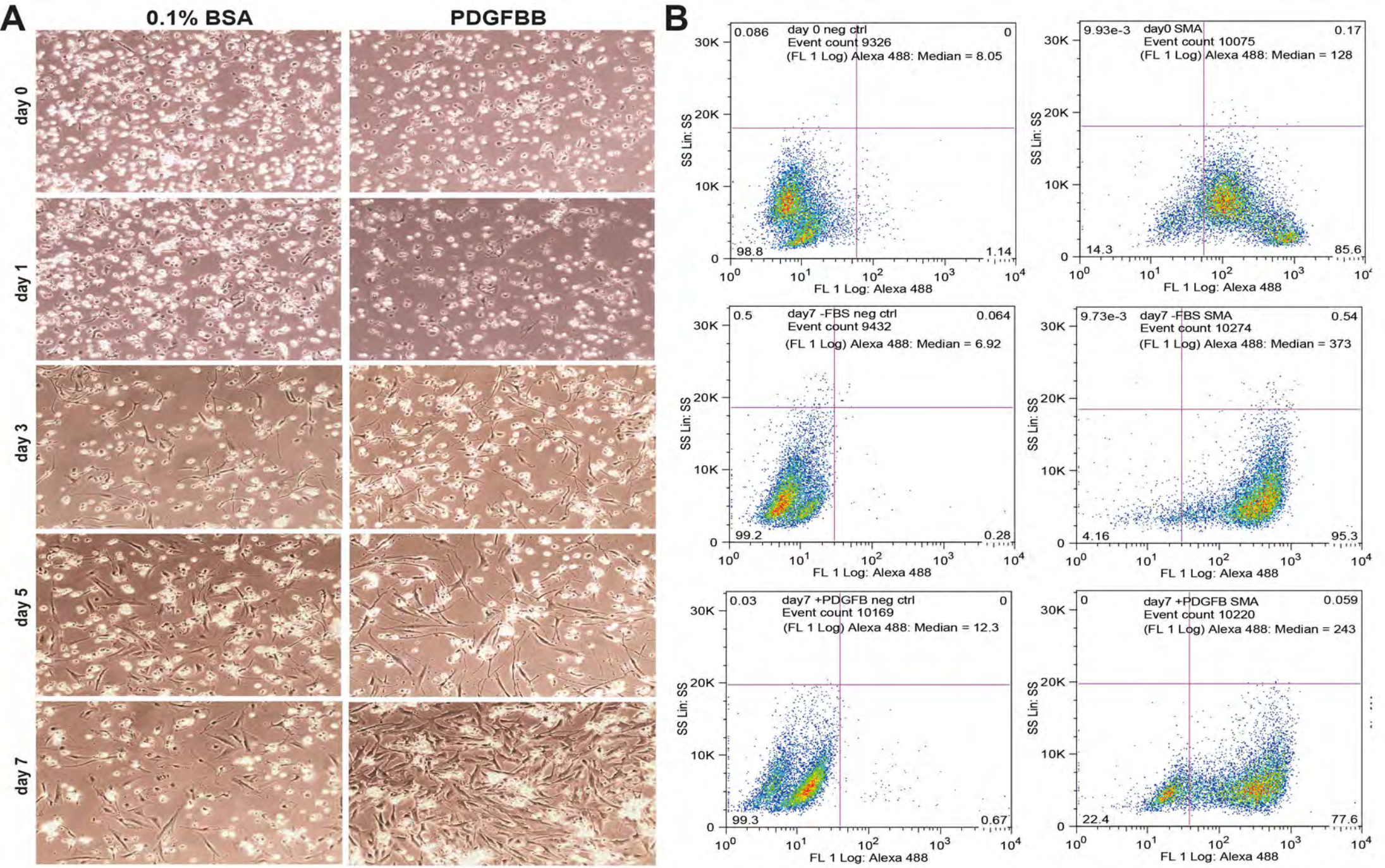

Supplementary Fig VII. Characterisation of isolated primary cells from rat aorta. Brightfield photomicrographs of rat SMCs cultured over 7 days in serum-free medium or stimulated with PDGFBB. Cells were attached on day 1 after isolation, filopodia and cytoplasmic extensions were notable on day 3 while well-spread cells were dominant on day 5 and 7 (A). Flow cytometry analysis shows that 85.6% of isolated cells were SMA+ positive directly after isolation from tissue and 95.3% at day 7 after isolation. After 7 days of stimulation with PDGFB the number of SMA+ cells was decreased to 77.6% (B).

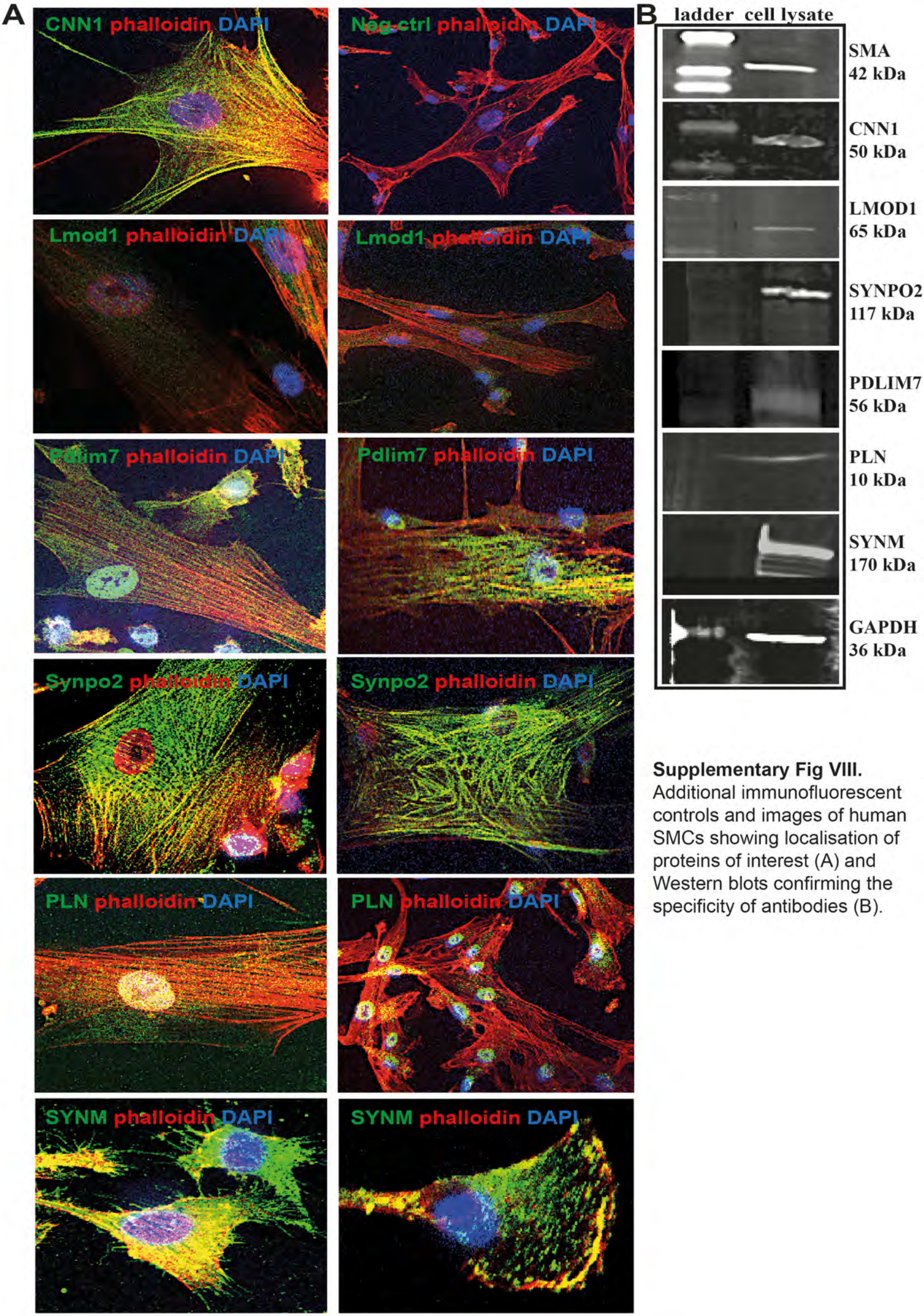

Supplementary Fig VIII.
Additional immunofluorescent controls and images of human SMCs showing localisation of proteins of interest (A) and Western blots confirming the specificity of antibodies (B).

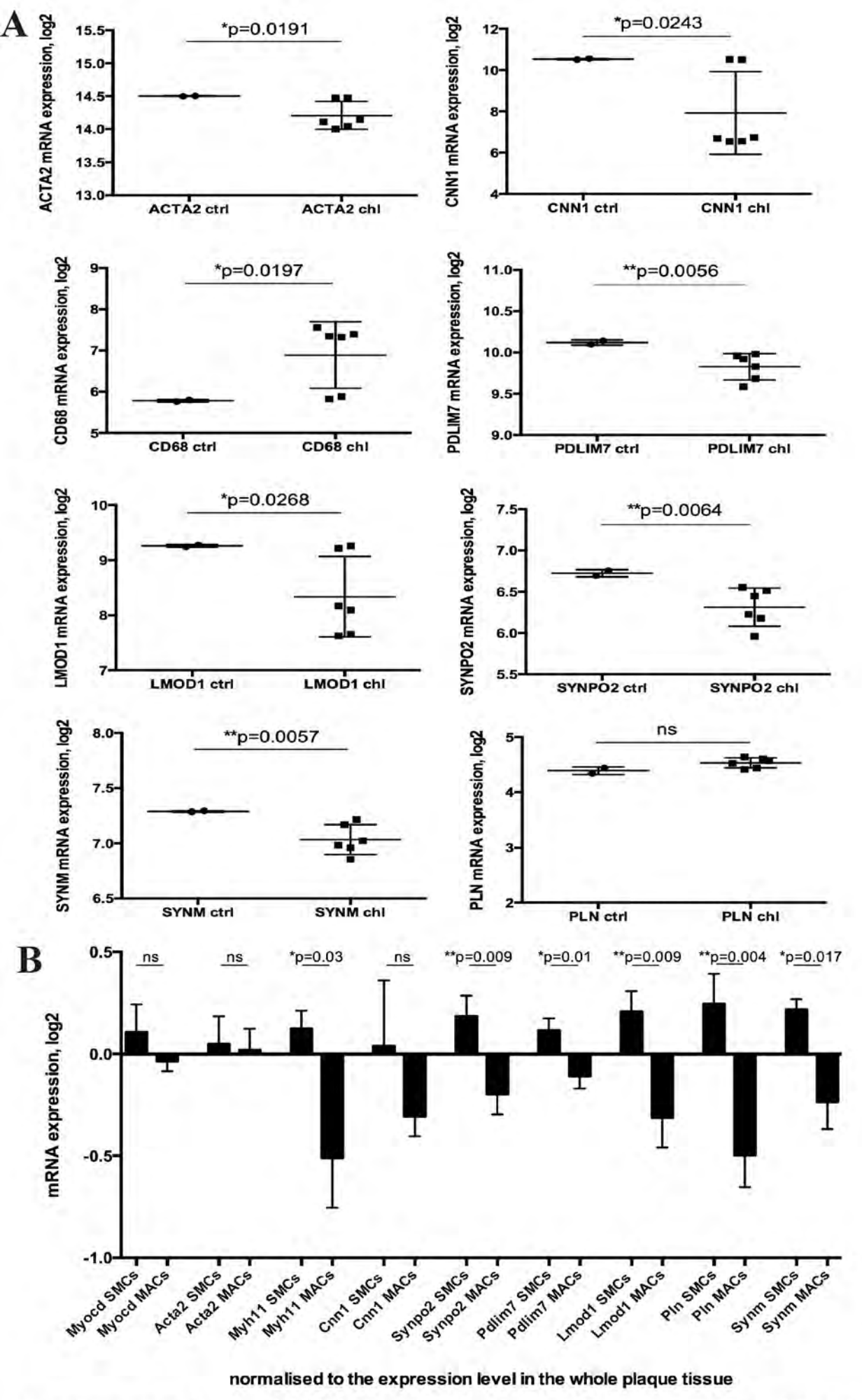

Supplementary figure IX. Validation of experimental data in available public microarray datasets. Processing of data from the public dataset GSE47744 for SMCs genes of interest, confirmed downregulation of novel and standard SMC markers and upregulation of macrophage marker CD68 upon treatment of primary mouse SMCs with cholesterol (A). In (B) expression of SMCs markers was analysed in the public dataset (GSE23303), comparing laser capture microdissected regions of human carotid plaques enriched with SMCs or macrophages (MACs).

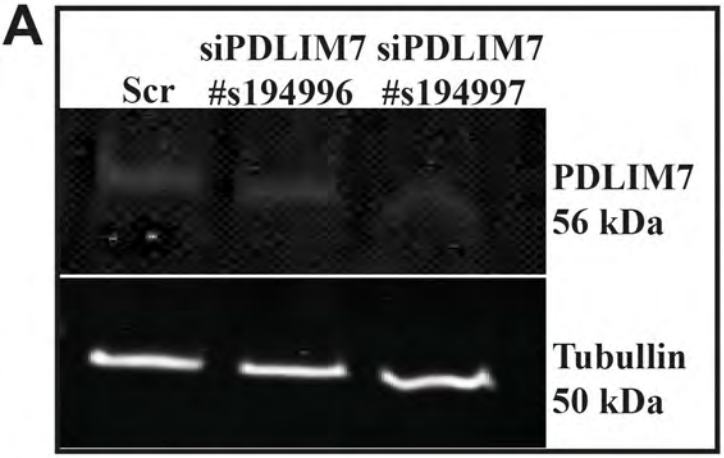

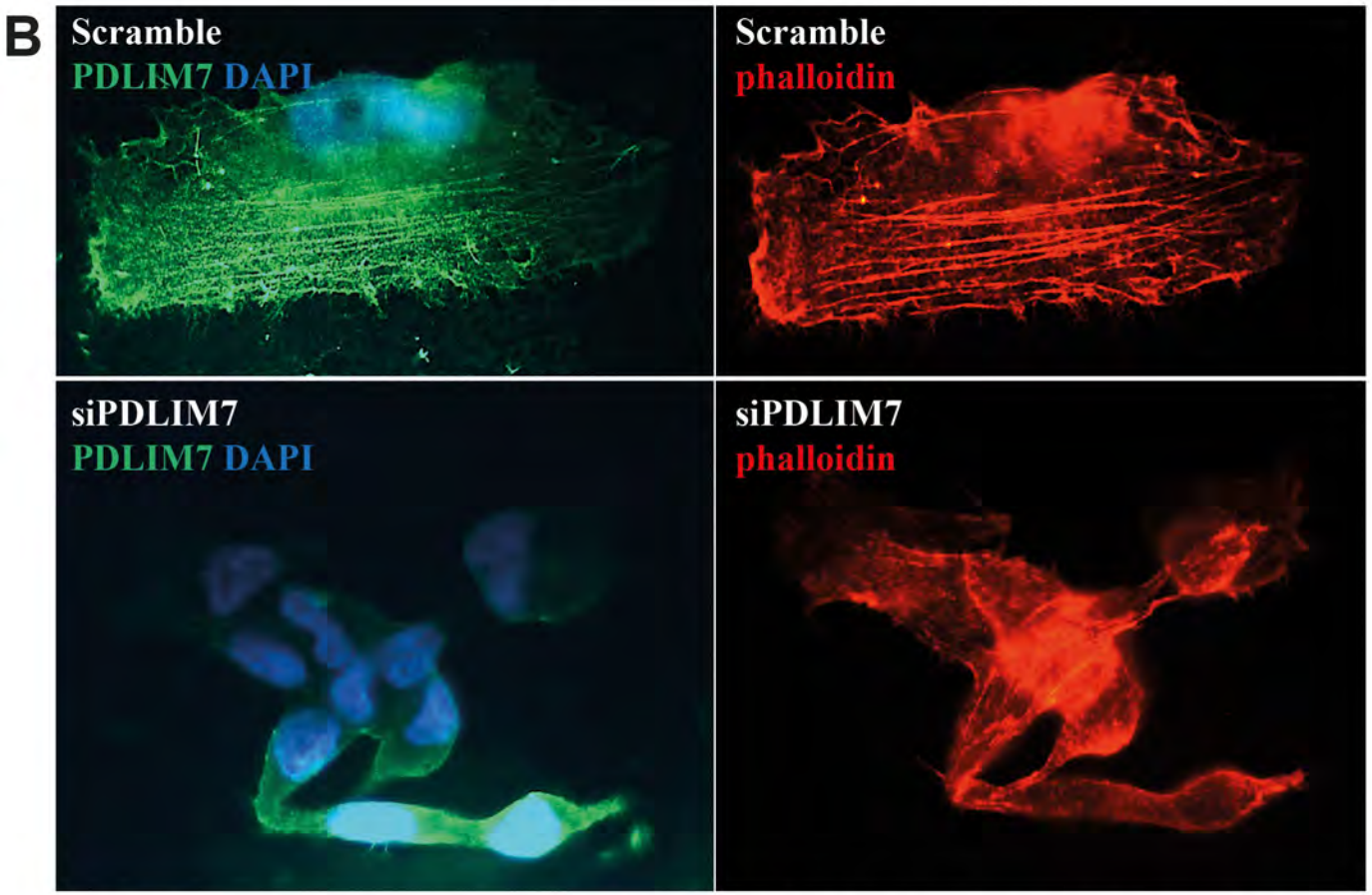

Supplementary Fig X. Controls for PDLIM7 silencing in vitro. Two siRNAs were tested initialy for silencing of PDLIM7 mRNA expression, of which #s194997 showed more efficient downregulation on the protein level by Western blot compared to missense scramble control (A). This siRNA was used in futher experiments. Immunofluorescent images showing decreased PDLIM7 protein signal in human SMCs upon silencing, as well as changes in cell morphology and actin cytoskeleton structure (by overlap with phalloidin, B).

Supplementary Table I: Pathway analysis of downregulated genes in BiKE plaque microarrays

plaques vs. normal arteries (n=127+10)

Gene Ontology Function	FDR
muscle system process	1.81E-21
muscle contraction	6.99E-21
contractile fiber	1.67E-10
actin cytoskeleton	2.54E-10
myofibril	3.79E-10
adherens junction	2.93E-09
cell-substrate junction	1.05E-07
extracellular matrix	1.80E-07
focal adhesion	5.49E-07
regulation of muscle system process	6.14E-07
smooth muscle contraction	1.37E-06
muscle structure development	1.66E-06
costamere	3.16E-06
regulation of muscle contraction	7.73E-06
sarcomere	8.31E-06
structural constituent of muscle	2.97E-05
actin binding	4.58E-05
actin-mediated cell contraction	8.33E-05
circulatory system process	1.43E-04
actomyosin	1.55E-04
muscle organ development	1.64E-04
actin filament organization	1.93E-04
actin filament-based movement	4.22E-04
cell junction assembly	6.14E-04
stress fiber	7.99E-04
angiogenesis	9.25E-04
actin filament bundle	9.25E-04
muscle cell differentiation	1.56E-03
heart contraction	1.87E-03
blood vessel development	2.56E-03
blood circulation	3.59E-03
regulation of heart contraction	6.61E-03
extracellular matrix organization	6.98E-03
extracellular structure organization	7.09E-03
cell-substrate adhesion	8.40E-03
regulation of smooth muscle contraction	1.19E-02
striated muscle cell differentiation	1.48E-02
calcium ion transport	1.92E-02
actin filament	3.50E-02
actin-myosin filament sliding	3.50E-02

symptomatic vs. asymptomatic plaques (n=87+40)

Gene Ontology Function	FDR
muscle contraction	1.20E-06
extracellular matrix	2.44E-06
muscle system process	2.44E-06
muscle structure development	7.58E-04
proteinaceous extracellular matrix	2.18E-03
actin cytoskeleton	2.56E-03
structural constituent of muscle	1.67E-02
kidney vasculature development	1.96E-02
contractile fiber part	3.21E-02
muscle organ development	3.74E-02

Supplementary Table II: Differential expression of candidate SMCs markers in microarrays from human plaque tissues

BiKE plaque n=127 vs. normal artery n=10

Gene symbol	Gene name	fold change (downregulation)	p-value
SYNPO2	synaptopodin 2	0.052286779	<0.0001
SYNM	synemin	0.190309568	<0.0001
LMOD1	leiomodin 1	0.197674681	<0.0001
PDLIM7	PDZ and LIM domain containing 7	0.165801619	<0.0001
PLN	phospholamban	0.311484008	<0.0001

BiKE symptomatic n=87 vs. asymptomatic n=40

Gene symbol	Gene name	fold change (downregulation)	p-value
SYNPO2	synaptopodin 2	0.773175056	<0.0001
SYNM	synemin	0.80189319	0.000295
LMOD1	leiomodin 1	0.698721288	<0.0001
PDLIM7	PDZ and LIM domain containing 7	0.663535703	<0.0001
PLN	phospholamban	0.660982509	<0.0001

BiKE plaque n=50 vs. normal arteries n=5

Gene symbol	Gene name	fold change (downregulation)	p-value
SYNPO2	synaptopodin 2	0.933482318	0.0272086
SYNM	synemin	0.208883436	< 0.0001
LMOD1	leiomodin 1	0.395286338	0.000341588
PDLIM7	PDZ and LIM domain containing 7	0.79699689	0.00220495
PLN	phospholamban	0.432496391	0.00469566

Saksi et al. dataset symptomatic n=12 vs. asymptomatic n=9

Gene symbol	Gene name	fold change (downregulation)	p-value
SYNPO2	synaptopodin 2	not found in dataset	not found in dataset
SYNM	synemin	0.348534	0.034546
LMOD1	leiomodin 1	0.574446	0.0371126
PDLIM7	PDZ and LIM domain containing 7	0.331987	0.045662
PLN	phospholamban	0.316845	0.040389

GSE43292 dataset: carotid plaques n=32 vs. matched adjacent tissue n=32

Gene symbol	Gene name	fold change (downregulation)	p-value
SYNPO2	synaptopodin 2	0.534923689	0.0000761
SYNM	synemin	0.599601518	0.0000835
LMOD1	leiomodin 1	0.531384871	0.0000753
PDLIM7	PDZ and LIM domain containing 7	0.735601461	0.0016719
PLN	phospholamban	0.479262555	0.0000984

GSE23303 dataset: carotid plaque SMCs-rich regions n=3 vs. macrophage-rich regions n=3, isolated by laser capture microscopy

Gene symbol	Gene name	fold change (upregulation)	p-value
SYNPO2	synaptopodin 2	10.1246213	0.006597
SYNM	synemin	15.8675976	0.0017057
LMOD1	leiomodin 1	13.8065034	0.0026328
PDLIM7	PDZ and LIM domain containing 7	11.6151913	0.0044314
PLN	phospholamban	12.1981667	0.0038319

ACTA2	smooth muscle actin	0.0535719	0.9481788
MYH11	myosin heavy chain 11	7.7847823	0.0135346
MYOCD	myocardin	33.1384268	0.0001432
CNN1	calponin	14.2453287	0.0023906

Suppementary Table III: Transcriptomic and proteomic expression correlations for candidate and typical SMCs markers

BiKE human carotid plaques microarrays

	LMOD1		SYNPO2		SYNM		PDLIM7		PLN	
SMC markers	Pearson r	p-value	Pearson r	p-value	Pearson r	p-value	Pearson r	p-value	Pearson r	p-value
ACTA2	0.7238	< 0.0001	0.6983	< 0.0001	0.7643	< 0.0001	0.3916	< 0.0001	0.7841	< 0.0001
SMTN	0.7069	< 0.0001	0.5411	< 0.0001	0.6398	< 0.0001	0.5964	< 0.0001	0.651	< 0.0001
CNN1	0.7583	< 0.0001	0.6011	< 0.0001	0.6797	< 0.0001	0.6227	< 0.0001	0.6574	< 0.0001
MYH11	0.7636	< 0.0001	0.7519	< 0.0001	0.7124	< 0.0001	0.5862	< 0.0001	0.8231	< 0.0001
MYOCD	0.638	< 0.0001	0.6493	< 0.0001	0.6402	< 0.0001	0.483	< 0.0001	0.7223	< 0.0001

BiKE human carotid plaques mass spectrometry, correlation matrix

Pearson r	SMA	CNN1	MYH11	PDLIM7	LMOD1	SYNPO2	SYNM
SMA		0.9682	0.9373	0.8936	0.9287	0.8631	0.4491
CNN1	0.9682		0.9721163	0.872647	0.9405631	0.877894	0.4386379
MYH11	0.9373	0.972116		0.822397	0.9350476	0.867897	0.448287
PDLIM7	0.8936	0.872647	0.8223968		0.8561276	0.753346	0.522256
LMOD1	0.9287	0.940563	0.9350476	0.856128		0.922575	0.4888232
SYNPO2	0.8631	0.877894	0.8678971	0.753346	0.9225745		0.418021
SYNM	0.4491	0.438638	0.448287	0.522256	0.4888232	0.418021	
p-value	SMA	CNN1	MYH11	PDLIM7	LMOD1	SYNPO2	SYNM
SMA		< 0.0001	< 0.0001	< 0.0001	< 0.0001	< 0.0001	0.0615
CNN1	< 0.0001		1.68E-11	2.32E-06	6.49E-09	1.68E-06	0.068615
MYH11	< 0.0001	1.68E-11		2.8E-05	1.30E-08	3.06E-06	0.0620676
PDLIM7	< 0.0001	2.32E-06	2.804E-05		5.819E-06	0.000307	0.0261917
LMOD1	< 0.0001	6.49E-09	1.30E-08	5.82E-06		5.08E-08	0.0395374
SYNPO2	< 0.0001	1.68E-06	3.056E-06	0.000307	5.08E-08		0.0842999
SYNM	0.0615	0.068615	0.0620676	0.026192	0.0395374	0.0843	

Rat carotid artery injury microarrays

	LMOD1		SYNPO2		SYNM		PDLIM7		PLN	
SMC markers	Pearson r	p-value	Pearson r	p-value	Pearson r	p-value	Pearson r	p-value	Pearson r	p-value
ACTA2	0.6576	< 0.0001	0.6612	< 0.0001	0.6566	< 0.0001	0.713	< 0.0001	0.6666	< 0.0001
SMTN	0.9676	< 0.0001	0.8661	< 0.0001	0.7919	< 0.0001	0.6891	< 0.0001	0.8093	< 0.0001
CNN1	0.8999	< 0.0001	0.8239	< 0.0001	0.7569	< 0.0001	0.7544	< 0.0001	0.8354	< 0.0001
MYH11	0.9498	< 0.0001	0.9363	< 0.0001	0.8831	< 0.0001	0.7108	< 0.0001	0.792	< 0.0001
MYOCD	0.7214	< 0.0001	0.7761	< 0.0001	0.7551	< 0.0001	0.8025	< 0.0001	0.7124	< 0.0001

	LMOD1		SYNPO2		SYNM		PDLIM7		PLN	
Cytokines	Pearson r	p-value	Pearson r	p-value	Pearson r	p-value	Pearson r	p-value	Pearson r	p-value
PDGFB	-0.3217	0.0156	-0.5135	< 0.0001	-0.5547	< 0.0001	-0.5472	< 0.0001	-0.2644	0.049
IGF1	-0.365	0.0057	-0.5846	< 0.0001	-0.6443	< 0.0001	-0.7011	< 0.0001	-0.2387	0.05
TGFB1	-0.56	< 0.0001	-0.4824	0.0002	-0.4911	< 0.0001	-0.4546	0.0004	-0.703	< 0.0001

Suppementary Table IV: Transcriptomic analysis of SMCs markers in mouse model of atherosclerotic plaque rupture

Ligation VS Normal

Gene Symbol	Fold Change	p-value	FDR
Pdlim7	-4.25	0.000001	0.000056
Synpo2	-114.39	9.85E-11	2.33E-07
Pln	-4.29	7.69E-07	0.000038
Lmod1	-45.05	2.32E-08	0.000003
Synm	-1.46	0.023435	0.106494

Rupture vs Stable

Gene Symbol	Fold Change	p-value	FDR
Pdlim7	-1.25	0.029730	0.494775
Synpo2	-1.61	0.060025	0.606094
Pln	-1.02	0.679074	0.986442
Lmod1	-1.99	0.017015	0.436322
Synm	-1.09	0.353552	0.922700

Supplementary Table V: RNAseq data comparing gene expression in human coronary artery SMCs cultured in serum vs. no serum

Gene symbol	Gene name	fold change	p-value
SYNPO2	synaptopodin 2	0.468746646	5.55E-17
LMOD1	leiomodin 1	0.419018145	1.22E-30
PDLIM7	PDZ and LIM domain containing 7	0.715969101	0.00416383
PLN	phospholamban	0.323119589	6.7E-09
SYNM	synemin	0.671463478	4.96E-05

Supplementary Table VI: ChIP seq data from primary human SMCs for H3K27ac active histone modification

Gene	chr	start	end	strand	Normalized Tag Count	region size	findPeaks Score	Total Tags	Control Tags (normalized to IP Exp)	Fold Change vs Control	p-value vs Control	Clonal Fold Change
LMOD1	chr1	2E+08	201915441	+	21	1000	37	38.5	7.4	5.19	1.71E-15	0.97
SYNPO2	chr4	1.2E+08	119772533	+	23.2	1515	41	54.2	9.5	5.71	2.45E-23	0.97
SYNPO2	chr4	1.2E+08	119813078	+	14.8	1000	39	34.7	8	4.33	7.45E-12	0.98
SYNPO2	chr4	1.2E+08	119827702	+	90.2	2456	89.5	211.1	43	4.91	5.45E-75	0.94
SYNPO2	chr4	1.2E+08	119833050	+	42.3	2039	42	99.1	22	4.51	3.04E-33	0.96
SYNPO2	chr4	1.2E+08	119842101	+	226.8	5320	43.5	531.2	71	7.48	1.17E-266	0.92
SYNPO2	chr4	1.2E+08	119869901	+	63.2	2574	44	148	24.5	6.04	4.23E-64	0.96
SYNPO2	chr4	1.2E+08	119878452	+	93.6	3652	62.5	219.1	42.5	5.16	1.72E-81	0.96
SYNPO2	chr4	1.2E+08	119906168	+	47.1	2008	82.5	110.2	23	4.79	5.02E-39	0.97
SYNPO2	chr4	1.2E+08	119912066	+	87.3	3118	35.5	204.5	47.5	4.3	2.56E-63	0.94
PDLIM7	chr5	1.8E+08	176924718	+	305.2	4529	89	714.8	143	5	4.19E-253	0.92
PLN	chr6	1.2E+08	118859467	+	20.5	1608	32	48	11	4.36	1.68E-16	0.97
PLN	chr6	1.2E+08	118869039	+	28.3	1775	45.5	66.2	10.5	6.31	1.50E-30	0.97
PLN	chr6	1.2E+08	118873479	+	30.6	1250	72	71.6	16	4.47	5.28E-24	0.96
PLN	chr6	1.2E+08	118881170	+	17.8	1000	36.5	41.8	8.5	4.92	9.72E-16	0.98
SYNM	ch15	1E+08	99710294	+	24.3	1000	63.5	56.9	13	4.38	9.88E-19	0.98

Supplementary Table VII: Putative transcription factors (TF) binding motifs enrichment analysis of candidate SMCs genes by MotifMap

Location	strand	FDR	Motif ID	TF Name	Gene	Distance from transcription start (bp)	Region
chr5:176932292..176932299	-	0	M00468	AP-2rep	PDLIM7	-7697	Upstream
chr5:176932115..176932121	+	0	M00704	TEF-1	PDLIM7	-7513	Upstream
chr5:176931912..176931919	-	0	M00468	AP-2rep	PDLIM7	-7317	Upstream
chr5:176930474..176930481	-	0	M00468	AP-2rep	PDLIM7	-5879	Upstream
chr5:176928139..176928159	-	0	M01259	CTCF	PDLIM7	-3557	Upstream
chr5:176928137..176928157	-	0	M01200	CTCF	PDLIM7	-3555	Upstream
chr5:176928137..176928156	-	0	MA0139	CTCF	PDLIM7	-3554	Upstream
chr5:176928137..176928156	-	0	LM2_CTCF	CTCF	PDLIM7	-3554	Upstream
chr5:176928041..176928047	-	0	M00704	TEF-1	PDLIM7	-3445	Upstream
chr5:176924073..176924079	-	0	M00704	TEF-1	PDLIM7	523	Downstream
chr5:176923860..176923873	+	0	M00517	AP-1	PDLIM7	742	Downstream
chr5:176923605..176923619	-	0	M01196	CTF1	PDLIM7	983	Downstream
chr5:176922810..176922831	+	0	M00512	PPARgamma:RXRalpha	PDLIM7	1792	Downstream
chr5:176922363..176922373	-	0	M00761	p53 decamer	PDLIM7	2229	Downstream
chr5:176921779..176921792	+	0	M00517	AP-1	PDLIM7	2823	Downstream
chr5:176920471..176920477	+	0	M00704	TEF-1	PDLIM7	4131	Downstream
chr5:176919482..176919489	-	0	M00468	AP-2rep	PDLIM7	5113	Downstream
chr5:176918675..176918694	+	0	MA0139	CTCF	PDLIM7	5927	Downstream
chr5:176918674..176918694	+	0	M01200	CTCF	PDLIM7	5928	Downstream
chr5:176917820..176917826	+	0	M00704	TEF-1	PDLIM7	6782	Downstream
chr5:176917140..176917147	-	0	M00468	AP-2rep	PDLIM7	7455	Downstream
chr5:176916962..176916969	-	0	M00468	AP-2rep	PDLIM7	7633	Downstream
chr5:176922239..176922248	-	0.003	M01705	TCF4	PDLIM7	2354	Downstream
chr5:176918672..176918692	+	0.003	M01259	CTCF	PDLIM7	5930	Downstream
chr5:176931920..176931928	-	0.004	M00973	E2A	PDLIM7	-7326	Upstream
chr5:176922029..176922048	-	0.007	MA0139	CTCF	PDLIM7	2554	Downstream
chr5:176921780..176921791	-	0.008	M00174	AP-1	PDLIM7	2811	Downstream
chr5:176919526..176919533	-	0.009	M01709	MAFA	PDLIM7	5069	Downstream
chr5:176922580..176922586	-	0.013	M01287	Neuro D	PDLIM7	2016	Downstream
chr5:176922580..176922586	+	0.013	M01287	Neuro D	PDLIM7	2022	Downstream
chr5:176922388..176922394	+	0.013	M01287	Neuro D	PDLIM7	2214	Downstream
chr5:176922388..176922394	-	0.013	M01287	Neuro D	PDLIM7	2208	Downstream
chr5:176919524..176919532	+	0.013	M00698	HEB	PDLIM7	5078	Downstream
chr5:176922814..176922827	+	0.015	M00762	PPAR, HNF-4, COUP, RAR	PDLIM7	1788	Downstream
chr5:176922031..176922051	-	0.016	M01259	CTCF	PDLIM7	2551	Downstream
chr5:176922029..176922048	-	0.016	LM2_CTCF	CTCF	PDLIM7	2554	Downstream
chr5:176922029..176922049	-	0.016	M01200	CTCF	PDLIM7	2553	Downstream
chr5:176919814..176919820	-	0.016	M01287	Neuro D	PDLIM7	4782	Downstream
chr5:176919814..176919820	+	0.016	M01287	Neuro D	PDLIM7	4788	Downstream
chr5:176930411..176930418	+	0.017	M01709	MAFA	PDLIM7	-5809	Upstream
chr5:176924267..176924278	+	0.017	M00174	AP-1	PDLIM7	335	Downstream
chr5:176916693..176916699	+	0.017	M01287	Neuro D	PDLIM7	7909	Downstream
chr5:176916693..176916699	-	0.017	M01287	Neuro D	PDLIM7	7903	Downstream

chr5:176918541..176918547	-	0.019	M01287	Neuro D	PDLIM7	6055	Downstream
chr5:176918541..176918547	+	0.019	M01287	Neuro D	PDLIM7	6061	Downstream
chr5:176922388..176922395	+	0.02	M00644	LBP-1	PDLIM7	2214	Downstream
chr5:176922814..176922827	-	0.021	M00764	HNF4 direct repeat 1	PDLIM7	1775	Downstream
chr5:176920298..176920304	+	0.021	M01287	Neuro D	PDLIM7	4304	Downstream
chr5:176920298..176920304	-	0.021	M01287	Neuro D	PDLIM7	4298	Downstream
chr5:176916692..176916699	-	0.021	M00644	LBP-1	PDLIM7	7903	Downstream
chr5:176924468..176924475	+	0.023	M01709	MAFA	PDLIM7	134	Downstream
chr5:176921287..176921294	-	0.024	M01709	MAFA	PDLIM7	3308	Downstream
chr5:176919814..176919821	+	0.025	M00644	LBP-1	PDLIM7	4788	Downstream
chr5:176919813..176919820	-	0.025	M00644	LBP-1	PDLIM7	4782	Downstream
chr5:176922820..176922827	-	0.028	M01269	NURR1	PDLIM7	1775	Downstream
chr5:176923861..176923872	-	0.029	M00174	AP-1	PDLIM7	730	Downstream
chr5:176917104..176917110	-	0.03	MA0095	YY1	PDLIM7	7492	Downstream
chr5:176917095..176917101	+	0.03	MA0095	YY1	PDLIM7	7507	Downstream
chr5:176932011..176932018	+	0.034	M01207	ETS2	PDLIM7	-7409	Upstream
chr5:176921439..176921450	-	0.038	M00174	AP-1	PDLIM7	3152	Downstream
chr5:176921722..176921729	-	0.039	M01269	NURR1	PDLIM7	2873	Downstream
chr5:176918415..176918427	+	0.045	M00414	AREB6	PDLIM7	6187	Downstream
chr5:176922662..176922668	+	0.048	MA0095	YY1	PDLIM7	1940	Downstream
chr5:176922445..176922452	-	0.051	M01207	ETS2	PDLIM7	2150	Downstream
chr5:176923863..176923871	+	0.054	M01267	FRA1	PDLIM7	739	Downstream
chr5:176922377..176922384	+	0.054	M01207	ETS2	PDLIM7	2225	Downstream
chr5:176921782..176921790	+	0.054	M01267	FRA1	PDLIM7	2820	Downstream
chr5:176921441..176921449	+	0.054	M01267	FRA1	PDLIM7	3161	Downstream
chr5:176921604..176921611	-	0.055	M01207	ETS2	PDLIM7	2991	Downstream
chr5:176930680..176930687	+	0.056	M01268	FXR	PDLIM7	-6078	Upstream
chr5:176922814..176922827	-	0.061	M00765	COUP direct repeat 1	PDLIM7	1775	Downstream
chr5:176920199..176920205	+	0.061	MA0095	YY1	PDLIM7	4403	Downstream
chr5:176930532..176930539	+	0.062	M01207	ETS2	PDLIM7	-5930	Upstream
chr5:176917089..176917096	-	0.062	M01207	ETS2	PDLIM7	7506	Downstream
chr5:176918771..176918777	-	0.067	MA0095	YY1	PDLIM7	5825	Downstream
chr5:176922237..176922243	+	0.068	MA0095	YY1	PDLIM7	2365	Downstream
chr5:176916870..176916877	+	0.068	M01207	ETS2	PDLIM7	7732	Downstream
chr5:176920548..176920554	-	0.072	MA0095	YY1	PDLIM7	4048	Downstream
chr5:176920746..176920752	+	0.074	MA0095	YY1	PDLIM7	3856	Downstream
chr5:176922814..176922828	+	0.076	M01031	HNF4	PDLIM7	1788	Downstream
chr5:176924328..176924335	-	0.077	M01207	ETS2	PDLIM7	267	Downstream
chr5:176928485..176928492	-	0.078	M01207	ETS2	PDLIM7	-3890	Upstream
chr5:176923605..176923619	-	0.078	MA0119	TLX1::NFIC	PDLIM7	983	Downstream
chr5:176921578..176921586	+	0.081	M00497	STAT3	PDLIM7	3024	Downstream
chr5:176930620..176930628	+	0.083	M00498	STAT4	PDLIM7	-6018	Upstream
chr5:176924133..176924141	-	0.089	M00500	STAT6	PDLIM7	461	Downstream
chr5:176924268..176924279	-	0.09	M00037	NF-E2	PDLIM7	323	Downstream
chr5:176924268..176924277	+	0.09	M00199	AP-1	PDLIM7	334	Downstream
chr5:176923862..176923871	+	0.101	M00199	AP-1	PDLIM7	740	Downstream

chr5:176921781..176921790	+	0.101	M00199	AP-1	PDLIM7	2821	Downstream
chr5:176921778..176921793	+	0.102	M00495	Bach1	PDLIM7	2824	Downstream
chr5:176921440..176921449	+	0.102	M00199	AP-1	PDLIM7	3162	Downstream
chr5:176928349..176928356	-	0.112	M01268	FXR	PDLIM7	-3754	Upstream
chr5:176921780..176921791	+	0.113	M00490	Bach2	PDLIM7	2822	Downstream
chr5:176921781..176921792	-	0.118	M00037	NF-E2	PDLIM7	2810	Downstream
chr5:176923859..176923874	+	0.121	M00495	Bach1	PDLIM7	743	Downstream
chr5:176918476..176918484	+	0.122	M00658	PU.1	PDLIM7	6126	Downstream
chr5:176923605..176923622	+	0.124	M00806	NF-1	PDLIM7	997	Downstream
chr5:176923861..176923872	+	0.15	M00490	Bach2	PDLIM7	741	Downstream
chr5:176924268..176924277	+	0.184	M00925	AP-1	PDLIM7	334	Downstream
chr5:176922441..176922457	+	0.186	M00007	Elk-1	PDLIM7	2161	Downstream
chr5:176919869..176919876	-	0.217	M00750	HMG IY	PDLIM7	4726	Downstream
chr5:176920352..176920359	-	0.218	M00750	HMG IY	PDLIM7	4243	Downstream
chr5:176932012..176932022	+	0.293	M01119	KAISO	PDLIM7	-7410	Upstream
chr5:176922817..176922823	+	0.294	M00805	LEF1	PDLIM7	1785	Downstream
chr5:176923933..176923948	-	0.301	M00215	SRF	PDLIM7	654	Downstream
chr5:176922687..176922702	-	0.301	M00215	SRF	PDLIM7	1900	Downstream
chr5:176924628..176924634	-	0.303	M00805	LEF1	PDLIM7	-32	Upstream
chr5:176924704..176924711	-	0.307	M01718	NFAT2	PDLIM7	-109	Upstream
chr5:176923419..176923427	-	0.314	M00493	STAT5A	PDLIM7	1175	Downstream
chr5:176916934..176916941	-	0.322	M01718	NFAT2	PDLIM7	7661	Downstream
chr5:176922699..176922709	-	0.328	M00051	NF-kappaB (p50)	PDLIM7	1893	Downstream
chr5:176919404..176919419	-	0.345	M00984	PEBP	PDLIM7	5183	Downstream
chr5:176932129..176932135	+	0.362	M00805	LEF1	PDLIM7	-7527	Upstream
chr5:176923937..176923952	+	0.378	M00252	TATA	PDLIM7	665	Downstream
chr5:176918405..176918417	+	0.381	MA0155	INSM1	PDLIM7	6197	Downstream
chr5:176920586..176920592	-	0.399	M00805	LEF1	PDLIM7	4010	Downstream
chr5:176920553..176920559	-	0.4	M00805	LEF1	PDLIM7	4043	Downstream
chr5:176922241..176922247	+	0.403	M00805	LEF1	PDLIM7	2361	Downstream
chr5:176920478..176920484	-	0.405	M00805	LEF1	PDLIM7	4118	Downstream
chr5:176930407..176930414	+	0.407	M01665	IRF8	PDLIM7	-5805	Upstream
chr5:176923397..176923404	-	0.412	M01733	MZF1	PDLIM7	1198	Downstream
chr5:176920225..176920231	-	0.414	M00805	LEF1	PDLIM7	4371	Downstream
chr5:176918150..176918157	+	0.429	M01733	MZF1	PDLIM7	6452	Downstream
chr5:176921638..176921645	+	0.434	M01733	MZF1	PDLIM7	2964	Downstream
chr5:176921785..176921791	-	0.44	M01227	MAFB	PDLIM7	2811	Downstream
chr5:176932112..176932118	+	0.449	MA0056	MZF1_1-4	PDLIM7	-7510	Upstream
chr5:176923954..176923960	+	0.455	M01227	MAFB	PDLIM7	648	Downstream
chr5:176922871..176922878	+	0.461	M01733	MZF1	PDLIM7	1731	Downstream
chr5:176918562..176918569	+	0.471	MA0133	BRCA1	PDLIM7	6040	Downstream
chr5:176923398..176923404	-	0.472	MA0056	MZF1_1-4	PDLIM7	1198	Downstream
chr5:176922006..176922012	+	0.472	M01227	MAFB	PDLIM7	2596	Downstream
chr5:176931707..176931713	-	0.473	M01227	MAFB	PDLIM7	-7111	Upstream
chr5:176918150..176918156	+	0.474	MA0056	MZF1_1-4	PDLIM7	6452	Downstream
chr5:176921638..176921644	+	0.477	MA0056	MZF1_1-4	PDLIM7	2964	Downstream

chr5:176923933..176923952	-	0.483	M01007	SRF	PDLIM7	650	Downstream
chr5:176922871..176922877	+	0.484	MA0056	MZF1_1-4	PDLIM7	1731	Downstream
chr5:176923935..176923949	+	0.487	M00186	SRF	PDLIM7	667	Downstream
chr5:176922091..176922098	-	0.488	M01733	MZF1	PDLIM7	2504	Downstream
chr5:176918335..176918342	+	0.492	M01733	MZF1	PDLIM7	6267	Downstream
chr5:176922689..176922707	+	0.493	M01257	SRF	PDLIM7	1913	Downstream
chr5:176922452..176922458	-	0.498	MA0056	MZF1_1-4	PDLIM7	2144	Downstream
chr1:201916734..201916743	-	0	M01721	PUR1	LMOD1	-1027	Upstream
chr1:201912172..201912181	+	0	M01721	PUR1	LMOD1	3544	Downstream
chr1:201921129..201921135	-	0	M00704	TEF-1	LMOD1	-5419	Upstream
chr1:201916951..201916957	+	0	M00704	TEF-1	LMOD1	-1235	Upstream
chr1:201915796..201915802	-	0	M00704	TEF-1	LMOD1	-86	Upstream
chr1:201914865..201914871	+	0	M00704	TEF-1	LMOD1	851	Downstream
chr1:201914021..201914027	-	0	M00704	TEF-1	LMOD1	1689	Downstream
chr1:201908243..201908249	-	0	M00704	TEF-1	LMOD1	7467	Downstream
chr1:201914483..201914492	+	0.002	M00927	AP-4	LMOD1	1233	Downstream
chr1:201912617..201912625	+	0.004	M00973	E2A	LMOD1	3099	Downstream
chr1:201907756..201907764	+	0.004	M00973	E2A	LMOD1	7960	Downstream
chr1:201910955..201910961	-	0.004	M01287	Neuro D	LMOD1	4755	Downstream
chr1:201910955..201910961	+	0.004	M01287	Neuro D	LMOD1	4761	Downstream
chr1:201910955..201910962	+	0.007	M00644	LBP-1	LMOD1	4761	Downstream
chr1:201910822..201910829	-	0.009	M01709	MAFA	LMOD1	4887	Downstream
chr1:201911162..201911169	+	0.009	M01131	SOX10	LMOD1	4554	Downstream
chr1:201908980..201908986	+	0.011	M01287	Neuro D	LMOD1	6736	Downstream
chr1:201908980..201908986	-	0.011	M01287	Neuro D	LMOD1	6730	Downstream
chr1:201907966..201907972	+	0.012	M01287	Neuro D	LMOD1	7750	Downstream
chr1:201907966..201907972	-	0.012	M01287	Neuro D	LMOD1	7744	Downstream
chr1:201914272..201914279	-	0.012	M01131	SOX10	LMOD1	1437	Downstream
chr1:201919156..201919162	-	0.015	M01287	Neuro D	LMOD1	-3446	Upstream
chr1:201919156..201919162	+	0.015	M01287	Neuro D	LMOD1	-3440	Upstream
chr1:201914259..201914266	-	0.015	M01131	SOX10	LMOD1	1450	Downstream
chr1:201914792..201914799	+	0.017	M01131	SOX10	LMOD1	924	Downstream
chr1:201918737..201918743	-	0.018	M01287	Neuro D	LMOD1	-3027	Upstream
chr1:201918737..201918743	+	0.018	M01287	Neuro D	LMOD1	-3021	Upstream
chr1:201909078..201909085	+	0.022	M01131	SOX10	LMOD1	6638	Downstream
chr1:201914485..201914491	+	0.025	M01287	Neuro D	LMOD1	1231	Downstream
chr1:201914485..201914491	-	0.025	M01287	Neuro D	LMOD1	1225	Downstream
chr1:201909006..201909013	-	0.025	M01131	SOX10	LMOD1	6703	Downstream
chr1:201918644..201918650	+	0.026	M01287	Neuro D	LMOD1	-2928	Upstream
chr1:201918644..201918650	-	0.026	M01287	Neuro D	LMOD1	-2934	Upstream
chr1:201914485..201914492	+	0.027	M00644	LBP-1	LMOD1	1231	Downstream
chr1:201912570..201912577	-	0.036	M01269	NURR1	LMOD1	3139	Downstream
chr1:201916563..201916570	+	0.043	M01268	FXR	LMOD1	-847	Upstream
chr1:201909232..201909238	+	0.043	MA0095	YY1	LMOD1	6484	Downstream
chr1:201911768..201911775	-	0.049	M01269	NURR1	LMOD1	3941	Downstream
chr1:201919064..201919072	-	0.051	M00926	AP-1	LMOD1	-3356	Upstream

chr1:201913597..201913605	+	0.054	M00498	STAT4	LMOD1	2119	Downstream
chr1:201918648..201918655	+	0.061	M01269	NURR1	LMOD1	-2932	Upstream
chr1:201920656..201920663	+	0.074	M01207	ETS2	LMOD1	-4940	Upstream
chr1:201913795..201913803	+	0.074	M00497	STAT3	LMOD1	1921	Downstream
chr1:201910756..201910764	+	0.074	M00500	STAT6	LMOD1	4960	Downstream
chr1:201918920..201918927	-	0.078	M01207	ETS2	LMOD1	-3211	Upstream
chr1:201915982..201915988	+	0.092	M01033	HNF4	LMOD1	-266	Upstream
chr1:201916513..201916521	-	0.095	M00658	PU.1	LMOD1	-805	Upstream
chr1:201914883..201914891	+	0.095	M01308	SOX4	LMOD1	833	Downstream
chr1:201916737..201916743	-	0.097	M01033	HNF4	LMOD1	-1027	Upstream
chr1:201922573..201922581	+	0.11	M01308	SOX4	LMOD1	-6857	Upstream
chr1:201913435..201913442	-	0.149	M00750	HMG IY	LMOD1	2274	Downstream
chr1:201912172..201912178	+	0.164	M01033	HNF4	LMOD1	3544	Downstream
chr1:201916603..201916614	-	0.171	M00691	ATF1	LMOD1	-898	Upstream
chr1:201916680..201916687	+	0.177	M01718	NFAT2	LMOD1	-964	Upstream
chr1:201908626..201908635	+	0.178	M00792	SMAD	LMOD1	7090	Downstream
chr1:201913748..201913754	+	0.18	M01033	HNF4	LMOD1	1968	Downstream
chr1:201912621..201912627	-	0.187	M01033	HNF4	LMOD1	3089	Downstream
chr1:201911125..201911132	+	0.19	M01665	IRF8	LMOD1	4591	Downstream
chr1:201915794..201915806	+	0.194	M01305	TEF	LMOD1	-78	Upstream
chr1:201922852..201922859	+	0.2	M00799	Myc	LMOD1	-7136	Upstream
chr1:201915783..201915790	-	0.205	M01665	IRF8	LMOD1	-74	Upstream
chr1:201908586..201908592	+	0.216	M01033	HNF4	LMOD1	7130	Downstream
chr1:201920688..201920694	+	0.228	M01033	HNF4	LMOD1	-4972	Upstream
chr1:201916850..201916857	-	0.252	M00240	Nkx2-5	LMOD1	-1141	Upstream
chr1:201915794..201915806	+	0.256	MA0090	TEAD1	LMOD1	-78	Upstream
chr1:201915793..201915813	+	0.267	M00034	p53	LMOD1	-77	Upstream
chr1:201916563..201916569	+	0.282	M01032	HNF4	LMOD1	-847	Upstream
chr1:201908151..201908157	+	0.293	M00805	LEF1	LMOD1	7565	Downstream
chr1:201915793..201915813	-	0.293	M00034	p53	LMOD1	-97	Upstream
chr1:201910853..201910859	+	0.303	M01032	HNF4	LMOD1	4863	Downstream
chr1:201914640..201914648	+	0.319	M00493	STAT5A	LMOD1	1076	Downstream
chr1:201910514..201910521	+	0.329	M01665	IRF8	LMOD1	5202	Downstream
chr1:201916781..201916795	-	0.343	M00209	NF-Y	LMOD1	-1079	Upstream
chr1:201910655..201910671	-	0.359	M01436	Crx	LMOD1	5045	Downstream
chr1:201911221..201911227	+	0.386	M01227	MAFB	LMOD1	4495	Downstream
chr1:201919399..201919405	+	0.387	M00805	LEF1	LMOD1	-3683	Upstream
chr1:201913577..201913583	+	0.404	MA0056	MZF1_1-4	LMOD1	2139	Downstream
chr1:201907806..201907812	+	0.406	M00805	LEF1	LMOD1	7910	Downstream
chr1:201910990..201910996	-	0.426	MA0056	MZF1_1-4	LMOD1	4720	Downstream
chr1:201911291..201911298	-	0.435	M01733	MZF1	LMOD1	4418	Downstream
chr1:201916848..201916859	-	0.435	M00220	SREBP-1	LMOD1	-1143	Upstream
chr1:201923669..201923677	+	0.44	M00690	AP-3	LMOD1	-7953	Upstream
chr1:201910709..201910716	+	0.44	MA0133	BRCA1	LMOD1	5007	Downstream
chr1:201911489..201911495	-	0.442	M01032	HNF4	LMOD1	4221	Downstream
chr1:201915741..201915747	-	0.442	MA0056	MZF1_1-4	LMOD1	-31	Upstream

chr1:201908090..201908097	+	0.446	MA0133	BRCA1	LMOD1	7626	Downstream
chr1:201911048..201911056	+	0.446	M01111	RBP-Jkappa	LMOD1	4668	Downstream
chr1:201921408..201921415	-	0.451	M00240	Nkx2-5	LMOD1	-5699	Upstream
chr1:201911559..201911565	-	0.458	M01032	HNF4	LMOD1	4151	Downstream
chr1:201911738..201911744	+	0.465	MA0056	MZF1_1-4	LMOD1	3978	Downstream
chr1:201914809..201914815	+	0.472	M01227	MAFB	LMOD1	907	Downstream
chr1:201911292..201911298	-	0.475	MA0056	MZF1_1-4	LMOD1	4418	Downstream
chr1:201922680..201922686	+	0.483	M01227	MAFB	LMOD1	-6964	Upstream
chr1:201920881..201920887	-	0.484	M01032	HNF4	LMOD1	-5171	Upstream
chr1:201908993..201908999	+	0.486	M01227	MAFB	LMOD1	6723	Downstream
chr6:118863507..118863513	-	0	M00704	TEF-1	PLN	-5928	Upstream
chr6:118870473..118870479	+	0	M00704	TEF-1	PLN	1032	Downstream
chr6:118871984..118871990	-	0	M00704	TEF-1	PLN	2549	Downstream
chr6:118872852..118872858	+	0	M00704	TEF-1	PLN	3411	Downstream
chr6:118872957..118872963	+	0	M00704	TEF-1	PLN	3516	Downstream
chr6:118873929..118873935	-	0	M00704	TEF-1	PLN	4494	Downstream
chr6:118868198..118868210	+	0.003	MA0055	Myf	PLN	-1243	Upstream
chr6:118868201..118868207	+	0.004	M01287	Neuro D	PLN	-1240	Upstream
chr6:118868201..118868207	-	0.004	M01287	Neuro D	PLN	-1234	Upstream
chr6:118868200..118868207	-	0.006	M00644	LBP-1	PLN	-1234	Upstream
chr6:118868201..118868208	+	0.006	M00644	LBP-1	PLN	-1240	Upstream
chr6:118869945..118869952	-	0.01	M01709	MAFA	PLN	511	Downstream
chr6:118862420..118862427	+	0.015	M01709	MAFA	PLN	-7021	Upstream
chr6:118867849..118867855	+	0.015	M01287	Neuro D	PLN	-1592	Upstream
chr6:118867849..118867855	-	0.015	M01287	Neuro D	PLN	-1586	Upstream
chr6:118862694..118862701	-	0.019	M01709	MAFA	PLN	-6740	Upstream
chr6:118869544..118869550	+	0.019	M01287	Neuro D	PLN	103	Downstream
chr6:118869544..118869550	-	0.019	M01287	Neuro D	PLN	109	Downstream
chr6:118869544..118869551	+	0.024	M00644	LBP-1	PLN	103	Downstream
chr6:118867848..118867855	-	0.026	M00644	LBP-1	PLN	-1586	Upstream
chr6:118874547..118874554	-	0.043	M01207	ETS2	PLN	5113	Downstream
chr6:118874476..118874483	+	0.043	M01268	FXR	PLN	5035	Downstream
chr6:118866178..118866185	+	0.074	M01207	ETS2	PLN	-3263	Upstream
chr6:118862584..118862591	-	0.078	M01207	ETS2	PLN	-6850	Upstream
chr6:118874518..118874526	+	0.108	M01308	SOX4	PLN	5077	Downstream
chr6:118868010..118868017	-	0.112	M00750	HMG IY	PLN	-1424	Upstream
chr6:118865459..118865467	-	0.112	M01308	SOX4	PLN	-3974	Upstream
chr6:118866338..118866345	-	0.147	M00750	HMG IY	PLN	-3096	Upstream
chr6:118872621..118872628	-	0.155	M00750	HMG IY	PLN	3187	Downstream
chr6:118873833..118873840	-	0.164	M00750	HMG IY	PLN	4399	Downstream
chr6:118865663..118865670	-	0.177	M00750	HMG IY	PLN	-3771	Upstream
chr6:118866030..118866037	-	0.179	M00750	HMG IY	PLN	-3404	Upstream
chr6:118865543..118865550	+	0.2	M00799	Myc	PLN	-3898	Upstream
chr6:118872445..118872453	+	0.2	M00671	TCF-4	PLN	3004	Downstream
chr6:118869775..118869781	-	0.201	M00805	LEF1	PLN	340	Downstream
chr6:118869748..118869754	-	0.202	M00805	LEF1	PLN	313	Downstream

chr6:118871658..118871665	-	0.203	M00750	HMG IY	PLN	2224	Downstream
chr6:118869369..118869383	-	0.203	M00209	NF-Y	PLN	-58	Upstream
chr6:118868181..118868196	+	0.203	M00215	SRF	PLN	-1260	Upstream
chr6:118870829..118870835	-	0.238	M00805	LEF1	PLN	1394	Downstream
chr6:118862600..118862607	+	0.248	M01718	NFAT2	PLN	-6841	Upstream
chr6:118868178..118868196	-	0.258	M00152	SRF	PLN	-1245	Upstream
chr6:118872338..118872344	+	0.26	M00805	LEF1	PLN	2897	Downstream
chr6:118869217..118869224	+	0.266	M01718	NFAT2	PLN	-224	Upstream
chr6:118873151..118873158	-	0.266	M01718	NFAT2	PLN	3717	Downstream
chr6:118866222..118866228	-	0.274	M00805	LEF1	PLN	-3213	Upstream
chr6:118868180..118868194	+	0.291	M00186	SRF	PLN	-1261	Upstream
chr6:118872178..118872184	+	0.293	M00805	LEF1	PLN	2737	Downstream
chr6:118871192..118871198	+	0.306	M00805	LEF1	PLN	1751	Downstream
chr6:118872446..118872452	-	0.307	M00805	LEF1	PLN	3011	Downstream
chr6:118869414..118869441	-	0.31	M00957	PR	PLN	0	Upstream
chr6:118862393..118862399	-	0.311	M00805	LEF1	PLN	-7042	Upstream
chr6:118863046..118863052	+	0.321	M00805	LEF1	PLN	-6395	Upstream
chr6:118872458..118872467	-	0.331	M00630	FOXM1	PLN	3026	Downstream
chr6:118866255..118866261	+	0.341	M00805	LEF1	PLN	-3186	Upstream
chr6:118861589..118861595	+	0.35	M00805	LEF1	PLN	-7852	Upstream
chr6:118872587..118872594	-	0.351	M01733	MZF1	PLN	3153	Downstream
chr6:118870078..118870085	+	0.357	M01665	IRF8	PLN	637	Downstream
chr6:118865891..118865898	+	0.357	M00240	Nkx2-5	PLN	-3550	Upstream
chr6:118868178..118868197	-	0.359	M01007	SRF	PLN	-1244	Upstream
chr6:118865261..118865267	+	0.361	M00805	LEF1	PLN	-4180	Upstream
chr6:118868177..118868196	+	0.366	M01007	SRF	PLN	-1264	Upstream
chr6:118868177..118868192	-	0.371	M00922	SRF	PLN	-1249	Upstream
chr6:118862113..118862120	+	0.374	M01665	IRF8	PLN	-7328	Upstream
chr6:118862836..118862842	+	0.374	M00805	LEF1	PLN	-6605	Upstream
chr6:118872588..118872594	-	0.398	MA0056	MZF1_1-4	PLN	3153	Downstream
chr6:118862921..118862928	-	0.398	M00240	Nkx2-5	PLN	-6513	Upstream
chr6:118871582..118871590	+	0.405	M00690	AP-3	PLN	2141	Downstream
chr6:118871469..118871476	+	0.405	M01665	IRF8	PLN	2028	Downstream
chr6:118872481..118872488	+	0.47	MA0133	BRCA1	PLN	3040	Downstream
chr6:118869571..118869577	+	0.47	M01227	MAFB	PLN	130	Downstream
chr6:118867379..118867386	-	0.475	M01733	MZF1	PLN	-2055	Upstream
chr6:118869814..118869821	+	0.484	M00747	IRF-1	PLN	373	Downstream
chr6:118868109..118868115	+	0.492	M01227	MAFB	PLN	-1332	Upstream
chr6:118865893..118865900	-	0.497	M00747	IRF-1	PLN	-3541	Upstream
chr6:118865900..118865907	-	0.499	M00747	IRF-1	PLN	-3534	Upstream
chr15:99639410..99639417	-	0	M00468	AP-2rep	SYNM	-5868	Upstream
chr15:99640307..99640313	-	0	M00704	TEF-1	SYNM	-4972	Upstream
chr15:99640509..99640515	+	0	M00704	TEF-1	SYNM	-4776	Upstream
chr15:99642703..99642709	-	0	M00704	TEF-1	SYNM	-2576	Upstream
chr15:99643359..99643365	+	0	M00704	TEF-1	SYNM	-1926	Upstream
chr15:99647195..99647201	+	0	M00704	TEF-1	SYNM	1910	Downstream

chr15:99648597..99648603	-	0	M00704	TEF-1	SYNM	3318	Downstream
chr15:99651624..99651630	+	0	M00704	TEF-1	SYNM	6339	Downstream
chr15:99652306..99652312	-	0	M00704	TEF-1	SYNM	7027	Downstream
chr15:99645142..99645161	+	0.003	MA0139	CTCF	SYNM	-143	Upstream
chr15:99645189..99645205	-	0.008	M00287	NF-Y	SYNM	-80	Upstream
chr15:99643198..99643204	+	0.011	M01287	Neuro D	SYNM	-2087	Upstream
chr15:99643198..99643204	-	0.011	M01287	Neuro D	SYNM	-2081	Upstream
chr15:99647124..99647130	+	0.011	M01287	Neuro D	SYNM	1839	Downstream
chr15:99647124..99647130	-	0.011	M01287	Neuro D	SYNM	1845	Downstream
chr15:99645192..99645203	-	0.012	M00687	alpha-CP1	SYNM	-82	Upstream
chr15:99638324..99638332	+	0.013	M00698	HEB	SYNM	-6961	Upstream
chr15:99647123..99647130	-	0.014	M00644	LBP-1	SYNM	1845	Downstream
chr15:99649137..99649143	+	0.014	M01287	Neuro D	SYNM	3852	Downstream
chr15:99649137..99649143	-	0.014	M01287	Neuro D	SYNM	3858	Downstream
chr15:99642941..99642947	+	0.015	M01287	Neuro D	SYNM	-2344	Upstream
chr15:99642941..99642947	-	0.015	M01287	Neuro D	SYNM	-2338	Upstream
chr15:99638612..99638618	-	0.016	M01287	Neuro D	SYNM	-6667	Upstream
chr15:99638612..99638618	+	0.016	M01287	Neuro D	SYNM	-6673	Upstream
chr15:99643198..99643205	+	0.017	M00644	LBP-1	SYNM	-2087	Upstream
chr15:99638164..99638171	+	0.021	M01131	SOX10	SYNM	-7121	Upstream
chr15:99646460..99646466	+	0.021	M01287	Neuro D	SYNM	1175	Downstream
chr15:99646460..99646466	-	0.021	M01287	Neuro D	SYNM	1181	Downstream
chr15:99651752..99651758	+	0.021	M01287	Neuro D	SYNM	6467	Downstream
chr15:99651752..99651758	-	0.021	M01287	Neuro D	SYNM	6473	Downstream
chr15:99642940..99642947	-	0.024	M00644	LBP-1	SYNM	-2338	Upstream
chr15:99642941..99642948	+	0.024	M00644	LBP-1	SYNM	-2344	Upstream
chr15:99649614..99649621	-	0.024	M01709	MAFA	SYNM	4336	Downstream
chr15:99649099..99649106	-	0.026	M01709	MAFA	SYNM	3821	Downstream
chr15:99646459..99646466	-	0.03	M00644	LBP-1	SYNM	1181	Downstream
chr15:99646460..99646467	+	0.03	M00644	LBP-1	SYNM	1175	Downstream
chr15:99652618..99652624	+	0.035	M01287	Neuro D	SYNM	7333	Downstream
chr15:99652618..99652624	-	0.035	M01287	Neuro D	SYNM	7339	Downstream
chr15:99643629..99643636	+	0.039	M01131	SOX10	SYNM	-1656	Upstream
chr15:99638681..99638688	+	0.041	M01269	NURR1	SYNM	-6604	Upstream
chr15:99639948..99639955	-	0.044	M01131	SOX10	SYNM	-5330	Upstream
chr15:99652617..99652624	-	0.044	M00644	LBP-1	SYNM	7339	Downstream
chr15:99643332..99643339	-	0.046	M01269	NURR1	SYNM	-1946	Upstream
chr15:99645016..99645023	-	0.049	M01269	NURR1	SYNM	-262	Upstream
chr15:99651357..99651364	+	0.05	M01207	ETS2	SYNM	6072	Downstream
chr15:99649359..99649365	-	0.052	MA0095	YY1	SYNM	4080	Downstream
chr15:99650986..99650993	-	0.055	M01268	FXR	SYNM	5708	Downstream
chr15:99638638..99638644	+	0.058	MA0095	YY1	SYNM	-6647	Upstream
chr15:99648047..99648053	+	0.059	MA0095	YY1	SYNM	2762	Downstream
chr15:99647463..99647471	+	0.067	M00498	STAT4	SYNM	2178	Downstream
chr15:99642731..99642738	+	0.071	M01207	ETS2	SYNM	-2554	Upstream
chr15:99652606..99652614	-	0.071	M00498	STAT4	SYNM	7329	Downstream

chr15:99640259..99640266	-	0.074	M01207	ETS2	SYNM	-5019	Upstream
chr15:99646778..99646786	-	0.074	M00921	GR	SYNM	1501	Downstream
chr15:99646227..99646233	-	0.075	MA0095	YY1	SYNM	948	Downstream
chr15:99640942..99640949	-	0.086	M01207	ETS2	SYNM	-4336	Upstream
chr15:99647028..99647036	-	0.097	M00494	STAT6	SYNM	1751	Downstream
chr15:99640483..99640491	+	0.1	M00497	STAT3	SYNM	-4802	Upstream
chr15:99646665..99646672	-	0.107	M00750	HMG IY	SYNM	1387	Downstream
chr15:99646759..99646765	+	0.124	M01033	HNF4	SYNM	1474	Downstream
chr15:99647075..99647083	-	0.128	M00494	STAT6	SYNM	1798	Downstream
chr15:99651521..99651528	-	0.174	M00750	HMG IY	SYNM	6243	Downstream
chr15:99642937..99642943	+	0.181	M01033	HNF4	SYNM	-2348	Upstream
chr15:99645193..99645206	-	0.181	M00775	NF-Y	SYNM	-79	Upstream
chr15:99643125..99643131	-	0.194	M01033	HNF4	SYNM	-2154	Upstream
chr15:99646286..99646292	+	0.195	M01033	HNF4	SYNM	1001	Downstream
chr15:99649403..99649409	-	0.195	M01033	HNF4	SYNM	4124	Downstream
chr15:99649210..99649216	-	0.201	M01033	HNF4	SYNM	3931	Downstream
chr15:99651374..99651381	-	0.202	M00799	Myc	SYNM	6096	Downstream
chr15:99645191..99645205	+	0.223	M00209	NF-Y	SYNM	-94	Upstream
chr15:99640879..99640885	-	0.224	M01033	HNF4	SYNM	-4400	Upstream
chr15:99651222..99651228	-	0.225	M00805	LEF1	SYNM	5943	Downstream
chr15:99646290..99646298	+	0.257	M01240	BEN	SYNM	1005	Downstream
chr15:99640884..99640892	+	0.268	M01240	BEN	SYNM	-4401	Upstream
chr15:99638218..99638226	+	0.272	M00690	AP-3	SYNM	-7067	Upstream
chr15:99638078..99638084	-	0.297	M00805	LEF1	SYNM	-7201	Upstream
chr15:99647465..99647472	+	0.303	M01718	NFAT2	SYNM	2180	Downstream
chr15:99643452..99643459	+	0.306	M01718	NFAT2	SYNM	-1833	Upstream
chr15:99651393..99651399	-	0.308	M01032	HNF4	SYNM	6114	Downstream
chr15:99645192..99645203	-	0.319	M00185	NF-Y	SYNM	-82	Upstream
chr15:99651775..99651782	+	0.323	M01718	NFAT2	SYNM	6490	Downstream
chr15:99643010..99643017	+	0.325	M01665	IRF8	SYNM	-2275	Upstream
chr15:99651411..99651418	+	0.334	M01658	AML1	SYNM	6126	Downstream
chr15:99651264..99651271	-	0.335	M01665	IRF8	SYNM	5986	Downstream
chr15:99643014..99643020	+	0.337	M00805	LEF1	SYNM	-2271	Upstream
chr15:99648000..99648006	+	0.343	M01032	HNF4	SYNM	2715	Downstream
chr15:99647719..99647725	-	0.346	M00805	LEF1	SYNM	2440	Downstream
chr15:99647954..99647960	-	0.349	M00805	LEF1	SYNM	2675	Downstream
chr15:99650987..99650993	-	0.361	M01032	HNF4	SYNM	5708	Downstream
chr15:99649480..99649487	-	0.364	M00240	Nkx2-5	SYNM	4202	Downstream
chr15:99651019..99651026	-	0.365	M01665	IRF8	SYNM	5741	Downstream
chr15:99643179..99643185	+	0.368	M00805	LEF1	SYNM	-2106	Upstream
chr15:99647398..99647404	+	0.391	M00805	LEF1	SYNM	2113	Downstream
chr15:99646818..99646824	+	0.44	M01227	MAFB	SYNM	1533	Downstream
chr15:99649531..99649538	-	0.442	M00240	Nkx2-5	SYNM	4253	Downstream
chr15:99651241..99651247	+	0.467	M01227	MAFB	SYNM	5956	Downstream
chr15:99638396..99638402	+	0.474	MA0056	MZF1_1-4	SYNM	-6889	Upstream
chr15:99643172..99643179	+	0.477	M01733	MZF1	SYNM	-2113	Upstream

chr15:99653272..99653279	-	0.479	M01733	MZF1	SYNM	7994	Downstream
chr15:99646360..99646366	+	0.481	MA0056	MZF1_1-4	SYNM	1075	Downstream
chr15:99648712..99648719	+	0.483	M01733	MZF1	SYNM	3427	Downstream
chr15:99640388..99640395	-	0.499	M01733	MZF1	SYNM	-4890	Upstream
chr4:119802949..119802955	+	0	M00704	TEF-1	SYNPO2	-7046	Upstream
chr4:119803010..119803016	-	0	M00704	TEF-1	SYNPO2	-6979	Upstream
chr4:119803653..119803659	-	0	M00704	TEF-1	SYNPO2	-6336	Upstream
chr4:119805740..119805750	+	0	M01211	PARP	SYNPO2	-4255	Upstream
chr4:119809198..119809209	-	0	M01596	GLI3	SYNPO2	-786	Upstream
chr4:119810339..119810345	+	0	M00704	TEF-1	SYNPO2	344	Downstream
chr4:119811424..119811443	-	0	LM2_CTCF	CTCF	SYNPO2	1448	Downstream
chr4:119813049..119813055	+	0	M00704	TEF-1	SYNPO2	3054	Downstream
chr4:119813609..119813616	-	0	M00468	AP-2rep	SYNPO2	3621	Downstream
chr4:119815381..119815388	-	0	M00468	AP-2rep	SYNPO2	5393	Downstream
chr4:119810534..119810540	+	0.006	M01287	Neuro D	SYNPO2	539	Downstream
chr4:119810534..119810540	-	0.006	M01287	Neuro D	SYNPO2	545	Downstream
chr4:119809309..119809316	+	0.009	M01709	MAFA	SYNPO2	-686	Upstream
chr4:119810353..119810360	-	0.009	M01709	MAFA	SYNPO2	365	Downstream
chr4:119809554..119809561	+	0.01	M01709	MAFA	SYNPO2	-441	Upstream
chr4:119809199..119809209	+	0.014	M01042	GLI1	SYNPO2	-796	Upstream
chr4:119809198..119809210	-	0.016	M01037	GLI	SYNPO2	-785	Upstream
chr4:119810762..119810769	-	0.024	M01269	NURR1	SYNPO2	774	Downstream
chr4:119812729..119812736	-	0.025	M01269	NURR1	SYNPO2	2741	Downstream
chr4:119802981..119802987	-	0.03	MA0095	YY1	SYNPO2	-7008	Upstream
chr4:119809199..119809208	-	0.037	M00449	Zic2	SYNPO2	-787	Upstream
chr4:119804259..119804265	-	0.044	MA0095	YY1	SYNPO2	-5730	Upstream
chr4:119814118..119814124	+	0.044	MA0095	YY1	SYNPO2	4123	Downstream
chr4:119804362..119804372	-	0.053	M01261	HNF3A	SYNPO2	-5623	Upstream
chr4:119804274..119804281	-	0.055	M01207	ETS2	SYNPO2	-5714	Upstream
chr4:119817819..119817825	-	0.057	MA0095	YY1	SYNPO2	7830	Downstream
chr4:119804248..119804255	-	0.06	M01207	ETS2	SYNPO2	-5740	Upstream
chr4:119813997..119814004	-	0.062	M01269	NURR1	SYNPO2	4009	Downstream
chr4:119803009..119803024	+	0.063	MA0137	STAT1	SYNPO2	-6986	Upstream
chr4:119805605..119805613	-	0.079	M00498	STAT4	SYNPO2	-4382	Upstream
chr4:119815830..119815838	-	0.086	M01308	SOX4	SYNPO2	5843	Downstream
chr4:119811418..119811432	-	0.087	MA0119	TLX1::NFIC	SYNPO2	1437	Downstream
chr4:119811180..119811187	-	0.109	M00750	HMG IY	SYNPO2	1192	Downstream
chr4:119815408..119815416	+	0.112	M00658	PU.1	SYNPO2	5413	Downstream
chr4:119803012..119803021	+	0.126	M00223	STATx	SYNPO2	-6983	Upstream
chr4:119809199..119809210	+	0.126	M01704	GLI3	SYNPO2	-796	Upstream
chr4:119816017..119816025	+	0.127	M00658	PU.1	SYNPO2	6022	Downstream
chr4:119809199..119809210	+	0.143	M01702	GLI1	SYNPO2	-796	Upstream
chr4:119811176..119811184	+	0.155	M01117	OTX	SYNPO2	1181	Downstream
chr4:119803009..119803024	+	0.195	M00459	STAT5B (homodimer)	SYNPO2	-6986	Upstream
chr4:119817251..119817257	+	0.195	M01033	HNF4	SYNPO2	7256	Downstream
chr4:119803009..119803024	+	0.199	M00457	STAT5A (homodimer)	SYNPO2	-6986	Upstream

chr4:119808995..119809002	+	0.205	M00750	HMG IY	SYNPO2	-1000	Upstream
chr4:119802703..119802709	-	0.207	M01033	HNF4	SYNPO2	-7286	Upstream
chr4:119809199..119809210	+	0.212	M01703	GLI2	SYNPO2	-796	Upstream
chr4:119809868..119809875	-	0.215	M00799	Myc	SYNPO2	-120	Upstream
chr4:119811364..119811371	-	0.217	M01665	IRF8	SYNPO2	1376	Downstream
chr4:119811361..119811367	-	0.219	M00805	LEF1	SYNPO2	1372	Downstream
chr4:119807973..119807981	-	0.237	M00671	TCF-4	SYNPO2	-2014	Upstream
chr4:119803363..119803369	+	0.261	M00805	LEF1	SYNPO2	-6632	Upstream
chr4:119817566..119817573	-	0.291	M01665	IRF8	SYNPO2	7578	Downstream
chr4:119812999..119813005	+	0.308	M00805	LEF1	SYNPO2	3004	Downstream
chr4:119814715..119814722	-	0.308	M01718	NFAT2	SYNPO2	4727	Downstream
chr4:119810799..119810815	+	0.314	M01317	HOXC13	SYNPO2	804	Downstream
chr4:119813728..119813734	-	0.315	M00805	LEF1	SYNPO2	3739	Downstream
chr4:119803810..119803817	-	0.321	M01665	IRF8	SYNPO2	-6178	Upstream
chr4:119803370..119803378	+	0.324	M00690	AP-3	SYNPO2	-6625	Upstream
chr4:119807974..119807980	+	0.334	M00805	LEF1	SYNPO2	-2021	Upstream
chr4:119804934..119804940	-	0.338	M00805	LEF1	SYNPO2	-5055	Upstream
chr4:119813940..119813947	+	0.342	M01665	IRF8	SYNPO2	3945	Downstream
chr4:119804444..119804450	-	0.351	M00805	LEF1	SYNPO2	-5545	Upstream
chr4:119813662..119813669	-	0.353	M01665	IRF8	SYNPO2	3674	Downstream
chr4:119803126..119803133	+	0.366	M00240	Nkx2-5	SYNPO2	-6869	Upstream
chr4:119813936..119813942	+	0.367	M00805	LEF1	SYNPO2	3941	Downstream
chr4:119815928..119815935	-	0.367	M01665	IRF8	SYNPO2	5940	Downstream
chr4:119816082..119816089	+	0.382	M01665	IRF8	SYNPO2	6087	Downstream
chr4:119810587..119810594	+	0.411	M01733	MZF1	SYNPO2	592	Downstream
chr4:119813754..119813761	+	0.417	M01733	MZF1	SYNPO2	3759	Downstream
chr4:119808047..119808054	-	0.432	M00240	Nkx2-5	SYNPO2	-1941	Upstream
chr4:119810709..119810715	+	0.434	MA0056	MZF1_1-4	SYNPO2	714	Downstream
chr4:119804709..119804716	-	0.439	M00240	Nkx2-5	SYNPO2	-5279	Upstream
chr4:119812059..119812065	+	0.439	MA0056	MZF1_1-4	SYNPO2	2064	Downstream
chr4:119810587..119810593	+	0.443	MA0056	MZF1_1-4	SYNPO2	592	Downstream
chr4:119803189..119803197	-	0.444	M01117	OTX	SYNPO2	-6798	Upstream
chr4:119805587..119805595	-	0.455	M01117	OTX	SYNPO2	-4400	Upstream
chr4:119809840..119809846	+	0.458	M01660	GABP-alpha	SYNPO2	-155	Upstream
chr4:119813754..119813760	+	0.458	MA0056	MZF1_1-4	SYNPO2	3759	Downstream
chr4:119802759..119802766	+	0.462	M01733	MZF1	SYNPO2	-7236	Upstream
chr4:119802998..119803005	-	0.472	M01243	MTF1	SYNPO2	-6990	Upstream
chr4:119817274..119817280	-	0.477	M01227	MAFB	SYNPO2	7285	Downstream
chr4:119804668..119804674	+	0.481	MA0056	MZF1_1-4	SYNPO2	-5327	Upstream
chr4:119812819..119812826	-	0.481	M00747	IRF-1	SYNPO2	2831	Downstream
chr4:119802759..119802765	+	0.487	MA0056	MZF1_1-4	SYNPO2	-7236	Upstream
chr4:119815379..119815385	-	0.493	MA0056	MZF1_1-4	SYNPO2	5390	Downstream

Supplementary Table VIII: Genetic analysis of candidate SMCs markers loci in association to carotid IMT phenotypes (raw p-values reported in Table; significance levels after Bonferroni correction and number of SNPs tested for each gene are indicated in the headlines; only SNPs with significant results are reported)

		PDLIM7 (n=16 SNPs tested, corrected significance p=0.003125)		PLN (n=637 SNPs tested, corrected significance p=9.29368E-05)		SYNPO2 (n=24 SNPs tested, corrected significance p=0.00208)
	CHR	5	5	6	6	4
	SNP	rs11746443	rs35716097	chr6:119185974	chr6:119186493	rs4833611
	BP	176798306	176806636	119079281	119079800	120147460
	A1	A	T	G	A	T
Max_CC	**BETA**	-0.005052	-0.008738	0.005459	-0.009305	0.0002154
	SE	0.002912	0.002868	0.002855	0.00362	0.002842
	P	0.08288	0.002332	0.05598	0.01021	0.9396
Mean_CC	**BETA**	-0.003273	-0.005266	0.003644	-0.0065	-0.0005459
	SE	0.001827	0.001799	0.001789	0.002268	0.001781
	P	0.07328	0.003452	0.04171	0.004175	0.7592
Max_l_CC	**BETA**	-0.00006758	-0.003169	0.006954	-0.01309	-0.0009964
	SE	0.002567	0.002529	0.00252	0.003189	0.002508
	P	0.979	0.2104	0.005813	0.00004144	0.6912
Mean_l_CC	**BETA**	-0.000216	-0.003566	0.005076	-0.008463	-0.0006467
	SE	0.001981	0.001952	0.00194	0.002457	0.001932
	P	0.9132	0.06784	0.008933	0.0005792	0.7378
Max_IMT	**BETA**	0.0003577	-0.0006055	0.01328	-0.01237	-0.0002705
	SE	0.004056	0.003998	0.003975	0.005045	0.00396
	P	0.9297	0.8796	0.0008466	0.01428	0.9455
Mean_IMT	**BETA**	-0.00008371	-0.002227	0.007917	-0.008392	-0.001366
	SE	0.002152	0.002121	0.002109	0.002677	0.002102
	P	0.969	0.2939	0.0001769	0.001731	0.5158
pr3_Max_1_CC	**BETA**	0.001717	0.0003846	-0.002659	0.006886	-0.007522
	SE	0.001879	0.00185	0.002198	0.002806	0.00221
	P	0.3608	0.8354	0.2264	0.01418	0.0006729
fastest	**BETA**	-0.01818	-0.01691	0.002048	-0.008911	-0.00563
progression	**SE**	0.005457	0.005372	0.00533	0.006805	0.005364
	P	0.0008743	0.001658	0.7009	0.1905	0.294

legend:

Chr: chromosome, A1: coded allele, P: p-value for association with IMT phenotypes

Max_CC: maximum IMT of the common carotid in a segment excluding the first cm proximal to the bifurcation

Max_l_CC: Max IMT value of the first centimetre of the common carotid arteries closest to the bifurcation (left and right)

Mean_l_CC: Mean IMT value of the first centimetre of the common carotid arteries closest to the bifurcation (left and right)

Max_IMT: maximum IMT measure considering the whole carotid tree derived from the segment-specific measurements

Mean_CC: average IMT of the common carotid in a segment excluding the first cm proximal to the bifurcation

Mean_IMT: average IMT composite value considering the whole carotid tree derived from the segment-specific measurements

pr3_Max_1_CC: 3 point progression of the maximum IMT of the first centimeter of Common Carotid artery (the one close to the bifurcation) right and left

fastest progression: fastest IMTmax progression detected in the whole carotid tree regardless of location

Supplementary Table IX: Functional data from REGULOME/ENCODE databases for SNPs associated with carotid IMT phenotypes from genetic analyses

TF-transcription factor

GENE	SNP	RegulomeDB TF binding score	TF binding and function	Proxy	RegulomeDB TF binding score	TF binding and function	Distance (bp)	RSquared	DPrime
PDLIM7	rs11746443	Likely to affect binding, top score	HEY1, cardiovascular development	rs4075958	Likely to affect binding, top score	ETS1, expression of cytokines, cell proliferation, differentiation, migration	13794	0.927	0.963
PDLIM7	rs11746443	Likely to affect binding, top score	HEY1, cardiovascular development	rs10866705	low		2825	0.754	0.955
PDLIM7	rs35716097	Likely to affect binding, high score	HNF4A, proliferation	rs10866705	low		5505	0.857	1
SYNPO2	rs4833611	low		rs12645079	low		47052	0.81	1
SYNPO2	rs4833611	low		rs2102541	low		32081	0.766	0.912
SYNPO2	rs4833611	low		rs7668423	low		30248	0.701	0.871
PLN	rs7742814	low		rs7765824	low		5363	1	1
PLN	rs7742814	low		rs17826675	low		31609	0.74	1
PLN	rs67456868	low		rs11153777	low		52374	0.797	0.942
PLN	rs67456868	low		rs11153778	low		79622	0.797	0.942
PLN	rs67456868	low		rs669978	low		226809	0.797	0.942
PLN	rs67456868	low		rs2295709	low		87174	0.749	0.889

GENE	SNP	Genomic location, nearby genes	Functional consequence	MAF
PDLIM7	rs11746443	RGS14	intronic variant	0.1773
PDLIM7	rs35716097	outside	unknown	0.3425
SYNPO2	rs4833611	USP53	intronic variant	0.3734
PLN	rs7742814	outside	unnown	0.3133
PLN	rs67456868	outside	unknown	0.0923

Supplementary Table X: Functional data from HAPLOREG database for SNPs associated with carotid IMT phenotypes

Query SNP: rs11746443 and variants with r2 >= 0.8

							freq	freq	freq	freq	histone marks	histone marks	bound	changed	GWAS hits	hits	hits	genes	func annot	location
chr	pos (hg38)	(r^2)	(D')	LD	variant		AMR	ASN	EUR	SiPhy	Enhancer	DNAse	Motifs	NHGRI/EBI	GRASP QTL	Selected eQTL	GENCODE	dbSNP		
5	177355217	0.8	0.94	rs13153019	T	C	0.07	0.25	0.17	0.26	BLD	6 tissues			AIRE,PU.1			17 hits	2.6kb 5' of RGS14	
5	177357511	0.89	0.95	rs4075958	G	A	0.08	0.26	0.17	0.27	7 tissues	14 tissues	8 tissues	MAX		1 hit	10 hits	26 hits	325bp 5' of RGS14	
5	177365742	0.89	0.95	rs11741640	G	A	0.05	0.26	0.17	0.27	SKIN, LIV	11 tissues	ESDR,BLD,LIV		6 altered motifs			20 hits	RGS14	intronic
5	177370342	0.96	1	rs4074995	G	A	0.09	0.25	0.17	0.28	SKIN, GI, MUS	18 tissues	BLD,PANC		IRC900814,STAT,Sp100	1 hit	2 hits	24 hits	RGS14	intronic
5	177371305	1	1	rs11746443	G	A	0.06	0.25	0.17	0.28	21 tissues	5 tissues	7 tissues	HEY1,POL2	5 altered motifs	1 hit		21 hits	RGS14	intronic
5	177373053	0.94	0.99	rs11748165	C	T	0.11	0.26	0.17	0.28	BLD	11 tissues	BLD,BLD		Hic1			22 hits	451bp 3' of RGS14	
5	177373360	0.96	0.99	rs11748297	G	A	0.1	0.26	0.17	0.28	BLD	8 tissues			DMRT5			21 hits	758bp 3' of RGS14	
5	177379813	0.8	0.95	rs138255156	TTTCC	T	0.04	0.24	0.17	0.25		BLD, LIV			EWSR1-FLI1,SP1				SLC34A1	

Query SNP: rs35716097 and variants with r2 >= 0.8

							freq	freq	freq	freq	histone marks	histone marks	bound	changed	GWAS hits	hits	hits	genes	func annot
chr	pos (hg38)	(r^2)	(D')	LD	variant		AMR	ASN	EUR	SiPhy	Enhancer	DNAse	Motifs	NHGRI/EBI	GRASP QTL	Selected eQTL	GENCODE	dbSNP	
5	177372991	0.84	0.99	rs10051765	T	C	0.49	0.32	0.26	0.33			BLD		E2A,Ik-1,LUN-1			30 hits	389bp 3' of RGS14
5	177379635	1	1	rs35716097	C	T	0.4	0.3	0.27	0.3	LIV, BLD	10 tissues	19 tissues	18 bound pro	AIRE,Rhox11			28 hits	SLC34A1

Query SNP: rs4833611 and variants with r2 >= 0.8

							freq	freq	freq	freq	histone marks	histone marks	bound	changed	GWAS hits	hits	hits	genes	func annot	location
chr	pos (hg38)	(r^2)	(D')	LD	variant		AMR	ASN	EUR	SiPhy	Enhancer	DNAse	Motifs	NHGRI/EBI	GRASP QTL	Selected eQTL	GENCODE	dbSNP		
4	119213621	0.92	0.96	rs12648052	A	C	0.42	0.43	0.25	0.33	23 tissues	BLD	6 tissues		Hsf,SRF,STAT			7 hits	USP53	intronic
4	119214039	0.97	0.99	rs4621411	A	G	0.4	0.43	0.25	0.33	23 tissues	4 tissues		CTCF	6 altered motifs			7 hits	USP53	intronic
4	119214980	0.98	0.99	rs10033031	G	A	0.42	0.43	0.25	0.32					4 altered motifs			7 hits	USP53	intronic
4	119217669	0.98	0.99	rs1134065	A	C,G,T	0.42	0.43	0.26	0.32		8 tissues	SKIN					7 hits	USP53	5'-UTR
4	119218028	0.98	0.99	rs74629660	G	C	0.4	0.43	0.26	0.32		8 tissues			Spz1			6 hits	USP53	intronic
4	119218998	0.98	0.99	rs144747687	T	TGCAT	0.41	0.42	0.26	0.32	SKIN	STRM, SKIN, VAS			10 altered motifs			1 hit	USP53	intronic
4	119219427	0.99	1	rs11943184	A	G	0.4	0.43	0.26	0.32	BRN	10 tissues			Hoxb8,SRF,YY1			6 hits	USP53	intronic
4	119221468	0.99	1	rs55903149	A	AG,AG	0.39	0.43	0.26	0.32		PLCNT						5 hits	USP53	intronic
4	119221647	0.99	0.99	rs35886000	G	A	0.4	0.43	0.26	0.33		PLCNT, MUS	SKIN,SKIN		Foxd1,Foxo,GCNF			6 hits	USP53	intronic
4	119221984	0.99	1	rs56090560	A	T	0.4	0.43	0.26	0.32					DBP,Hdx			6 hits	USP53	intronic
4	119222111	0.99	1	rs62326359	G	A	0.4	0.43	0.26	0.32					5 altered motifs			6 hits	USP53	intronic
4	119222703	0.99	1	rs62328360	G	A	0.4	0.43	0.26	0.32		FAT			MIZF,Smad			6 hits	USP53	intronic
4	119222882	0.96	1	rs200152715	A	AT	0.39	0.42	0.26	0.32		FAT			24 altered motifs			7 hits	USP53	intronic
4	119225485	0.99	1	rs12643221	G	A	0.4	0.43	0.26	0.32					E2A,TBX5,ZEB1			6 hits	USP53	intronic
4	119226305	1	1	rs4833611	C	T	0.42	0.43	0.26	0.33		FAT, SKIN	THYM	POL2	4 altered motifs			8 hits	USP53	intronic
4	119227213	0.99	1	rs11946597	A	C	0.39	0.43	0.26	0.32		LNG, FAT, SKIN			5 altered motifs			8 hits	USP53	intronic
4	119227355	0.99	1	rs76546029	A	G	0.39	0.43	0.27	0.32		4 tissues			7 altered motifs			6 hits	USP53	intronic
4	119228507	0.99	1	rs61015834	C	G	0.42	0.43	0.26	0.32		FAT						7 hits	USP53	intronic

Query SNP: rs7742814 and variants with r2 >= 0.8

							freq	freq	freq	freq	histone marks	histone marks	bound	changed	GWAS hits	hits	hits	genes	func annot
chr	pos (hg38)	(r^2)	(D')	LD	variant		AMR	ASN	EUR	SiPhy	Enhancer	DNAse	Motifs	NHGRI/EBI	GRASP QTL	Selected eQTL	GENCODE	dbSNP	
6	118757157	0.91	0.96	rs62424023	A	G	0.39	0.33	0.24	0.33		BLD, THYM			NRSF			5 hits	47kb 5' of CEP85L
6	118757161	0.95	1	rs62424024	G	A	0.36	0.32	0.23	0.32		BLD, THYM			Pbx-1			6 hits	47kb 5' of CEP85L

6	118758118	1	1	rs7742814	A	G	0.37	0.32	0.24	0.33	BLD	4 tissues				7 hits	48kb 5' of CEP85L
6	118760311	0.96	1	rs7745728	T	A	0.34	0.33	0.24	0.34		BLD		Hoxd10,Pax-4		7 hits	50kb 5' of CEP85L
6	118760407	0.96	1	rs9320667	A	G	0.34	0.33	0.24	0.34		BLD		Foxp1,Irx		7 hits	50kb 5' of CEP85L
6	118762772	1	1	rs7740511	A	G	0.3	0.31	0.24	0.33		BLD		Cdx2,Hoxb8		5 hits	51kb 3' of MCM9
6	118763481	1	1	rs7765824	T	G	0.27	0.31	0.24	0.33	BLD	BLD		RBP-Jkappa		6 hits	50kb 3' of MCM9
6	118764003	0.95	1	rs6909006	G	C	0.3	0.31	0.24	0.32		BLD		7 altered motifs		5 hits	49kb 3' of MCM9

Query SNP: rs67456868 and variants with r2 >= 0.8

							freq	freq	freq	freq	histone marks	histone marks	bound	changed	GWAS hits	hits	hits	genes	func annot
chr	pos (hg38)	(r^2)	(D')	LD	variant		AMR	ASN	EUR	SiPhy	Enhancer	DNAse	Motifs	NHGRI/EBI	GRASP QTL	Selected eQTL	GENCODE	dbSNP	
6	118747670	0.8	-0.92	rs10691836	T	TAC	0.71	0.85	0.98	0.84					RREB-1			1 hit	38kb 5' of CEP85L
6	118758637	1	1	rs67456868	G	A	0.11	0.13	0.03	0.17	BLD	BLD, BRN						2 hits	49kb 5' of CEP85L
6	118782616	0.94	0.97	rs12194135	T	G	0.12	0.14	0.03	0.17		ESDR						3 hits	31kb 3' of MCM9
6	118792308	0.9	0.97	rs12194458	C	G	0.11	0.13	0.03	0.16								3 hits	21kb 3' of MCM9

DATA SUPPLEMENT

Phenotypic modulation of smooth muscle cells in atherosclerosis is associated with downregulation of *LMOD1, SYNPO2, PDLIM7, PLN* and *SYNM*

- Markers of smooth muscle cells -

Perisic L, Rykaczewska U, Razuvaev A, Sabater-Lleal M, Lengquist M, Miller CL, Ericsson I, Röhl S, Kronqvist M, Aldi S, Magné J, Vesterlund M, Li Y, Yin H, Gonzalez Diez M**,** Roy J, Baldassarre D, Veglia F, Humphries SE, de Faire U, Tremoli E, on behalf of the IMPROVE study group, Odeberg J, Vukojević V, Lehtiö J, Maegdefessel L, Ehrenborg E, Paulsson-Berne G**,** Hansson GK, Lindeman JHN, Eriksson P, Quertermous T, Hamsten A, Hedin U

Materials and Methods

Human material

Patients undergoing surgery for symptomatic (S) or asymptomatic (AS), high-grade (>50% NASCET) [1] carotid stenosis at the Department of Vascular Surgery, Karolinska University Hospital, Stockholm, Sweden were consecutively enrolled in the study and clinical data recorded on admission. Symptoms of plaque instability were defined as transitory ischemic attack (TIA), minor stroke (MS) and amaurosis fugax (AF). Patients without qualifying symptoms within 6 months prior to surgery were cathegorized as AS and indication for carotid endarterectomy (CEA) based on results from the Asymptomatic Carotid Surgery Trial (ACST) [2]. Carotid endarterectomies (carotid plaques, CP) and blood samples were collected at surgery and retained within the **Bi**obank of **K**arolinska **E**ndarterectomies (BiKE). The BiKE study cohort demographics, details of sample collection, processing and analyses were as previously described [3]. The microarray dataset is available from Gene Expression Omnibus (GSE21545). For immunohistochemistry additional tissues were used: normal radial arteries obtained at coronary by-pass surgery, one internal carotid artery from a 61-year-old male treated for a neck tumor, and in-stent stenosis (intimal hyperplasia) tissue obtained from a patient after treatment of a traumatic aortic transection with a stent graft.

The SOKRATES study comprises progressive aortic atherosclerotic lesions collected during organ transplantation, covering all age groups and the whole spectrum of atherosclerotic disease. Briefly, two centimetres of excessive aorta proximal and distal from the ostium of the renal artery was removed and lesions were classified according to adapted American Heart Association (AHA) classification [4] as proposed by Virmani et al [5]. Details of sample collection, demographics of the cohort along with tissue processing and full histological classification have been described previously [6].

The database of IMPROVE, a large, multicenter, European longitudinal cohort study IMPROVE (acronym: Carotid **I**ntima **M**edia Thickness (IMT) and IMT-**PR**ogression as Predictors of **V**ascular **E**vents in a High-Risk European Population) was used for studying single nucleotide polymorphism (SNP) associations with various cIMT measures. IMPROVE was set up for the study of cIMT measures as predictors of incident coronary events, and enrolled n=3711 subjects with at least three independent CAD risk factors. Detailed descriptions of IMPROVE, including the protocols for carotid ultrasound measures and SNP genotyping on Illumina CardioMetabochip and Immunochip arrays, have been reported [7-9]. In the present study, a total of n=3378 subjects were available for the genetic association analyses. All samples were collected with informed consent from patients, organ donors or their guardians. All human studies were approved by the regional Ethical Committees.

Antibodies

The following primary antibodies obtained from Human Protein Atlas (HPA) were used: anti-Lmod1 (HPA030097), Synpo2 (HPA030665), Pdlim7 (HPA048815), Pln (HPA026900). Anti-Synm antibody was purchased from Proteintech (20735-1-AP). For stainings of rat samples additional antibodies were purchased: anti-Pln (ab85146, Abcam) and Synpo2 (ab50192, Abcam).

Quantitative PCR (qPCR)

For quantitative PCR, total RNA was reverse-transcribed using High Capacity RNA-to-cDNA kit (4387406, Applied Biosystems, Life Technologies Corporation, Carlsbad, CA). PCR amplification was done in 96-well plates in 7900 HT real-time PCR system (Applied Biosystems), using TaqMan® Universal PCR Master Mix (Applied Biosystems) and TaqMan® Gene Expression Assays (LMOD1 Rn01483340_m1, SYNM Rn00711100_m1, SYNPO2 Rn04244800_m1, PDLIM7 Rn01441766_m1, PLN Rn01434045_m1; MYOCD Rn01786178_m1, ACTA2 Rn01759928_g1, MYH11 Rn01530317_m1; Applied Biosystems). All samples were measured in triplicates. Results were normalized to the equal mass of total RNA as well as the Ct values of RPLPO housekeeping control (Hs99999902_m1). The relative amount of target gene mRNA was calculated by $2^{-\Delta\Delta Ct}$ method and presented as fold change.

In situ RNA detection

All reagents for in situ RNA detection were from Advanced Cell Diagnostics (ACDbio, USA). RNA detection was performed using RNAscope 2.0 HD Detection Kit Brown (#310033) on fresh frozen paraffin embedded tissues sectioned to 5 um thickness. Briefly, slides were heated to 57°C, deparaffinised, pretreated and probe hybridisation performed according to manufacturers instructions. All incubations were done in the HybEZ hybridisation oven. Probes targeting RNA of interest were the following: ACTA2 (311811), CNN1 (444131), PLN (444181), SYNPO2 (444161), LMOD1 (444141), PDLIM7 (444171), SYNM (444191), MYH11 (444151).

Immunohistochemistry (IHC)

All IHC reagents were from Biocare Medical (Concord, CA). Tissues were fixed for 24-48 hours in 2% Zn-formaldehyde at room temperature and paraffin-embedded. Isotype rabbit and mouse IgG were used as negative controls. In brief, 5 µm sections were deparaffinized in Tissue Clear and rehydrated in graded ethanol. For antigen retrieval, slides were subjected to high-pressure boiling in DIVA buffer (pH 6.0). After blocking with Background Sniper, primary antibodies were diluted in Da Vinci Green solution, applied on slides and incubated at room temperature for 1 hour. For colocalizations, antibodies for SMC-specific markers were used: anti-Myosin heavy chain 11 (MYH11, sc65735, Santa Cruz), Calponin (ab700, Abcam), Smooth muscle α-actin (SMA, M0851, DAKO). A double-stain probe-polymer system containing

alkaline phosphatase and horseradish peroxidase was applied, with subsequent detection using Warp Red and Vina Green. Slides were counterstained with Hematoxylin QS (Vector Laboratories, Burlingame, CA), dehydrated and mounted in Pertex (Histolab, Gothenburg, Sweden). Images were taken using an automated ScanScope slidescanner or a Nikon OPTIPHOT-2 microscope equipped with a digital camera and processed with NIS-Elements software. Magnifications are indicated in figure legends.

Immunofluorescence (IFL)

Cells grown on glass coverslips were fixed in 4% paraformaldehyde for 10 minutes at room temperature, permeabilized with 0.1 % Triton X-100/PBS for 5 min, followed by blocking with 5% normal goat serum/PBS for 1 hour. Cells were then incubated with primary antibodies diluted in the blocking solution for 1 hour at room temperature, washed with PBS and counterstained with Alexa Fluor 488 or 568-conjugated secondary antibodies (Invitrogen). Nuclei were stained with diamidino-2-phenylindole (DAPI) and fibrous-actin with Rhodamine-conjugated phalloidin. Images were taken in a multitrack mode, one channel at a time, using the Zeiss LSM510 confocal laser scanning microscope system and 100× oil immersion objective.

Flow cytometry

Cells were fixed with 4% paraformaldehyde and permeabilised with 0.1% Triton X-100/PBS for 5 min. Unspecific binding was blocked by incubation with 0.1% BSA/PBS and cell were stained with primary (SMA, M0851, DAKO) and secondary antibodies (Alexa 488, Invitrogen) diluted in 0.1% BSA/PBS for 1h at room temperature. Analysis was performed on the CyAn flow cytometer (Beckman Coulter) and data processed using the FlowJo software.

Primary rat aortic SMCs culture

For isolation of primary rat SMCs (rSMCs), whole aortas were harvested, as previously described [10]. Adventitia was removed and vessels were cut into 1 mm pieces and digested in 0.1% collagenase in Ham's medium F-12 supplemented with 0.1% BSA, 10 mM Hepes, 10mM Tes (pH 7.3), 50 □g/ml of L-ascorbic acid, and 50 □g/ml of penicilin-streptomycin (medium F-12/0.1% BSA) for 10h. Cells were seeded (50 000 cells/cm^2) on fibronectin-coated Petri dishes and cultured for 7 days either in medium F-12/0.1% BSA (serum-free condition) or in medium F-12/0.1% BSA with 30ng/ml platelet derived growth factor BB (PDGFBB) [11]. Cells were harvested for experiments after 1, 3, 5 and days 7 of culture. Intact artery tissue was also used as reference when measuring expression levels of genes of interest. All cell culture experiments were repeated three times and representative images are shown.

Primary human carotid artery SMCs culture and silencing of PDLIM7

Low passage (3-4) primary human carotid artery artery SMCs (3014-05a, Cell Applications), were grown in 5% CO2 humidified environment at 37°C, in

complete medium (311-500, Cell Applications). For siRNA transfections, growth medium was replaced with Opti-MEM (Gibco, Thermo Fisher Scientific) medium supplemented with 0.2% fetal bovine serum (FBS, Gibco). Cells were transiently transfected using Lipofectamine 2000 (Invitrogen) according to the manufacturer**'**s recommendations, separately with 2 siPDLIM7 (s194996 and s194997, Applied Biosystems**)** and mismatch (scrambled, 4390843, Applied Biosystems) control oligonucleotides diluted in Opti-MEM and applied at 200 pmol/well for a 6-well plate. After 48 hrs of silencing, downregulation of PDLIM7 protein was evaluated by Western blot and immunofluorescence, and PDLIM7 siRNA s194997 was used in further experiments (Supplementary Figure X).

Cell culture assays

Human carotid SMCs were plated on fibronectin (PHE0023, Invitrogen) coated 6-well plates and left to adhere. After overnight serum-starvation, cells were treated with 20 ng/ml IFNγ (285-IF-100, R&D Systems) and collected at several time-points (2h, 4h, 8h and 24h) for RNA isolation and qPCR analyses.

Cell proliferation was assessed using the colorimetric immunoassay based on the BrdU incorporation during DNA synthesis (11647229001, Roche), according to manufacturer protocol. Cell adhesion was assessed on fibronectin-coated 96-well plates, using a colorimetric assay according to standard protocol[12]. Briefly, cells were fixed with 4% paraformaldehyde, stained with 0.1% (w/v) Crystal Violet, 200 mM MES, pH 6.0 and thereafter treated with 10% (v/v) acetic acid. Cell spreading was quantified after 2 hours of plating, by measuring cell area using ImageJ software.

Lipid-loading assays we performed in human aortic SMCs following the previously published protocol [13]. Briefly, cells were incubated with oxLDL (XXX *μ*g/ml, Company???) in 0.2% (w/v) BSA for 48 and 72 h. Cells incubated with 0.2% BSA without oxLDL treatment at corresponding time-points, served as controls. All cell culture experiments were repeated three times, samples were measured in triplicates and representative results shown.

Commento [LP1]: Joelle, please check/rewrite this if needed

Western blots

Cells were treated with RIPA buffer on ice for extraction of proteins. Samples were reduced with β-mercaptoethanol and heated to 95ºC for 10 minutes. Proteins were separated using Mini-Protean® TGX™ Precast Gels 4-20% (BIORAD, California, USA) and transferred to Immun-Blot® PVDF membrane (BIORAD) for 1h. Blocking was done with 5% bovine serum albumin (BSA)/milk in 1xTTBS to minimize unspecific signal. Primary antibodies were added to the membranes in recommended dilutions and incubated in +4C ON. After washing in 1xTTBS the fluorescent IRDye800CW or IRDye680RD (Odyssey) secondary antibodies were incubated for 1h at RT. The membranes were analyzed in LICOR ODYSSEY scanner.

RNA-sequencing

Human carotid artery SMCs were cultured in serum-free or 10% serum-supplemented media for 48 hours (n=3 per condition) and total RNA was purified from $5x10^5$ cells using the Qiagen miRNeasy kit. RNA libraries were prepared with the Illumina TruSeq library kit as described by the manufacturer and RNA sequenced using Illumina HiSeq 2500 (2x101). Reads contained in raw fastq files were mapped to hg19 using the RNA-seq aligner STAR (v2.4.0i). Mapped reads were counted using the htseq-count script distributed with the HTSeq Python package (https://pypi.python.org/pypi/HTSeq). Differential expression of exons, genes, and transcripts were assayed using the DESeq2 R package from Bioconductor (http://bioconductor.org/packages/release/bioc/html/DESeq2.html), which uses negative binomial distribution to estimate dispersion and model differential expression such as to permit biological variability to be different among tested genes (transcripts).

ChIP-sequencing

Human carotid artery SMCs were cultured in normal 5% serum-supplemented media for 48 hours and fixed in 1% formaldehyde to cross-link chromatin, followed by quenching with glycine. $2x10^7$ cells were collected, and nuclear lysates were prepared as previously described [14]. Chromatin nuclear lysates were then sheared to fragments of 100-500bp using a Bioruptor Pico sonicator (Diagenode) according to the manufacturer. 5ug H3K27ac antibody (Abcam) was added to sheared chromatin to immunoprecipitate protein-DNA complexes overnight at 4C. Following capture of the antibody-protein-DNA complexes to Protein G beads, the complexes were washed and eluted as previously described. Protein-DNA crosslinks were reversed and ChIP DNA was recovered using Qiagen PCR Purification kits. To generate the ChIP library, Illumina TruSeq adapters were ligated to the ChIP DNA, followed by PCR amplification and gel electrophoresis on a 2% agarose gel. ChIP DNA library fragments around 300bp were selected for PCR amplification. ChIP DNA library concentrations were quantitated by Qubit fluorometric and bioanalyzer analyses. Libraries were sequenced on an Illumina HiSeq 2500 (2x101) to obtain approximately 45-50 million reads per barcoded sample. Resulting fastq files were aligned to human genome hg19 using bowtie2 to generate bam files and peaks were called using HOMER findPeaks with treatment sample as H3K27ac and control sample as IgG using the local filtering model, peak size of 1000, and an FDR threshold of 0.001. Fold change and p-value in H3K27ac vs. control were determined using a cumulative Poisson distribution.

LC-MS/MS analysis and protein identification

Atherosclerotic plaques from n=20 BiKE patients (n=10 symptomatic + 10 asymptomatic; matched for male gender, age and statin medication) were

Commento [LP2]: Mattias, please check/rewrite if needed. Please keep the description very brief for this particular manuscript.

analysed using LC-MS/MS as previously described [15]. Briefly, protein samples were iTRAQ labeled and pooled samples were separated on IPG strips. After separation, peptides were eluted into 72 fractions for each strip. These fractions were one by one subjected to reversed phase LC-MS/MS, where the peptides were fragmented to obtain the amino acid sequences. LC-MS was performed on a hybrid LTQ-Orbitrap Velos mass spectrometer (Thermo Fischer Scientific, San Jose, CA, USA). The fragment spectra from the mass spectrometer were matched to a database consisting of theoretical fragment spectra from all human proteins to obtain protein identities. Quantitative information was acquired by using the iTRAQ reporter ion intensities.

Rat carotid artery balloon injury

Carotid artery balloon injury was performed on male Sprague-Dawley rats, as previously described [16]. The left carotid artery was dissected under isoflurane inhalation anesthesia, an arteriotomy performed in the external carotid artery and the common carotid artery de-endothelialized 3 times with a 2F Fogarty catheter. Animals were euthanized with isoflurane directly after injury (0h) or after 2h, 20h, 2 days, 5 days, 2 weeks, 6 weeks and 12 weeks after vascular injury and both the left (injured) and right (uninjured) common carotid arteries harvested (n=6 or 7 animals at each time point). Arteries were rinsed with PBS to remove blood. Eight additional animals were sacrificed and uninjured carotid arteries used as controls (intact). Arteries were divided in a proximal segment used for RNA isolation and a distal segment used for histology. Total RNA was used for microarray analysis with Affymetrix GeneTitan Rat Gene ST v1.1 arrays (part of a manuscript in preparation). Experiments were performed according to the protocols approved by the Regional Animal Ethic committee, Stockholm, and institutional guidelines for animal care were followed.

Mouse model of atherosclerotic plaque vulnerability

Commento [LP3]: Hong and Daniel, please check this part.

Analyses of gene expression were performed in an atherosclerotic carotid plaque rupture model in ApoE-deficient mice and contralateral control carotid arteries of the same mice [17, 18]. The model in brief consists of an incomplete ligation (Vicryl 5-0 suture, Ethicon Endo-Surgery Inc, Blue Ash, USA) of the common right carotid artery (just below the bifurcation) for 4 weeks, which triggers intimal hyperplasia and non-ruptured carotid atherosclerotic lesions. To provoke rupture of the developed plaque, a conical polyethylene cuff is placed proximal to the ligation site for 4 days. Approximately 50% of the 16 week old male mice display features of ruptured plaques, such as endothelial cracks or ulcers, and intraluminal thrombus formation. All experiments have been approved by the Stockholm Regional Board for Experimental Animal Ethics.

Bioinformatic and statistical analyses

Gene expression and pathway analyses of the human plaque microarrays were previosly described in details [3]. Pearson correlations were calculated to determine the association between mRNA expression levels from microarrays. Functional coupling network based on extended protein-protein interactions was constructed using FunCoup software (http://funcoup.sbc.su.se) and the one based on co-expression using GeneMania (www.genemania.org). Transcription factors binding motif analysis was performed using MotifMap (http://motifmap.ics.uci.edu) and MSigDB (Broad Institute) softwares, considering those with FDR<0.05. For genetic analyses, all SNPs in the region ±200 000 kb around the gene from the 1000 genomes pilot 1 CEU reference were tested that were present on the Illumina CardioMetabochip and Immunochip arrays. Linear regression analyses were performed between the SNPs and different cIMT measures using PLINK (v1.07) [19], assuming an additive genetic model and adjusting for age, gender and population stratification. All cIMT variables were logarithmically transformed before statistical analysis because of skewed distributions. Group comparisons were evaluated by the T-test, Mann-Whitney test or ANOVA when appropriate. In all analyses p-values were Bonferroni-corrected and $p<0.05$ after correction for multiple comparisons considered to indicate statistical significance.

References

1. Naylor AR, Rothwell PM, Bell PR. Overview of the principal results and secondary analyses from the european and north american randomised trials of endarterectomy for symptomatic carotid stenosis. *European journal of vascular and endovascular surgery : the official journal of the European Society for Vascular Surgery*. 2003;26:115-129
2. Halliday A, Harrison M, Hayter E, Kong X, Mansfield A, Marro J, Pan H, Peto R, Potter J, Rahimi K, Rau A, Robertson S, Streifler J, Thomas D, Asymptomatic Carotid Surgery Trial Collaborative G. 10-year stroke prevention after successful carotid endarterectomy for asymptomatic stenosis (acst-1): A multicentre randomised trial. *Lancet*. 2010;376:1074-1084
3. Perisic L, Aldi S, Sun Y, Folkersen L, Razuvaev A, Roy J, Lengquist M, Akesson S, Wheelock CE, Maegdefessel L, Gabrielsen A, Odeberg J, Hansson GK, Paulsson-Berne G, Hedin U. Gene expression signatures, pathways and networks in carotid atherosclerosis. *Journal of internal medicine*. 2015
4. Stary HC. Natural history and histological classification of atherosclerotic lesions: An update. *Arteriosclerosis, thrombosis, and vascular biology*. 2000;20:1177-1178
5. Virmani R, Kolodgie FD, Burke AP, Farb A, Schwartz SM. Lessons from sudden coronary death: A comprehensive morphological classification scheme for atherosclerotic lesions. *Arteriosclerosis, thrombosis, and vascular biology*. 2000;20:1262-1275
6. van Dijk RA, Virmani R, von der Thusen JH, Schaapherder AF, Lindeman JH. The natural history of aortic atherosclerosis: A systematic histopathological evaluation of the peri-renal region. *Atherosclerosis*. 2010;210:100-106
7. Baldassarre D, Hamsten A, Veglia F, de Faire U, Humphries SE, Smit AJ, Giral P, Kurl S, Rauramaa R, Mannarino E, Grossi E, Paoletti R, Tremoli E, Group IS. Measurements of carotid intima-media thickness and of interadventitia common carotid diameter improve prediction of cardiovascular events: Results of the improve (carotid intima media thickness [imt] and imt-progression as predictors of vascular events in a high risk european population) study. *Journal of the American College of Cardiology*. 2012;60:1489-1499
8. Baldassarre D, Veglia F, Hamsten A, Humphries SE, Rauramaa R, de Faire U, Smit AJ, Giral P, Kurl S, Mannarino E, Grossi E, Paoletti R, Tremoli E, Group IS. Progression of carotid intima-media thickness as predictor of vascular events: Results from the improve study. *Arteriosclerosis, thrombosis, and vascular biology*. 2013;33:2273-2279
9. Gertow K, Sennblad B, Strawbridge RJ et al. Identification of the bcar1-cfdp1-tmem170a locus as a determinant of carotid intima-media thickness and coronary artery disease risk. *Circulation. Cardiovascular genetics*. 2012;5:656-665
10. Roy J, Tran PK, Religa P, Kazi M, Henderson B, Lundmark K, Hedin U. Fibronectin promotes cell cycle entry in smooth muscle cells in primary culture. *Experimental cell research*. 2002;273:169-177

11. Hedin U, Bottger BA, Forsberg E, Johansson S, Thyberg J. Diverse effects of fibronectin and laminin on phenotypic properties of cultured arterial smooth muscle cells. *The Journal of cell biology*. 1988;107:307-319
12. Humphries MJ. Cell adhesion assays. *Molecular biotechnology*. 2001;18:57-61
13. Vengrenyuk Y, Nishi H, Long X, Ouimet M, Savji N, Martinez FO, Cassella CP, Moore KJ, Ramsey SA, Miano JM, Fisher EA. Cholesterol loading reprograms the microrna-143/145-myocardin axis to convert aortic smooth muscle cells to a dysfunctional macrophage-like phenotype. *Arteriosclerosis, thrombosis, and vascular biology*. 2015;35:535-546
14. Miller CL, Anderson DR, Kundu RK, Raiesdana A, Nurnberg ST, Diaz R, Cheng K, Leeper NJ, Chen CH, Chang IS, Schadt EE, Hsiung CA, Assimes TL, Quertermous T. Disease-related growth factor and embryonic signaling pathways modulate an enhancer of tcf21 expression at the 6q23.2 coronary heart disease locus. *PLoS genetics*. 2013;9:e1003652
15. Branca RM, Orre LM, Johansson HJ, Granholm V, Huss M, Perez-Bercoff A, Forshed J, Kall L, Lehtio J. Hirief lc-ms enables deep proteome coverage and unbiased proteogenomics. *Nature methods*. 2014;11:59-62
16. Razuvaev A, Henderson B, Girnita L, Larsson O, Axelson M, Hedin U, Roy J. The cyclolignan picropodophyllin attenuates intimal hyperplasia after rat carotid balloon injury by blocking insulin-like growth factor-1 receptor signaling. *Journal of vascular surgery*. 2007;46:108-115
17. Sasaki T, Nakamura K, Kuzuya M. Plaque rupture model in mice. *Methods in molecular medicine*. 2007;139:67-75
18. Sasaki T, Kuzuya M, Nakamura K, Cheng XW, Shibata T, Sato K, Iguchi A. A simple method of plaque rupture induction in apolipoprotein e-deficient mice. *Arteriosclerosis, thrombosis, and vascular biology*. 2006;26:1304-1309
19. Purcell S, Neale B, Todd-Brown K, Thomas L, Ferreira MA, Bender D, Maller J, Sklar P, de Bakker PI, Daly MJ, Sham PC. Plink: A tool set for whole-genome association and population-based linkage analyses. *American journal of human genetics*. 2007;81:559-575